THE 4TH INTERNATIONAL WORKSHOP ON INNOVATIVE SIMULATION FOR HEALTH CARE

SEPTEMBER, 21-23 2015
BERGEGGI, ITALY

EDITED BY
AGOSTINO BRUZZONE
MARCO FRASCIO
FRANCESCO LONGO
YURY MERKURYEV
VERA NOVAK
JERZY W. ROZENBLIT

PRINTED IN RENDE (CS), ITALY, SEPTEMBER 2015

ISBN 978-88-97999-53-9 (Paperback)
ISBN 978-88-97999-62-1 (PDF)

ISBN 978-88-97999-53-9 (Paperback)
ISBN 978-88-97999-62-1 (PDF)

THE 4TH INTERNATIONAL WORKSHOP ON INNOVATIVE SIMULATION FOR HEALTH CARE, IWISH 2015

SEPTEMBER 21-23 2015, BERGEGGI, ITALY

ORGANIZED BY

DIME – UNIVERSITY OF GENOA

LIOPHANT SIMULATION

SIMULATION TEAM

IMCS – INTERNATIONAL MEDITERRANEAN & LATIN AMERICAN COUNCIL OF SIMULATION

DIMEG, UNIVERSITY OF CALABRIA

MSC-LES, MODELING & SIMULATION CENTER, LABORATORY OF ENTERPRISE SOLUTIONS

MODELING AND SIMULATION CENTER OF EXCELLENCE (MSCOE)

LATVIAN SIMULATION CENTER – RIGA TECHNICAL UNIVERSITY

LOGISIM

LSIS – LABORATOIRE DES SCIENCES DE L'INFORMATION ET DES SYSTÉMES

MIMOS – MOVIMENTO ITALIANO MODELLAZIONE E SIMULAZIONE

MITIM PERUGIA CENTER – UNIVERSITY OF PERUGIA

BRASILIAN SIMULATION CENTER, LAMCE-COPPE-UFRJ

MITIM - MCLEOD INSTITUTE OF TECHNOLOGY AND INTEROPERABLE MODELING AND SIMULATION – GENOA CENTER

M&SNET - MCLEOD MODELING AND SIMULATION NETWORK

LATVIAN SIMULATION SOCIETY

ECOLE SUPÉRIEURE D'INGÉNIERIE EN SCIENCES APPLIQUÉES

FACULTAD DE CIENCIAS EXACTAS. INGEGNERIA Y AGRIMENSURA

UNIVERSITY OF LA LAGUNA

CIFASIS: CONICET-UNR-UPCAM

INSTICC - INSTITUTE FOR SYSTEMS AND TECHNOLOGIES OF INFORMATION, CONTROL AND COMMUNICATION

NATIONAL RUSSIAN SIMULATION SOCIETY

CEA - IFAC

UNIVERSITY OF BORDEAUX

UNIVERSITY OF CYPRUS

I3M 2015 INDUSTRIAL SPONSORS

CAL-TEK SRL

LIOTECH LTD

MAST SRL

SIM-4-FUTURE

I3M 2015 MEDIA PARTNERS

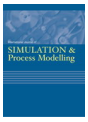

INDERSCIENCE PUBLISHERS – INTERNATIONAL JOURNAL OF SIMULATION AND PROCESS MODELING

INDERSCIENCE PUBLISHERS – INTERNATIONAL JOURNAL OF CRITICAL INFRASTRUCTURES

INDERSCIENCE PUBLISHERS – INTERNATIONAL JOURNAL OF ENGINEERING SYSTEMS MODELLING AND SIMULATION

INDERSCIENCE PUBLISHERS – INTERNATIONAL JOURNAL OF SERVICE AND COMPUTING ORIENTED MANUFACTURING

IGI GLOBAL – INTERNATIONAL JOURNAL OF PRIVACY AND HEALTH INFORMATION MANAGEMENT

HALLDALE MEDIA GROUP: MILITARY SIMULATION AND TRAINING MAGAZINE

HALLDALE MEDIA GROUP: THE JOURNAL FOR HEALTHCARE EDUCATION, SIMULATION AND TRAINING

SAGE
SIMULATION TRANSACTION OF SCS

EUROMERCI

DE GRUYTER

DE GRUYTER
INTERNATIONAL JOURNAL OF FOOD ENGINEERING

EDITORS

AGOSTINO BRUZZONE
MITIM-DIME, UNIVERSITY OF GENOA, ITALY
agostino@itim.unige.it

MARCO FRASCIO
UNIVERSITY OF GENOA, ITALY
mfrascio@unige.it

FRANCESCO LONGO
DIMEG, UNIVERSITY OF CALABRIA, ITALY
f.longo@unical.it

YURI MERKURYEV
RIGA TECHNICAL UNIVERSITY, LATVIA
merkur@itl.rtu.lv

VERA NOVAK
BETH ISRAEL DEACONESS MEDICAL CENTER, HARVARD MEDICAL SCHOOL, USA
vnovak@bidmc.harvard.edu

JERZY W. ROZENBLIT
UNIVERSITY OF ARIZONA, USA
jr@ece.arizona.edu

THE INTERNATIONAL MULTIDISCIPLINARY MODELING AND SIMULATION MULTICONFERENCE, I3M 2015

GENERAL CO-CHAIRS

AGOSTINO BRUZZONE, *MITIM DIME, UNIVERSITY OF GENOA, ITALY*
YURI MERKURYEV, *RIGA TECHNICAL UNIVERSITY, LATVIA*

PROGRAM CO-CHAIRS

FRANCESCO LONGO, *DIMEG, UNIVERSITY OF CALABRIA, ITALY*
EMILIO JIMÉNEZ, *UNIVERSITY OF LA RIOJA, SPAIN*

THE 4TH INTERNATIONAL WORKSHOP ON INNOVATIVE SIMULATION FOR HEALTH CARE, IWISH 2015

GENERAL CO-CHAIRS

VERA NOVAK, *BETH ISRAEL DEACONESS MEDICAL CENTER, HARVARD MEDICAL SCHOOL, USA*
JERZY W. ROZENBLIT, *UNIVERSITY OF ARIZONA, USA*

PROGRAM CHAIR

MARCO FRASCIO, *UNIVERSITY OF GENOA, ITALY*

IWISH 2015 International Program Committee

Maja Atanasijevic-Kunc, *University of Ljubljana, Slovenia*
Werner Backfrieder, *University of Applied Sciences, Upper Austria*
Jerry Batzel, *University of Graz, Austria*
Felix Breitenecker, *TU Vienna, Austria*
Eva Bruballa, *Escuelas Universitarias Gimbernat, Spain*
Agostino Bruzzone, *University of Genoa, Italy*
Eduardo Cabrera, *Universidad autonoma de Barcelona, Spain*
Gianluca De Leo, *Old Dominium University, USA*
Lucio Tommaso De Paolis, *University of Salento, Italy*
Rafael Diaz, VMASC Virginia Modeling, Analysis and Simulation Center, Virginia, *Usa*
Gottfried Endel, *Association of Austrian Social Security, Austria*
Gionata Fragomeni, *University Magna Graecia, Italy*
Marco Frascio, University of Genoa, Italy
Nandu Goswami, *Medical University of Graz, Austria*
Amir Hussain, *University of Stirling, Scotland, UK*
Witold Jacak, Upper Austria UAS, Austria
Franz Kappel, *University of Graz, Austria*
Rihard Karba, *University of Ljubljana, Slovenia*
Korina Katsaliaki, *International Hellenic University, Greece*
Helmut Lackner, *Medical University of Graz, Austria*
Zhengchun Liu, *Universidad Autonoma de Barcelona, Spain*
Francesco Longo, *University of Calabria, Italy*
Marina Massei, *University of Genoa, Italy*
Navail Mustafee, *University of Exeter, UK*
Muaz Niazi, Bahria *University of Islamabad, Pakistan*
Letizia Nicoletti, *Cal-Tek Srl, Italy*
Vera Novak, *Harvard Medical School, USA*
Mette Olufsen, *North Carolina State University, USA*
Johhny Ottesen, *Roskilde University, Denmark*
Stephan Onggo, *University of Lancaster, UK*
Niki Popper, *DWH Simulation Services Vienna, Austria*
Paolo Proietti, *Mimos, Italy*
Joseph Rosen, *Thayer School of Engineering at Darmouth, USA*
Jerzy Rozenblit, University of Arizona, USA
Gudrin Schappacher-Tilp, *University of Graz, Austria*
Manel Taboada, *Escuelas Universitarias Gimbernat, Spain*
Hien Tran, *North Carolina State University, Usa*
Alberto Tremori, *NATO STO CMRE, Italy*
Gerald Zwettler, *Upper Univ. of Applied Science, Austria*

Tracks and Workshop Chairs

Application of Simulation for Healthcare Supply Chains
Chairs: Navonil Mustafee, University of Exeter, UK; Korina Katsaliaki, International Hellenic University, Greece

Healthcare and Public Health M&S
Chairs: Rafael Diaz, VMASC Virginia Modeling, Analysis and Simulation Center, USA; Eduardo Cabrera, Universidad Autonoma de Barcelona, Spain

Modeling and Simulation for Cognitive Computation
Chairs: Muaz Niazi,Bahria University, Pakistan; Amir Hussain University of Stirling, UK

Studying Biomechanical Problems for Cardiothoracic and Cardiovascular Clinical Problems: Models, Designing Tools, Simulation Environments and Critical Condition Prediction for Surgical Interventions.
Chair: Gionata Fragomeni, University Magna Graecia, Italy

Patient Specific Modeling of the Cardiovascular-Respiratory System: Interdisciplinary Approaches to Theory and Practice
Chairs: Jerry Batzel, University of Graz, Austria; Nandu Goswami, Medical University of Graz, Austria; Mette Olufsen, North Carolina State University, USA

Mathematical Modeling and Health Technology Assessment
Chairs: Niki Popper, dwh Simulation Services Vienna, Austria; Felix Breitenecker, Vienna Univ. of technology, Austria; Gottfried Endel, Main Association of Austrian Social Security Institutions, Austria

Modelling and Simulation in Physiology and Medicine (common track IWISH-EMSS)
Chairs: Maja Atanasijevic-Kunc, Univ. Ljubljana, Slovenia; Felix Breitenecker, Vienna Uiv. of Technology, Austria

Simulation and Modeling in Computer Aided Therapy
Chairs: Werner Backfrieder, University of Applied Sciences, Upper Austria; Witold Jacak, University of Applied Sciences, Upper Austria

CHAIRS' MESSAGE

On behalf of the Organization Committee of the International Workshop on Innovative Simulation for Healthcare (I-WISH 2015) we are pleased to welcome all the delegates.

Starting from 2012, I-WISH mission is to stimulate discussion on new methods and topics in the emerging field of healthcare bringing together scientists from medicine, engineering, natural and life sciences. Thanks to the excellent work of authors and Program Committee members, I-WISH offers an extensive as well as comprehensive view of novel simulation-based approaches and methods but not only. Indeed, the conference program holds original scientific contributions that provide meaningful results and applications dealing with the complexity and the huge diversity of healthcare.

As in previous years, I-WISH provides an excellent forum to discuss and get acquainted with the latest developments and early achievements in terms of models, approaches and technologies giving an important opportunity of networking and interaction on challenging multidisciplinary problems.

In addition to the scientific program, social events will be a good chance for people to meet and establish fruitful relations while enjoying the warm Italian hospitality.

The conference venue is Bergeggi, a nice town located in Italy on the Italian Riviera, which offers the perfect backdrop for meeting both new and old acquaintances and share researches and practices with colleagues.

Finally we would like to convey our best wishes to the participants for a very productive and rewarding event, as well as to the visitors for a most enjoyable stay in Italy.

Vera Novak
Harvard Medical School, USA

Marco Frascio
University of Genoa
Italy

ACKNOWLEDGEMENTS

The IWISH 2015 International Program Committee (IPC) has selected the papers for the Conference among many submissions; therefore, based on this effort, a very successful event is expected. The IWISH 2015 IPC would like to thank all the authors as well as the reviewers for their invaluable work.
A special thank goes to all the organizations, institutions and societies that have supported and technically sponsored the event.

I3M 2015 INTERNAL STAFF

AGOSTINO G. BRUZZONE, *DIME, UNIVERSITY OF GENOA, ITALY*
MATTEO AGRESTA, *SIMULATION TEAM, ITALY*
TERESA BARBIERI, *CAL-TEK SRL, ITALY*
CHRISTIAN BARTOLUCCI, *SIMULATION TEAM, ITALY*
LUIGI BRUNO, *DIMEG, UNIVERSITY OF CALABRIA*
ALESSANDRO CHIURCO, *DIMEG, UNIVERSITY OF CALABRIA, ITALY*
MARIO COSENTINI, *CAL-TEK SRL, ITALY*
RICCARDO DI MATTEO, *SIMULATION TEAM, ITALY*
CATERINA FUSTO, *DIMEG, UNIVERSITY OF CALABRIA, ITALY*
FRANCESCO LONGO, *DIMEG, UNIVERSITY OF CALABRIA, ITALY*
GIANLUCA MAGLIONE, *CAL-TEK SRL*, ITALY
MARINA MASSEI, *LIOPHANT SIMULATION, ITALY*
LETIZIA NICOLETTI, *CAL-TEK SRL*
ANTONIO PADOVANO, *DIMEG, UNIVERSITY OF CALABRIA, ITALY*
ALBERTO TREMORI, *SIMULATION TEAM, ITALY*
MARCO VETRANO, *CAL-TEK SRL, ITALY*

This International Workshop is part of the I3M Multiconference: the Congress leading **Simulation around the World and Along the Years**

Index

TOWARDS A HYBRID VIRTUAL/PHYSICAL NUSS PROCEDURE SURGICAL SIMULATOR

Mohammad F. Obeid[(a)], Eun-sil Heo[(b)], Krzysztof J. Rechowicz[(c)], Robert E. Kelly[(d)], Frederic D. McKenzie[(e)]

[(a),(b),(e)]Dept. of Modeling, Simulation and Visualization Engineering
Old Dominion University Norfolk, USA
[(c)]Virginia Modeling, Analysis and Simulation Center
Old Dominion University Norfolk, USA
[(d)]Pediatric Surgery, Children's Hospital of The King's Daughters and Eastern Virginia Medical School, Norfolk, USA

[(a)]mobei001@odu.edu, [(b)]eheox002@odu.edu, [(c)]krechowi@odu.edu, [(d)]robert.kelly@chkd.org, [(e)]rdmckenz@odu.edu

ABSTRACT
Surgical simulation is embraced by many for training and skill transfer purposes of non-trivial minimally invasive procedures. Some systems utilize haptic feedback within an anatomically-correct virtual environment whereas others use manikins, synthetic components and box trainers. This paper explores the challenges and implications of reproducing the Nuss procedure on both a solely-virtual and a solely-physical environment. This work then describes a roadmap for a hybrid system that employs a best-of-both approach integrating both physical and virtual schemes to achieve a mixed reality implementation of the primary steps of the Nuss procedure.

Keywords: surgery simulator, mixed reality, hybrid simulation, Nuss procedure

1. INTRODUCTION

Over the past two decades, minimally invasive procedures (MIP) have influenced the popularity of conventional approaches with regards to scarring, recovery times and pain medication aspects. It is often argued, however, that such procedures pose a prolonged learning curve for most novice surgeons. Preoperative training and proper surgical planning can alleviate such limitations. In the early stages, such planning existed in the form of collaboration between radiologists and surgeons using three-dimensional representations of organs and body components constructed from MRI and/or CT images for preoperative planning such as for colonoscopy (Vining 1997) and craniofacial surgery (Altobelli, Kikinis et al. 1993). In principle, high fidelity surgical simulators can be employed for surgical training and education and proved to be an advantageous part of a teaching curricula (Satava 2001).

Today, a number of commercially available and under development simulators exist for most common endoscopic, laparoscopic, and, in general, minimally invasive procedures. SimSurgery's Educational Platform for laparoscopic procedures (SimSurgery 2015), Simbionix's numerous mentors for laparoscopic, endoscopic, arthroscopic, endovascular and other procedures (Simbionix 2015), SurgicalScience's procedural simulation systems for cholecystectomy, appendectomy, suturing and anastomosis (Surgical Science 2015), and Mentice's Minimally Invasive Surgical Trainer (MIST) (Mentice 2015), are all examples of such simulation systems.

Others are developing simulation and training systems in medical robotics. Among those are projects that aim for skill transfer and training for operating the da Vinci surgical robot. Although Mimic's dV-Trainer (Mimic 2015) is a pioneer in this area, Simulate Surgical Systems' RoSS (Simulated Surgical Systems 2015) and Simbionix's Robotix Mentor (Simbionix 2015) are not far behind.

According to Milgram and Kishino (Milgram and Kishino 1994), the conventional view of a *virtual reality* (VR) environment is one where the user views, and interacts with, a completely synthetic world that consists of virtual objects. On the other extreme of the virtuality continuum, a *real environment* is one that consists solely of real objects. A display system that falls somewhere between the two and involves a merge of real and virtual worlds is referred to as *mixed reality* (MR). This concept of mixed reality is carried on in this work and will be used with the term *hybrid* interchangeably.

Many of the aforementioned surgical simulators use physical components when simulating external behaviors such as a tool insertion process, whereas others utilize haptic feedback. A simulator that integrates a physical component representing an anatomically correct part of the body (a manikin) with a virtual environment displayed on a monitor is referred to, in this work, as a *hybrid simulator*. This definition of a hybrid excludes simulators that use physical ports mounted on arbitrary objects like a box or hemisphere and focuses on those that use an anatomical manikin.

Pectus Excavatum (PE) is a congenital chest wall deformity that affects children and young adults exhibiting a sunken or funnel anterior chest wall (Huddleston 2004). In the Nuss Procedure, two small incisions are made on either sides of the chest to insert a pre-bent steel bar from the side of the chest to be placed and secured beneath the funneled area to elevate and support the sternum pushing out the sunken part of the ribcage. The surgeon uses a thoracoscope to monitor the procedure internally in addition to the external view of the patient's torso (Nuss and Kelly 2008).

The need to, pre-operatively, enhance surgical skills of trainees as well as alleviate risks of complications during surgery drove the development of a surgical simulator. The Nuss Procedure Surgical Simulator (NPSS), (Rechowicz, Obeid et al. 2014; Rechowicz, Obeid and McKenzie 2014), utilizes patient-specific data to create a computer generated virtual model of the patient and the deformity and allows the user to interact with the environment through a haptic interface. Simultaneously, an anatomically correct manikin was developed combining 3D-printed components with synthetic materials to create a physical simulator for the procedure. This work aims to compare the two implementations against relevant criteria derived from the nature of the surgery to identify potentials and weaknesses of each setup in order to pave the road for a hybrid model that combines the best of both.

2. RELATED WORK AND STATE OF THE ART

Relating to Milgram and Kishino's virtuality continuum model but in a more related context, ASERNIP-S's systematic review describes, among others, three types of surgical simulators: virtual reality (VR), physical, and hybrid (Sturm, Windsor et al. 2007).

2.1. Virtual Reality (VR) Simulators

In virtual reality surgical simulators, computer generated instruments are used to manipulate computer generated objects in a virtual environment through specially designed interfaces. A high-fidelity simulator of this type is usually expensive but provides objective performance measurements, error tracking and tactile (haptic) feedback.

Peterisk et. al. worked on reproducing haptic volume interactions for bone surgery simulations. Recently, VOXEL-MAN commercialized their fully-virtual Tempo and Dental simulators for training surgical access to the structures of the middle ear, and for training on dental procedures, respectively (Petersik, Pflesser et al. 2002; Voxel-Man 2015). A similar all-virtual surgical simulator was developed by Choi *et al.* for the phacoemulsification procedures of the cataract surgery (Choi, Soo and Chung 2009). Heng et. al. built a tailored force feedback device that compensates for all related forces within the surgical simulation for arthroscopic surgery (Heng, Cheng et al. 2004).

Many others have developed and commercialized VR simulators for endoscopic procedural tasks such as camera navigation, instrument manipulation, perceptual-motor skills coordination, grasping, cutting, clipping, dissection, and suturing. SimSurgery's Education Platform (SimSurgery 2015), Surgical Science's LapSim (Surgical Science 2015), Simbionix's LapMentor (Simbionix 2015), and CAE Healthcare's LapVR (CAE Healthcare 2015) are such products for laparoscopic surgery. For other endoscopic procedures, Surgical Science's EndoSim (Surgical Science 2015), Simbionix's Bronch Mentor (Simbionix 2015), and CAE Healthcare's EndoVR (CAE Healthcare 2015) are available.

2.2. Physical Simulators

Physical (synthetic) models and box trainers use models of plastic, rubber and latex to render different organs and pathologies (Cisler and Martin 2006). This type is generally used as a low-cost, portable platform for part-task trainers but is limited in aspects such as time required to replace components, level of realism, haptic forces, and lack of inherent metrics of performance.

Delletec provides several synthetic components for simulating various surgical procedures including appendectomy, breast biopsy, laparoscopy, and many others (Delletec 2015). SimuLab offers synthetic and physical models and manikins for numerous open and laparoscopic surgeries as well as box trainer modules. TraumaMan is considered one of their popular systems (SimuLab 2015).

2.3. Hybrid Simulators

Hybrid simulators are a combination of physical simulators and VR simulators, where a physical object (usually a manikin) is linked to a computer program that provides visual images and/or feedback (Satava 2001). The virtual component, i.e., the computer program, produces patient responses and simulation dynamics, whereas the physical component provides the ability to interact with the patient's physical constructs.

Many systems have proven a more practical, realistic and efficient reproduction of surgical procedures when composed of an integration of a physical manikin with a virtual environment. Such a mixed reality implementation was developed by Li *et al.* for arthroscopic knee surgery simulation. In their system, they used an artificial knee joint from Pacific Research Laboratories. As the user manipulates the actual tools and arthroscopic camera used in the surgery, the display shows a synchronized 3D computer generated model of the joint.

Simbionix commercializes Arthro Mentor for arthroscopic training which combines fiberglass/polyurethane anatomical models (shoulder, knee and hip) with 3D images and a haptic interface, allowing the user to operate the actual instruments and the arthroscopic camera (Simbionix 2015). CAE Healthcare provides VirtaMed ArthroS for knee and shoulder arthroscopy training in a mixed reality environment that integrates anatomical rubber models of a knee or shoulder with a corresponding virtual environment, also allowing the user to train on the original surgical tools (CAE Healthcare 2015).

3. METHODS

Simulating a non-laparoscopic (involves instruments other than common laparoscopic graspers, scissors, dissectors and clip-appliers) minimally invasive procedure can be challenging due to the nature of the used surgical tools. Depending on the procedure, a physical constituent can be of great significance to enhance realism aspects. This section describes methods used to construct the fully-virtual NPSS and introduces the under-development fully-physical NPSS. The two schemes are then compared against critical tasks of the Nuss procedure to demonstrate where each setup adds more value.

3.1. Nuss Procedure Tasks

In collaboration with surgeons who frequently perform the Nuss procedure, a task breakdown was performed for the surgery and a (high, medium, or low) evaluation of priority was assigned to all tasks and subtasks of the procedure. This evaluation reflects the importance of each subtask in the training context, i.e., the significance of a correct skill-transfer for that particular subtask. This task analysis was used as an assessment platform for the various constructs of the NPSS. Table 1 shows how each subtask is executed on both the virtual and the physical setting of the NPSS. An initial assessment of each implementation is done by displaying the one that is anticipated to perform more efficiently and satisfactory in bold).

3.2. A Solely Virtual Setup

As thoroughly explained in (Rechowicz, Obeid et al. 2014) and (Chemlal, Rechowicz et al. 2014), a virtual version of the NPSS was developed by integrating a virtual environment with a haptic interface. A generic low polygon model of the patient's torso was adjusted to a skinny posture, a skeletal model based on the Visible Human Project (Ackerman 1998) was used to create the ribcage, the pericardium was modeled based on an anatomical atlas, and generic models of the lungs and the diaphragm were obtained from a 3D models repository. The main tool used in the procedure -the introducer- was modeled using orthogonal photographs. The virtual environment also includes a thoracoscopic camera that follows the surgical tool and shows the real-time dynamics including collisions, deformations and heart beating. As explained in (Rechowicz, Obeid and McKenzie 2014), the patient's model as well as the reproduced PE deforming are formed according to patient-specific data. Table 1 describes how the simulator performs each of the Nuss procedure tasks.

In the actual surgery, since the introducer's movement is limited at the insertion point within the selected intercostal space and by the room of motion inside the body, these constraints can be simulated in the haptic interface by applying corresponding forces that vary depending on the stiffness of the simulated tissue or surrounding organs. The haptic device's forces approximate a virtual pivot (Obeid, Chemlal et al. 2014) constraining the tool from motion in the local x- and y-directions by applying high stiffness forces while allowing translation in the z-direction only for further insertion.

3.3. A Solely Physical Setup

In a prototyped fully-physical version of the simulator, rapid prototyping, 3D printing and form casting techniques are utilized to create a physical manikin simulator of a patient's torso with a PE deformity. The skeletal model from the Visible Human Project (Ackerman 1998) is used to create a 3D model of a deformed ribcage. The ribs are then 3D-printed and mounted on the apparatus along with synthetic skin and muscle and incorporated with casted organs. The synthetic skin and muscle are replaceable to allow for repetitive training. A metal hinge is inserted into the sternum to introduce the PE deformity as an added elastic connector pulls the sternum posteriorly toward the spine. In addition to a small camera mounted on a steel rod for thoracoscopy, the user is able to operate the actual surgical tools including, among others: introducer, Kelly clamp, pectus bar, and bar flipper. Table 1 describes how the simulator performs each of the Nuss procedure tasks.

4. DISCUSSION AND NEW APPROACH

As can be observed in Table 1. Each setup varies in its successful implementation of different aspects of the procedure. In this section, the advantages and disadvantages of each setup will be discussed and a new hypothesized improved setup will be introduced.

4.1. Merits and Limitations

For each of the two setups, some steps of the procedure are better and more accurately reproduced. In this section, the merits, advantages and limitations of each setup will be discussed to shed light on the areas where each setup contributes more in order to define areas of strength for each.

4.1.1. Solely Virtual Simulator

Given the nature of a generic (3-DOF) haptic device's end-effector, no insertion mechanism can be performed without moving the stylus' natural pivot along. Therefore, although the force models for constraining the haptic device's motion and simulating collisions are a successful approximation of the tool's pivoting behavior, a discrepancy is present where the end-effector is always carried along causing the stylus' physical joint to be located, at some instances, at coordinates that correspond to the inside of the patient.

Furthermore, the virtual implementation of the simulator lacks visual cues such as an exterior visualization of intercostal spaces (tasks 2b, 2c, and 3 in Table 1). It is also not, or at least not easily, possible in such setup to utilize the haptic device to operate instruments such as a bar flipper, Kelly clamp, suture needle and umbilical tape (tasks 4 and 10 in Table 1).

In this setup, however, patient-specific modeling is used to create a planning platform where dimensions and parameters describing the patient's torso and deformity

are extracted from CT data to, consequently, tailor the models (task 2a in Table 1). Furthermore, the virtual environment allows for introducing surgical scenarios and complications to the procedure for training aspects. Another benefit from a virtual setup is the ability to accurately reproduce forces with the aid of the haptic device and associated physics-based models.

4.1.2. Solely Physical Simulator

The physical setup clearly adds value to tasks that require the use of surgical instruments where fine movements are expected such as making an incision, creating a suture and securing the stabilizer. The reproduction of the mechanical behavior and pivoting motion of the surgical tools are flawless here as they, the tools, are inserted into the manikin just like they are in the actual surgery. Additionally, not only does the physical setup provide the user with visual cues regarding the external landmarks such as the intercostal spaces, deepest point of depression, and introducer's progress in the subcutaneous tunnel, but also the ability determine their location in a tactile manner.

In a physical setup, however, no real-time dynamics and interactions are present such as the beating heart, fluid emission and the possibility to puncture the pericardial sac by mistake (task 7b in Table 1). Although these can be added with some difficulty and expense, the system is also unable to introduce procedural complications and pre-modeled scenarios to the simulation which makes the training scope and resolution somewhat limited. Furthermore, this setup is not an efficient platform for patient-specific planning as it requires an offline, and a rather long, changeover. Therefore, an average or standardized set of parameters that describe the patient and deformity populations are assumed to suffice.

4.2. A Hybrid Approach

From previous sections, the comparison between the two setups shows how each scheme has merits that the other cannot provide. In this section, a best-of-both approach will be undertaken to describe a design of a hybrid virtual/physical construction for the simulator.

Since the physical setup showed very strong potential for implementing aspects that are relevant to the external visual and tactile cues of the simulator, a 3D-printed ribcage with synthetic skin and muscle will be adopted in the new approach. This will allow for tool insertion, subcutaneous tunneling, popping into and out of the thoracic cavity, as well as making sutures and installing the stabilizer. Implementing this physical component in the hybrid simulator provides the ability to use the original surgical tools and to perform fundamental tasks such as making incisions and using the umbilical tape.

The thoracoscopic view of the patient, however, will convey from the virtual setup. Patient-specific modeling of the patient's PE deformity will be reproduced from a parameterized ribcage system explained in (Rechowicz, Obeid and McKenzie 2014), the organs and tool movement inside the chest will be part of a virtual environment utilizing the haptic interface. However, to overcome the discrepancy introduced by the virtual setup regarding the pivoting motion of the tool, the generic haptic device is augmented with an extension that implements a mechanism to utilize the device's natural pivot, while allowing the tool to be inserted into the physical manikin.

At insertion, the haptic device prevents motion in all directions. As the user attempts to move the tool through the insertion point (in the z-direction), the tool (not the end-effector itself) slides through the developed extension. The tool's translational motion is monitored using a rotary encoder (potentiometer) which controls the surgical tool in the simulation. Upon collision with an organ in the simulation, the mechanism will trigger a rubber wheel to descend vertically pushing onto the tool; thus reproducing force that would hinder the tool's motion. In this implementation, the forces generated upon colliding with the organs and moving inside the chest are calculated according to a physics-based model that studies the force-displacement profile as measured from a constructed phantom. Information regarding the force's behavior over time or versus displacement and velocity is directly obtainable using this phantom.

The mechanism for haptic augmentation has been prototyped using 3D printed components and implemented on the Arduino platform. The methods used for developing this mechanism as well as the constructed phantom for force-displacement measurement are thoroughly explained in (Obeid, Chemlal et al. 2014).

To control the virtual thoracoscope, the user is able to choose between the first mode where the camera constantly follows the tip of the introducer as in the case for the fully-virtual setup, and the second mode where the user is able to control the thoracoscopic camera in real-time using a Wiimote. Since the hybrid setup utilizes a physical manikin, the Wiimote can be attached to a steel rod and inserted in any intercostal space the surgeon decides. The Wiimote’s pitch, roll and yaw motions control the rotation of the virtual camera which is equipped with a 30° tilt as in the real surgery.

The dynamics involved in the simulated surgery will convey from the virtual setup. Physics-based interactions were modeled to deliver realistic behavior of the pericardium. To simulate the beating heart, a non-uniform scaling deformation of the pericardial sac was constructed to reproduce systole and diastole motions. The amount and shape of PE depression can be adjusted according to patient-specific data and the pericardial sac is pushed laterally to the left as severity increases. Additionally, a framework is implemented for puncturing detection to trigger blood or pericardial fluid emission, depending on puncturing depth.

Table 1: A comparison in implementation for the virtual and physical surgical simulators against the Nuss Procedure tasks. Training significance for each subtask is identified and the corresponding more efficient setup is marked in bold.

#	Task Description	Subtasks "*High (H), Medium (M), Low (L) significance for training*"	Virtual Simulator Approach	Physical Simulator Approach
1	Positioning patient appropriately	a. Patient placed in supine position with back against operating table. "*M*"	**Patient's avatar is positioned supine with arms spread and right side facing user.**	**Manikin is mounted down in correct position. Surgical drapes provided to simulate actual operation.**
		b. Patient's arms are spread. "*M*"		
2	Visualizing external landmarks:	a. Deepest part of sternum. "*M*"	**PE deformity is reproduced by affecting sternum, associated costal cartilage and external skin of patient's avatar with a deformation model with a falloff according to parameters collected from CT data.**	PE deformity created with a physical elastic force attached to xiphoid process. Elastic force holding the bottom half of the sternum may be pulled up to show a corrected chest.
		b. Intercostal spaces. "*M*"	Deepest depression can be visualized. However, tactile determination of landmarks is absent and intercostal spaces are not visible externally. AAL and MAL can only be approximated.	**Exterior landmarks can be located by visualizing and feeling through synthetic skin on 3D-printed ribcage. AAL and MAL can be approximated.**
		c. Anterior axillary line (AAL) and mid axillary line (MAL). "*M*"		
3	Visualizing and marking necessary incision areas:	a. Deepest point of sternum. "*M*"	**User interface is incorporated with marking tool to mark skin externally using haptic device (not implemented). Intercostal spaces not visible externally.**	**Synthetic skin may be marked with a marker. Intercostal spaces can be assigned externally.**
		b. Intercostal spaces horizontal to deepest point of sternum. "*M*"		
		c. Entry and exit sites outside pectoralis muscle. "*M*"		
4	Preparing bar	a. Measure patient's chest according to landmark indicated in 2c. "*M*"	**The bar can be bent to fit patient specific data and incorporated in the UI (not implemented).**	The bar is already bent to fit the ribcage of the manikin. Verbal and visual instructions are necessary.
		b. Determine length of the bar (Bar should be 1 inch shorter than measurement). "*M*"		
		c. Shape bar using bending device.		
		d. Check final shape with patient's chest. "*M*"		
		e. Mark each end of bar (incision areas). "*M*"		
5	Thoracoscopy	a. Incision made for thoracoscope. "*H*"	a. Incision for thoracoscope is assumed to already exist.	**a. Incision can be made on replaceable synthetic skin.**
		b. Inspect deepest part of sternum internally. "*M*"	b. Camera is available to visualize interior of virtual chest and semi-translucent thoracic cavity.	**b. A camera is mounted on a long steel rod and can be inserted to visualize interior of chest.**
		c. Surgeon's assistant guides thoracoscope, focusing on tip of introducer. "*M*"	c. Virtual camera follows the introducer's tip at all times according to haptic device's motion. A 30° angle is incorporated.	**c. Assistant can maneuver the camera for the best view.**
6	Subcutaneous tunnel	a. Small incisions are made on right entry site marked in task 3. "*H*"	a. Incisions can be made (not implemented).	**a. Incisions can be made on the synthetic skin as it is replaceable.**
		b. Using tonsil or Kelly clamp or finger, make a pocket subcutaneously outside of pectoralis muscle. "*H*"	b. Subcutaneous tunneling is achievable by eliminating force feedback in plane between skin and muscle. Approximated with friction. (not implemented)	**b. Necessary tools are available. An extra layer of synthetic muscle is present beneath the synthetic skin, allowing separation between them.**
		c. Introducer is used to puncture the pectoralis muscle through the intercostal muscle. "*H*"	**c. Virtual muscle can be punctured (not implemented).**	c. Synthetic muscle can be punctured as it is replaceable.

7	Substernal tunnel	a. With aid of thoracoscope, guide introducer under sternum avoiding puncturing heart. "*M*"	a. The camera follows tip of introducer. Targeted areas can be viewed by aiming introducer towards them.	**a. Maneuver camera to visualize targeted area. Synthetic organs in sight.**
		b. Determine correct tunneling plane by putting small force brushing downwards with introducer on undersurface of sternum. Separation of tissue indicates safe spot to proceed. "*H*"	**b. Pericardial sac can be seen beating in view, a thin layer can be identified between the pericardial sac and the sternum.**	b. Tunneling plane can be determined between synthetic pericardial sac and sternum. Tissue separation is observed.
		c. Gently dissect off the pleura and pericardium under the sternum with the guide of thoracoscope. "*H*"	**c. User is able to pry along defined plane to dissect tissue and make pathway while heart is beating (implemented but slow).**	c. Brushing motion may be performed similar to surgery.
		d. When tunneling is achieved, puncture through exit site, examining externally. "*H*"	**d. Puncturing can be done to exit from other side with associated force feedback (not implemented).**	**d. Puncturing is done through the other side of the synthetic muscle.**
		e. Pull tip of introducer out through established left incision site. "*M*"	e. Will require moving the external camera to left side and making another incision (not implemented).	**e. Introducer tip can be pulled from left incision.**
8	Sternal elevation	a. Once introducer is through both incision sites, lift introducer up holding from both sides for 10-15 seconds for three times to mold the chest. "*M*"	a. Sternal elevation can be achieved by moving the end-effector of the haptic device (not implemented).	**a. Introducer can be lifted for the required duration elevating the sternum.**
		b. Link an umbilical tape to tip of introducer, pull through chest while introducer is slowly withdrawn from the chest with end of the string still remaining on left. "*M*"	b. Tying an umbilical tape to the introducer and pulling it inwards can be very difficult to implement (not implemented).	**b. An umbilical tape can be linked to the introducer.**
9	Bar insertion and rotation	a. Link umbilical tape to bar prepared in task 2. "*M*"	Tying an umbilical tape to the bar and pulling it inwards can be very difficult to implement (not implemented).	**The bar can be inserted into the simulator in a similar manner as in the surgery and the provided camera can be used for monitoring the process.** **A Bar Flipper is provided to flip the bar.**
		b. Insert prepared bar into right incision site upside down through subcutaneous tunnel. "*M*"		
		c. With guide of umbilical tape, introduce bar through under-sternal chest cavity. "*M*"	User can change the held instrument into a pectus bar and insert it into chest using haptic device's end-effector (not implemented).	
		d. Use finger in the left subcutaneous tunnel to guide tip of bar. "*M*"		
		e. Without displacing bar, use Bar Flipper to rotate bar clockwise or counter-clockwise. "*H*"	User can change held instrument into a Bar Flipper to rotate the bar (not implemented).	
		f. Ensure that patient's chest looks corrected. "*M*"		
10	Bar fixation	a. Place stabilizer in the space in left subcutaneous tunnel. "*M*"	Stabilizer fixation, suturing and stitching is difficult to achieve on a virtual setup (not implemented).	**3D-printed ribs can be used for stabilization and can be replaced when necessary. User can visualize corrected pectus interior and exterior of the chest using the provided camera.**
		b. Fix stabilizer and bar using a fiber wire. "*M*"		
		c. Ensure thoracoscope is used to assess the bar's current location. "*M*"		

The hybrid setup of the simulator is, therefore, able to combine the merits of having a physical external manikin that allows for realistic tactile assessment of the torso and the use of actual surgical tools with the power of a virtual environment that integrates an interactive and realistic patient-specific model of the patient's torso and deformation with the ability to generate accurate haptic force feedback. Complications and educational scenarios can be introduced to this setup to enhance training aspects.

5. CONCLUSION

Realistic simulation of a full surgical procedure is not a feasible goal with current technology. A more dominantly practical approach is to follow a task breakdown procedure of the surgery to identify the most relevant aspect to be included in the simulation. This paper presented this task breakdown for the Nuss procedure and, based on experts' opinion, identified the significance of each task.

This paper then compared a fully-virtual platform for simulating the procedure that utilizes a virtual environment setup integrated with a haptic interface, to a fully-physical manikin-based platform for the simulation that uses a 3D-printed ribcage and synthetic body components. The comparison resulted with an identification of the areas where each setup is more powerful and allowed for a preliminary structure of a hybrid virtual/physical Nuss procedure surgical simulator.

Following this work, the hybrid simulator will be put to evaluation and assessment by surgical experts and feedback will be reported in a validation study.

ACKNOWLEDGMENTS

This work was made possible by members of Children's Surgical Specialty Group and Children's Hospital of The King's Daughters, the authors would like to thank them for their generous support.

REFERENCES

Ackerman, M. J., 1998. The Visible Human Project. Proceedings of the IEEE. 86 (3): 504-511.

Altobelli, D. E., R. Kikinis, J. B. Mulliken, H. Cline, W. Lorensen and F. Jolesz, 1993. Computer-assisted three-dimensional planning in craniofacial surgery. Plastic and Reconstructive Surgery. 92 (4): 576-585.

CAE Healthcare, 2015. EndoVR. Available from: http://caehealthcare.com/eng/interventional-simulators/endovr [Accessed 04 April 2015].

CAE Healthcare, 2015. LapVR. Available from: http://caehealthcare.com/eng/interventional-simulators/lapvr [Accessed 04 April 2015].

CAE Healthcare, 2015. VirtaMed ArthroS. Available from: http://caehealthcare.com/eng/interventional-simulators/virtamed-arthros [Accessed 04 April 2015].

Chemlal, S., K. J. Rechowicz, M. F. Obeid, R. E. Kelly and F. D. Mckenzie, 2014. Developing Clinically Relevant Aspects of the Nuss Procedure Surgical Simulator. In: J. D. Westwood, S. W. Westwood, L. Felländer-Tsai et al., eds. Medicine Meets Virtual Reality 21. Amsterdam, The Netherlands: IOS Press, 51-55.

Choi, K.-S., S. Soo and F.-L. Chung, 2009. A virtual training simulator for learning cataract surgery with phacoemulsification. Computers in Biology and Medicine. 39 (11): 1020-1031.

Cisler, J. J. and J. A. Martin, 2006. Logistical considerations for endoscopy simulators. Gastrointestinal endoscopy clinics of North America. 16 (3): 565-575.

Delletec, 2015. Surgical Simulators. Available from: http://www.delletec.com/surgical_sims.htm [Accessed 04 April 2015].

Heng, P.-A., C.-Y. Cheng, T.-T. Wong, Y. Xu, Y.-P. Chui, K.-M. Chan and S.-K. Tso, 2004. A virtual-reality training system for knee arthroscopic surgery. IEEE Transactions on Information Technology in Biomedicine. 8 (2): 217 - 227.

Huddleston, C. B., 2004. Pectus Excavatum. Seminars in Thoracic and Cardiovascular Surgery. 16: 225–232.

Mentice, 2015. Our Simulators. Available from: http://www.mentice.com/our-simulators [Accessed 04 April 2015].

Milgram, P. and F. Kishino, 1994. A taxonomy of mixed reality visual displays. IEICE Transactions on Information Systems. E77-D (12)

Mimic, 2015. dV-Trainer. Available from: http://www.mimicsimulation.com/products/dv-trainer [Accessed 04 April 2015].

Nuss, D. and R. E. Kelly, 2008. Minimally invasive surgical correction of chest wall deformities in children (Nuss procedure). Advances in Pediatrics. 55: 395-410.

Obeid, M. F., S. Chemlal, K. J. Rechowicz, E.-s. Heo, R. E. Kelly and F. D. McKenzie, 2014. Improvement of a virtual pivot for minimally invasive surgery simulators using haptic augmentation. In: C. A. Linte, Z. Yaniv, P. Fallavollita et al., eds. Augmented Environments for Computer-Assisted Interventions. Cham, Switzerland: Springer International Publishing, 70-79.

Petersik, A., B. Pflesser, U. Tiede, K. H. Hhne and R. Leuwer, 2002. Realistic haptic volume interaction for petrous bone surgery simulation. In: H. U. Lemke, K. Inamura, K. Doi et al., eds. CARS 2002 Computer Assisted Radiology and Surgery. Berlin, Germany: Springer Berlin Heidelberg, 252-257.

Rechowicz, K. J., M. F. Obeid, S. Chemlal and F. D. McKenzie, 2014. Simulation of the critical steps of the Nuss procedure. Computer Methods in Biomechanics and Biomedical Engineering: Imaging & Visualization. 2: 1-15.

Rechowicz, K. J., M. F. Obeid and F. D. McKenzie, 2014. Patient specific modeling of pectus excavatum for the Nuss procedure simulation. In: J. M. R. S. Tavares, X. Luo and S. Li, eds. Bio-Imaging and Visualization for Patient-Customized Simulations. Cham, Switzerland: Springer International Publishing, 113-125.

Satava, R. M., 2001. Accomplishments and challenges of surgical simulation. Surgical endoscopy. 15 (3): 232-241.

Satava, R. M., 2001. Surgical education and surgical simulation. World Journal of Surgery. 25 (11): 1484-1489.

Simbionix, 2015. Arthro Mentor Available from: http://simbionix.com/simulators/arthro-mentor [Accessed 04 April 2015].

Simbionix, 2015. Bronch Mentor. Available from: http://simbionix.com/simulators/bronch-mentor [Accessed 04 April 2015].
Simbionix, 2015. Robotix Mentor. Available from: http://simbionix.com/simulators/robotix-mentor [Accessed 04 April 2015].
Simbionix, 2015. Simbionix Simulators. Available from: http://simbionix.com/simulators [Accessed 04 April 2015].
SimSurgery, 2015. SimSurgery SEP Products. Available from: http://www.simsurgery.com/sep-products.html [Accessed 04 April 2015].
SimuLab, 2015. Products: Surgery. Available from: http://www.simulab.com/products/surgery [Accessed 04 April 2015].
Simulated Surgical Systems, 2015. What is RoSS? Available from: http://www.simulatedsurgicals.com/what-is-ross.htm [Accessed 04 April 2015].
Sturm, L., J. Windsor, P. Cregan, P. Hewett, P. Cosman and G. Maddern, 2007. Surgical simulation for training: Skills transfer to the operating room ASERNIP-S Report No. 61.
Surgical Science, 2015. EndoSim. Available from: http://www.surgical-science.com/endosim-endoscopy-simulator [Accessed 04 April 2015].
Surgical Science, 2015. LapSim. Available from: http://www.surgical-science.com/lapsim-the-proven-training-system [Accessed 04 April 2015].
Surgical Science, 2015. Surgical Science Products. Available from: http://www.surgical-science.com/products [Accessed 04 April 2015].
Vining, D. J., 1997. Virtual colonoscopy. Gastrointestinal Endoscopy Clinics of North America. 7 (2): 285-291.
Voxel-Man, 2015. VOXEL-MAN Surgical Simulators. Available from: http://www.voxel-man.com [Accessed 04 April 2015].

AUTHORS BIOGRAPHY

Mohammad F. Obeid is a Ph.D. student and graduate Teaching/Research Assistant at the Modeling, Simulation and Visualization Engineering (MSVE) Department at Old Dominion University in Norfolk, Virginia. He received his BS degree in Industrial Engineering from the German-Jordanian University in Amman, Jordan in 2011; and his MS degree in Modeling and Simulation Engineering from Old Dominion University in Norfolk, Virginia in 2013. Currently, he is involved with research projects in virtual/augmented reality applications for simulated, surgical and computer assisted interventions. His research interests include medical modeling and simulation, surgery simulation, biomedical engineering and virtual environments.

Eun-sil (Helen) Heo was born in Busan, Korea. Ms. Heo received her B.S. in Mechanical Engineering and M.E. in Modeling and Simulation, both from Old Dominion University (ODU) in Norfolk, Virginia USA. She was a Graduate Research Assistant in the Modeling, Simulation and Visualization Engineering (MSVE) Department at ODU. After graduation in 2015, she joined Children's Surgical Specialty Group-Orthopedic Surgery and Sports Medicine/ Plastic Surgery at Children's Hospital of The King's Daughter as a Clinical Research Associate.

Krzysztof Rechowicz is a Research Assistant Professor at the Virginia Modeling, Analysis and Simulation Center of Old Dominion University. He also serves as a researcher and university representative at the Commonwealth Center for Advanced Manufacturing. He previously served as a Postdoctoral Research Associate at Old Dominion University from 2012 to 2014. In 2006, Dr. Rechowicz received his M.Eng. jointly with his B.Eng. in Mechanics and Machine Construction from the Warsaw University of Technology. He went on to receive his Ph.D. in Engineering with a Concentration in Modeling and Simulation from the Old Dominion University in 2012. Dr. Rechowicz's research interests center on applications of virtual and augmented reality, visualization and adequate user interfaces to medicine and manufacturing. Some of his past projects include the development of a haptically-enabled virtual surgical simulator and planner for a minimally surgical procedure that repairs a congenital chest wall deformity. Furthermore, he designed a surgical tool for removing chest implants without the need of larger skin openings. He has also applied his research experience to solve real world problems of the manufacturing industry, and his work has been sponsored by companies like Rolls-Royce, Sandvik and Newport News Shipbuilding. He has worked on the development of a flexible augmented reality system for integrating digital design and process information with a worker's physical environment for feedback and control of manufacturing processes with special emphasis on user's safety and user interface. He also provided visualization for special manufacturing processes which allowed to better understand influence of process variables on its outcome.

Dr. Robert E. Kelly, Jr., M.D. received his medical degree from The Johns Hopkins University in 1985. He completed his General Surgery Residency at Vanderbilt University School of Medicine and his Pediatric Surgery Fellowship at Children's Hospital of Buffalo. Dr. Kelly also completed an ECMO and Surgical Research Fellowship at UCLA School of Medicine. In 1994, Dr. Kelly joined Children's Surgical Specialty Group-Pediatric Surgery and has been the Chairman of the Department of Surgery at Children's Hospital of The King's Daughters since 1998. He is also a Professor of Clinical Surgery and Pediatrics in the Department of Surgery at Eastern Virginia Medical School. Dr. Kelly lives in Norfolk, Virginia with his wife, Dr. Cynthia Kelly, and their three children.

Frederic (Rick) D. McKenzie, Ph.D. was born in Kingston, Jamaica. Dr. McKenzie has a B.S. in engineering, M.S. in computer engineering, and a Ph.D. in computer engineering all from the University of Central Florida in Orlando, Florida U.S.A. Currently, he is the Department Chair in the new Modeling, Simulation and Visualization Engineering (MSVE) Dept. and a joint faculty member in the Department of Electrical and Computer Engineering (ECE) at Old Dominion University in Norfolk, Virginia U.S.A. In addition, Dr. McKenzie is the director of the Medical Imaging, Diagnosis, and Analysis (MIDA) Laboratory, Adjunct Associate Professor of Eastern Virginia Medical School (EVMS) in the School of Health Professions, and Graduate Faculty Scholar at University of Central Florida (UCF) in the School of Electrical Engineering and Computer Science. Before coming to Old Dominion University, he spent 6 years in the simulation industry at Science Applications International Corporation (SAIC) as a senior scientist. Dr. McKenzie's research has been in medical modeling and simulation, human behavior representation, and simulation architectures often focusing on aspects of scientific visualization and virtual reality.

POPLITEAL ARTERY ANEURYSM: A BIOENGINEERING STUDY ON PATHOGENESIS.

Francesca Condemi[(a)], Raffaele Serra[(b)], Stefano de Franciscis[(c)], Gionata Fragomeni[(d)]

[(a),(d)] Bioengineering Unit *"Magna Graecia"* University, Catanzaro, 88100, Italy
[(b),(c)] Vascular Surgery Unit *"Magna Graecia"* University, Catanzaro, 88100, Italy

[(a)]fccondemi@gmail.com, [(b)]rserra@unicz.it,[(c)]defranci@unicz.it[(d)]fragomeni@unicz.it

ABSTRACT
This study regards a computational fluid dynamics (CFD) model and a fluid structure interaction (FSI) model to describe the "Functional Entrapment Syndrome of Popliteal Artery" (PAES).
A stack of 127 slices, were acquired from RM of the right knee. The segmentation of the region of interest was performed on 3D Slicer, using the Single Region Growing. The final geometry was created in Comsol Multiphysics through the measure obtained by segmentation. To optimize the model's elaboration, we performed only the region of interest: the flow, the artery walls and the muscles soleus, medial gastrocnemius, plantaris and popliteus. CFD and FSI were performed using the commercial software Comsol Multiphysics 5.0 (COMSOL, Inc., Stockholm, Sweden). In CFD section, in agreement with the experimental data, the popliteal blood velocity varied from 30[cm/s] to 70 [cm/s]. In FSI phase, the entrapment due to the gastrocnemius muscle caused a maximum displacement of the popliteal artery walls of 0.16 [mm]. When the entrapment is due to soleus muscle, the maximum displacement of the artery is about 0.3947 [mm]. The most important observation is the variation of contact pressure in two cases of entrapment. In fact, when the occlusion is due to soleus muscle, the pressure is higher than the precedent case.
The CFD model and the FSI model resulted in a detailed description of fluid dynamic and fluid-structure interactions useful to evaluate the pathology's features, independently, from the obstacles of in vivo analysis. These models can define the sites more solicited where there is the most probability to have an aneurysm.

Keywords: PAES, CFD model, FSI model, popliteal artery aneurysm

1. INTRODUCTION

Popliteal artery represents most common region of aneurysms after aorta.[1-3]In the period 1999-2007, 21patients (19 males and 2 females), (Age range 50-88), (mean age 69), with popliteal aneurysm were treated at our department.

We noted that 4 Patients (all males) with the right leg affected were bus driver. A bus driver uses repeatedly, for at least 6 hours per day, his right foot on the accelerator and break pedal of the bus and popliteal artery has an important anatomical relation with the muscles that control the movement of the foot. The evaluation of the leg muscles with MR imaging after the execution of particular movement of the foot and the leg, elaborated with mathematical and bioengineering tools, may correlate with the mechanical stress on the artery that may lead to the aneurysm formation.
This findings may identify those persons at risk of developing popliteal aneurysm especially in those subject (workers, athletes, etc) that acts repeatedly movement with the lower limbs.

2. METHODS

2.1. Bioengineering Study

The study, which was developed, regards the analysis of the popliteal artery aneurysm in people who aren't familiar history to atherosclerotic disease, abnormal anatomy of the muscles of the popliteal cavity or deviations of the popliteal artery course.
According to recent studies, in these situations, the formation of aneurismal sacs is attributable to the PAES[4].In this case, there is a regular anatomy of the popliteal pit, but during walking, competitive activities or any other effort to induce an involvement of the lower limb, it's possible that the axis of arterial leg from the groin to the foot, can be compressed, invarious levels, from bone structures - muscle - tendon. In the case of this study, the movement analyzed is flexion-extension of the foot. In this regard, we proposed a description of the type of movement exercised when driving a truck, the articulation of the foot and the affected muscles. Such movement repeated over time can induce muscle hypertrophy, in particular, at the level of the soleus muscle and medial gastrocnemius. For this reason, the drivers would be among the

categories that are more susceptible to the popliteal artery functional entrapment syndrome, which may lead to aneurysm formation.

2.2. Image Acquisition

Data, 127 slices, were acquired from RM of the right knee. The subject was a healthy woman of 47 years old. 2D images have a resolution of 512 x 512 pixel, slice thickness of 4 mm, slice distance of 4mm and pixel dimension of 0.65 mm, Figure 1.

2.3. Geometry Reconstruction

The segmentation of the region of interest was performed on 3D Slicer, open-source software package for visualization and image analysis. In the first phase, the images were initialized using the definition of the Window/Level to discriminate little differences of density (of 0.5%), that are represented by different levels of gray, so we could increase the contrast of images. After the initialization, the segmentation was done using the Single Region Growing. The geometry was restituted in STL format (Standard Tessellation Language, native to the stereolithography CAD software created by 3D Systems of Valencia, CA, USA), Figure 1.

The final geometry was created in Comsol Multiphysics through the measure obtained by segmentation, Table 4. To optimize the model's elaboration, we performed only the region of interest: the flow, the artery and the muscles soleus, medial gastrocnemius, plantaris and popliteus, Figure 2.

Whereas, adipose tissue and the skin were simplified through a cylinder. The geometry was finished through form union, so it was only solid but the software could discriminate her different parts.

Finally, the meshing was realized using a free mesher that automatically created an unstructured mesh formed by tetrahedral and triangular elements. The mesh was chosen Fine and it restituted 56880 elements, Figure 2.

2.4. CFD Solver

CFD was performed using the commercial software ComsolMutiphysics. Therefore was used the module Fluid Dynamics – Incompressible Navier-Stokes.

Blood was assumed to be incompressible with a density of 1.050 kg/m^3 and dynamic viscosity of 0.0045 Pa*s.

The Navier-Stokes equation for a Newtonian and incompressible fluid formed a partial differential equation system[5-6]:

$$\rho\frac{\delta u}{\delta t} + \rho(u * \nabla) = \nabla * [-pI + \mu(\nabla u + (\nabla u^T)] + F$$

$$\rho\nabla * u = 0 \quad (3)$$

where v is the velocity field [m/s], F are the volume forces such as gravity [N/m^3], p is the pressure [Pa], ρ is the density of fluid[kg/m^3], μ is dynamic viscosity [Pa s].

To model the behavior of the arterial flow were specified the boundary conditions Inlet/Outlet pressure, no viscous stress, that are ideal because the variations of pressure, respect aorta, are known.

Therefore, we have been defined two functions that describe the variations from systole to diastole values, that characterized peripheral pulses, Figure 3. Finally, we have been imposed the condition of adhesions, i.e. a fluidin direct contact with a solid walladheresdue toviscous effectswithout giving rise to a relative flow. The condition Wall/No slipis precisely the adherence to a solid wall fixed in space.The Study of Time Dependent has been defined with t=(0:0.05:1), by which we derived the values of pressure and velocity along the artery.

2.5. FSI Solver

The module Structural Mechanics – Solid, Stress-Strain allowed to carry out structural analysis static or dynamic of all

types of geometry (3D, 2D and axial symmetry) and with various stresses (plane stress or plane strain, …). This module was exploited in order to consider the stresses suffered by artery that can induce the formation of an aneurysm. So, in this study, the problem has been addressed considering that:

- The surfaces of artery are in contact with the fluid, therefore, are subject to the forces due to pressure of the same.
- In functional popliteal artery entrapment syndrome, the walls are subjected to stress due to pressure exerted by the muscle.

In the first case, is set the rest condition of the knee, then the constraints relate to the

muscles around it. For the plantar muscle and popliteal has been imposed the condition of zero displacement, in this way the muscles can deform around the artery, but without inducing a load on it. For the muscles soleus and medial gastrocnemius, instead, in agreement to data reported on the literature, has been set a force of 758,313 [N], which varies parametrically, in such a way as to define the motion of the muscle. In the rest condition, the parameter that causes a change of this force is set equal to zero.

The value of the forces exerted by the fluid in contact with the wall is defined as:

$$F_A = \sigma * n \quad (4)$$

where F_A is the force per unit area [N/m^2], σ is the normal stress [N/m^2], n is the unit vector normal to the surface.

The PDE problems were solved using the solver PARDISO, by the solver Steady State Parametric, the parameter considered is the time.

It has been defined the time interval between zero and one, i.e. the time necessary for there to be the evolution

from the phase of systole to that of diastole, according to the course of pressure default.
In the second case, was analyzed the stress due to the load exerted from the soleus muscle, in the distal section, and from the medial gastrocnemius, in that medial.
This condition, in particular, is found in the lorry drivers, for whose posture, in the movement of flexion-extension of the foot is induced a constant stress of these muscles, which undergo hypertrophy and, consequently, in the exercise, they intermittently compress the artery. Therefore, has been defined a maximum force, as a function of which the muscles undergo a shift, such as to cause the trapping of the artery, it has been defined to be zero along x and z, while along y the force varies according to a parametric function:

P_max·((para<=1)·para+(para>1)·(2-para)) (5)

where the parameter, para, varies between zero and one, so the initial condition is the rest state, then the trapping and again the release of the artery.
In the case where the entrapment is exercised by the soleus muscle such a force acts on it.
It follows the movement of the muscle in the flexion-extension of the foot and the subsequent entrapment of the artery in the distal region.
For the plantar muscle, popliteal and gastrocnemius is imposed the condition of zero displacement, in this way the muscles can deform around the artery, but without inducing a load on it.
Conversely, in case where the entrapment is charged to the medial. In this case, the displacement of the plantar muscles, soleus and popliteal is set to zero along the three cartesian axes. While there is provided, according to the same principle of the soleus muscle, the displacement of the gastrocnemius along the y-axis, (Eq 5).
The solution of this study is for medal ways in the stationary case, with respect to time, and dependent upon the parameter that indicates the shift of the muscles involved.
In both cases, the mechanical properties of the soleus, medial gastrocnemius, plantar, popliteus and external tissue are: Lamé constant (μ) 7.20e6 [Pa], Lamé constant (λ) 20· μ-2· μ/3 [Pa], Density 1200 [kg/m^3].For walls Lamé constant (μ) 6.20e6 [Pa], Lamé constant (λ) 20·μ-2· μ/3 [Pa], Density 960 kg/m^3.

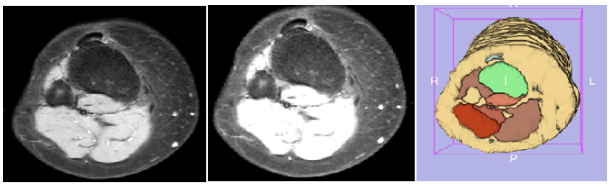

Figure 1: The first figure on the left represents one of 127 slices were scanned, the second the same slice pre-processed, the last on the right shows the segmentation result in 3D Slicer.

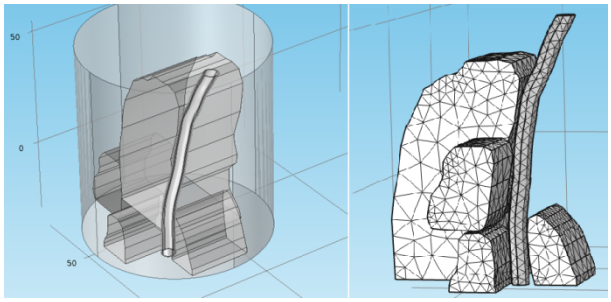

Figure 2: On the left is represented the full geometry, on the right the mesh.

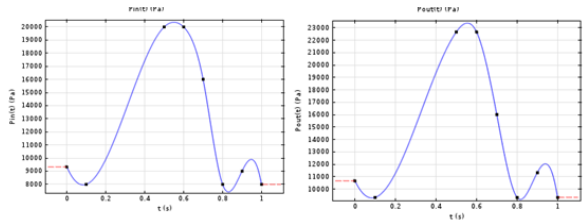

Figure 3: On the left inlet pressure, on the right outlet pressure that characterized peripheral pulses due to the peripheral resistance.

3. RESULTS

3.1. CFD results

The results for the values of pressure and velocity of the fluid have been developed in the first part of the analysis. We were imposed as boundary conditions the pressure, which evolve over a period of one second, from thediastolic value in the systolic, then defining the pulsation that characterized the peripheral pulses. Therefore, the values of the average speed, for each instant of time, vary between about 70 [cm/s] and 30[cm/s], Table 1. Assuming thatthe artery has constant cross section, these results show that the speed varies with the cardiac cycle. Furthermore, having assumed that the flow islaminar, the speed at the centerof the vessel is greater than that which is locatedat the edges andthisphenomenon is called *Parabolic Profile Velocity*.

3.2. FSI results for the rest condition

In the analysishas been supposed that the flow is continuous due to the elasticity of the arterial walls: they, after having dilated during the cardiac systole to accommodate the blood, in diastole retract thereby ensuring a forward thrust to the mass of blood. The arteryis affected by the compression force of blood flow, as a function of which will have in the systole phase an increase in diameter of the wall, which is equal

to $4.1 \cdot 10^{-3} \cdot 10$ [mm], while t = 1 [s], during diastole, is equal to $1.85 \cdot 10^{-3} 10$[mm].
The average pressure suffered by the wall varies between about 2900[Pa], in diastole, and 6000[Pa], in systole.
However, the hypotheses of the study are: young and healthy patients who did nothave risk factors or family history of atherosclerotic disease. Under these assumptions, the analysis does not focuson the definition of Shear Stress suffered by thevessel wall, which can be, also, a risk factorfor the onset of aneurismal disease.
However, even thisstage of the analysis has a certain importance in order to consider, first of all, the physiological condition of the artery and the stresses it undergoes in this case, and secondly, a full analysis can't be separated fromall the phenomenathat may occur.

3.3. FSI results duringthe flexion-extension of foot

The purpose of this experimental study is to define the prevalence of the popliteal artery occlusion during the active plantar flexion-extension, in young volunteers who lead physical activity. The analysis was carried out in such a way that could be induced the same condition suffered by the wall in case of exercise repeated.[7]
In the pathological case, we have distinguished two conditions: the first caused by entrapment soleus and the second by medial gastrocnemius muscle. Whereas the force exerted by the gastrocnemius muscle, the maximum displacementof the wall is about 0.16 [mm].
Comsol Multiphisycs provides a series of tools by means of which it is possible to derive the pressure over the entire wall. The value of the pressure undergone by the vessel is obtained by integrating the value of the pressure with respect to the surface of the wall itself:

$$P = \int_A pdA \quad (1)$$

The average pressure is calculated by simply dividing the load applied to the area of the wall:

$$p_m = \frac{P}{A} (2)$$

The values, obtained, were plotted with respect to the variation of the force and the time, Figure 4 (a-b). The latter part of the analysis made possible to compare the physiological and pathological data, Table 2.
As was expected, there is a marked increase in the average pressure over the entire artery. In addition, Figure 4 (a) shows how varying the pressure on the vessel as a function of the movement of the muscle: it is verified that the occlusion of the artery occurs intermittently, therefore, the rising phase of the function indicates the trapping during exercise, in the second part indicates the release of the artery, returning to the resting.
Finally, it was considered the pressure experienced by the side section of the artery, in contact with the muscle Figure 4 (c), according to equations 1 and 2, and subsequently, has been considered the stress undergone by that section, Figure 4 (d). It is evident, Figure 4 (c), that at the medial, that is, considering the length of the artery of 80 mm to about 40 mm, there is a peak pressure. This peak corresponds with the region where the trapping occurs due to the gastrocnemius muscle[8] compression on the artery.
Moreover, comparing the two curves of Figure 4 (c) and the two curves of Figure 4 (d), these show that in the region urged there is a pressure increase of an order of magnitudean increase in stress on artery and, therefore, according to the experimental data that are now known[9], these repeated stresses may be such as to induce a reduction in the elasticity of the artery, resulting in the expansion and formation of an aneurysm sac.
The same type of analysis has allowed to solve the problem in the case where the occlusion is due to the force exerted by the soleus muscle. In this case,the maximum displacementof the wall is about 0.3947[mm].
We have been defined the variation of pressure respect force and time, Figure 5 (a-b), the contact pressure and the stress suffered by vessel, Figure 5 (c-d). What it should be emphasized is, in this case, the pressure increase in the pathological condition, compared to the case previously considered, Table 3. About this, today, there are not sure explanations. The only assumption that can be advanced is that: the soleus muscle is characterized by a high pinnation and by I type fibers, while the gastrocnemius has a pinnation lower and prevalence of II type fibers, so the first serves to generate for a long time static force, the second generates lessforce, for less time, but faster. Consequently, for a given applied force, since the application time increased, the pressure and the induced stress will be higher.

4. DISCUSSION

Popliteal aneurysms constitute 70% of peripheral aneurysms with an incidence of 4.5-7.5 new cases out of 100.000 inhabitants per year in the world[1-3].
Natural story of poplitea artery aneurysms is characterized by high rate of thrombotic and thromboembolic complications which may determine an increased risk towards aserious damage of peripheral artery vessels.
Their clinical interest is due to frequent serious complications which may cause limb amputation. Various trials report a frequency rate of 18 -57 % ofcomplications like embolism, thrombosis and rarely rupture [10-12]
Acute ischemia may occur for acute thrombosis of aneurysm, chronic ischemia
is usually due to progressive occlusion for multiple thrombotic apposition in aneurismal sac [13].

About one third of patients are asymptomatic at first diagnosis [10]. Acute or chronic peripheral ischemia for thrombosis or distal embolism are most common clinical presentation [1,14].
Less frequent symptoms, often underestimate or not known, are those related to aneurysm compression on adjacent venous and nervous structures. Symptomatology, in these cases, may vary from pain (nervous irritation, venous outflow obstruction),oedema (marked venous outflow obstruction) to popliteal vein thrombosis (related to aneurismal sac dimension) [15].
Anatomy. The popliteal artery is the continuation of the superficial femoral artery, and courses through the popliteal fossa. It extends from the opening in the
Adductor magnus, at the junction of the middle and lower thirds of the thigh, downward and lateral ward to the intercondyloid fossa of the femur, and then vertically downward to the lower border of the Popliteus, where it divides into anterior and posterior tibial arteries. In front of the artery from above downward are the popliteal surface of the femur (which is separated from the vessel by some fat), the back of the knee-joint, and the fascia covering the Popliteus. Behind, it is overlapped by the Semimembranosus above, and is covered by the Gastrocnemius and Plantaris below. In the middle part of its course the artery is separated from the integument and fasciæ by a quantity of fat, and is crossed from the lateral to the medial side by the tibial nerve and the popliteal vein, the vein being between the nerve and the artery and closely adherent to the latter. On its lateral side, above, are the Biceps femoris, thetibial nerve, the popliteal vein, and the lateral condyle of the femur; below, thePlantaris muscle, the lateral head of the Gastrocnemius and the Soleus muscle. On its medial side, above, are the Semimembranosus and the medial condyle of the femur; below, the tibial nerve, the popliteal vein, and the medial head of the Gastrocnemius [16]. Popliteal artery is located in a compartment in which different muscles work. These muscles, expecially Gastrocnemius and Soleus, after specific movements apply pressure force on the vessel itself.
Erdoes LS et al. showed that, in normal population, sonographic examination can show arterial compression elicited by maneuvers such as plantar flexion and dorsiflexion of the feet. Although this finding is consistent with the diagnosis of popliteal artery entrapment syndrome, previous studies have shown occlusion in up to 59% of asymptomatic subjects. In those patients, normal anatomy was confirmed on MRI, and the popliteal artery occlusion was at the soleal sling site as a result of compression by the soleus muscle, lateral head of the gastrocnemius muscle, plantaris muscle, and popliteus muscle.
In the period 1999-2007, 21 patients (19 males and 2 females), (Age range 50-88), (mean age 69), with popliteal aneurysm were treated at our department.
We noted that 4 Patients (all males) with the right leg affected were bus driver.

This kind of working activity may represent a risk factor for popliteal aneurysm formation as bus drivers generally use repeatedly, for at least 6 hours per day, his right foot on the accelerator and break pedal of the bus. The break pedal offer, in fact, a certain resistance to the flexion of the foot. In this condition the generation of anomalous local forces in the popliteal fossa may attempt the arterial wall integrity that may
lead to aneurysm formation.

Table 1: Values assumed by the speed input and output in the different phases of the cardiac cycle.

t	Average velocity input[cm/s]	Average velocity output [cm/s]
0	0.00661	0.00472
0.55418	0.74669	0.41618

Table 2: The Table shows the data physiological and pathological for the time instants which indicate the transition from diastole to systole and vice versa.

t	Pressure in the physiological case [Pa]	Pressure in the pathological case [Pa]
0	2988.76593	2780.45252
0.45	5991.35984	11989.54278
0.5	6352.6332	12645.33149
1	2797.42349	30899.26342

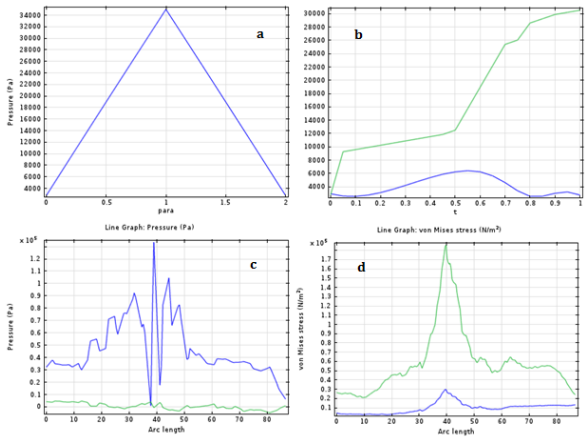

Figure 4: (a) Variation of the pressure exerted by the muscle; (b) in blue is shown the average pressure acting on the vessel in the physiological case, in green in the pathological case; (c) pressure suffered by the side section of the artery in contact with the muscle, the physiological condition in green, blue in the pathological; (d) the blue line represents the stress suffered by vessel under physiological conditions, the green stress in pathological conditions.

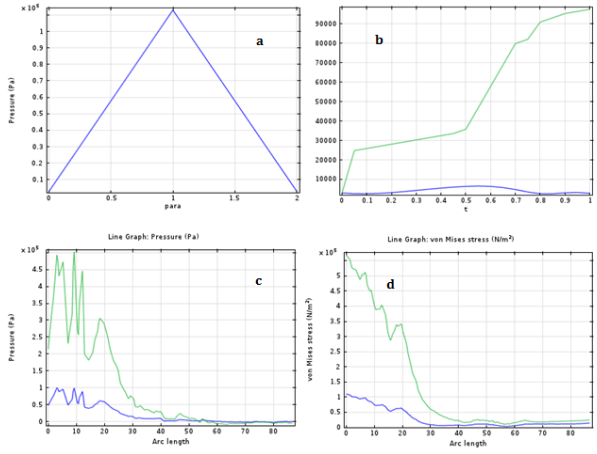

Figure 5: Variation of the pressure exerted by the soleus muscle; (b) the blue line represents the stress sufferedby vessel under physiological conditions, the green stress in pathological conditions; (c) pressure suffered by the side section of the artery in contact with the soleus muscle, the physiological conditionin green, blue in the pathological; (d) the blue line represents the stress suffered by wall sunder physiological conditions, the green stress in pathological conditions.

Table 3: The Table shows the data physiological and pathological for the time instants which indicate the transition from diastole to systole and vice versa.

t	physiological case (Pa)	pathological case gastrocnemio(Pa)	pathological case soleus (Pa)
0	2988.76593	2780.45252	2797.42345
0.45	5991.35984	11989.54278	33569.644
0.5	6352.6332	12645.33149	35769.99161
1	2797.42349	30899.26342	97510.95427

5. CONCLUSIONS

In functional popliteal artery entrapment syndrome, the walls are subjected to stress due to pressure exerted by the muscle. This is the final aspect studied in this analysis, from the consideration that: in young patients, who aren't familiar history to atherosclerotic disease, in fact, the increase in diameter of the artery due to stress caused by the fluid is negligible. In fact, what causes the pathological condition, i.e. the formation of the aneurysm sac, is the stress due to the load exerted from the soleus muscle, in the distal section, or from the medial gastrocnemius, in that medial.

REFERENCES

1. Shortell CK, Deweese JA, Ouriel K, Green RM. Poplital artery aneurisms: a 25-year surgical experience. J VascSurg 1991; 14:771-9.
2. Johnston KW, Rutherford RB, Tilson MD, Shah DM, Hollier L, Stanley JL. Suggested standards for reporting on arterial aneurysms. J VascSurg 1991; 13:440-50.
3. Lawrence FL, Lorenzo-Rivero S, Lyon J. The incidence of iliac, femoral, and popliteal artery aneurysms in hospitalized patients. J VascSurg 1991; 22:345-51.
4. Inada K, Hirose M, Iwashima Y, Matsumoto K. *Popliteal artery entrapment syndrome: a case report*. Br J Surg 1978; 65:613–5. [PubMed]
5. Fragomeni G., Rossi M., Condemi F., Mazzitelli R., SerraionoG.F., Renzulli A. *"Apicoaorticconduit and cerebralperfusion in mixedaortic valve disease: a computationalanalysis"* Interactive CardioVascular and ThoracicSurgery (2013) 1–6 doi:10.1093/icvts/ivt379.
6. M V Caruso, V Gramigna M Rossi, G F Serraino, A Renzulli, G Fragomeni *"A computationalfluiddynamicscomparisonbetweendifferentoutflowgraftanastomosislocations of Left Ventricular Assist Device (LVAD) in apatient-specificaortic model"* International Journal for NumericalMethods in BiomedicalEngineering 2015; e02700 DOI: 10.1002/cnm.2700
7. Ulrich Hoffmann, MD, Julia Vetter, MS, Lisa Rainoni, RVT, Anders J. Leu, MD, and Alfred Bollinger, MD, *Popliteal artery compression andactive plantar flexion in younghealthy volunteersforce.*Zurich, Switzerland
8. Rich NM, Collins GJ Jr, McDonald PT*, et al. Popliteal vascular entrapment. Its increasing interest. Arch Surg. 1979;114(12): 1377-1384.*
9. VedranRadonić, MD, PhD, Stevan Koplić, MD, Lovel Giunio, MSc, MD, Ivo
10. Božić, MSc, MD, Josip Mašković, MD, PhD, and Ante Buća, MSc, MD.*Popliteal Artery Entrapment Syndrome: Diagnosis and Management, with Report of Three Cases.*.
11. Lowell RC, Gioviczki P, Hallet JW Jr, NaessensJM,Maus TP, Cherry KJ, et al. Popliteal artery aneurysm: long term follow-up of aneurismal disease and results of surgical treatment. J VascSurg 13:398-407, 1991.
12. Shortell CK, De Weese JA, Ouriel K. Popliteal aneurysms: A 25-year surgical experience. J VascSurg 1991; 14:771-9.
13. Whitehouse WM, Wakefield TW, Graham LM. Limb-threatening potential of arteriosclerotic popliteal aneurysms. Surgery 1983; 93(5):694-9.
14. Buchbinder D, McCullough GM, Melick CF. Patients evaluated for venous disease may have other pathologic conditions contributing to

symptomatology. Am J Surg 1993; 166(2):211-5.
15. Walsh JJ, Williams LR, Driscoll JL, Lee JF. Vein compression by arterial anurysm. J VascSurg 1988; 8 (4): 465-9.

SITTING VS STANDING: A COMPUTATIONAL COMPARISON OF HEMODYNAMICS IN CAROTID BIFURCATION

Maria Vittoria Caruso[(a)], Raffaele Serra[(b)], Paolo Perri[(c)], Stefano de Franciscis[(d)], Gionata Fragomeni[(e)]

[(a),(e)]Bioengineering Group, *"Magna Graecia"* University, Catanzaro, 88100, Italy
[(b),(c),(d)]Operative Unit of Vascular Surgery, *"Magna Graecia"* University, Catanzaro, 88100, Italy

[(a)] mv.caruso@unicz.it, [(b)] rserra@unicz.it, [(c)] paolop83@yahoo.it, [(d)] defranci@unicz.it, [(e)] fragomeni@unicz.it

ABSTRACT
Sedentary lifestyle is very important in the etiology of atherosclerotic cardiovascular diseases. Furthermore, atherosclerotic plaques tend to occur near arterial bifurcation, as carotid one. Different studies have been conduced to investigate the physiological changes that occurred due to prolonged postural positions, but no computational analysis has been carried out. Aim of this study was to numerical explore the hemodynamic changes due to prolonged sitting or standing (1 hour respectively) in a carotid bifurcation, using the computational fluid dynamic (CFD) approach. In-vivo non-invasive measurements of anatomy, pressure field and velocity pattern were recorded in a cohort of 10 volunteers and used as boundary conditions for the simulations. The results showed that the worse hemodynamic profile occurs after sitting position near to the bifurcation - low velocity and wall shear stress (WSS), high stasis and chaotic flow - suggesting that a high risk of plaque formation and of stenosis could happen.

Keywords: carotid bifurcation, computational analysis, fluid dynamics, sitting, standing

1. INTRODUCTION

Atherosclerosis is the major cause of cardiovascular diseases (CVD), such as coronary heart disease, heart attack or stroke (Frostegard 2013). One important risk factor for its development is the lifestyle, which can favor plaque formation in the arteries in case of sedentary behavior, such as sitting or standing time. Indeed, prolonged sitting position is associated with CVD, but frequent short breaks in sedentary time may impart unique benefit (Owen et al. 2010), such as a significant reductions in postprandial glucose and insulin action (Dunstan et al. 2012).
The brain is perfused by means of the internal carotid arteries, vessels highly exposed to thromboembolic events (Malek et al. 1999), which can cause stroke. For this reason different studies have investigated what happens in these arteries considering different lifestyles and so, different postural positions. A comparison of waveforms in young, middle-aged and older groups has highlighted that regular aerobic exercise- trained increases velocity in respect to sedentary life in the carotid artery (Azhim et al. 2007, Azhim et al. 2011). The sedentary time is also associated with an increase in carotid intima media thickness (IMT) (Kozàkovà et al. 2010, García-Hermoso et al. 2015) and the carotid stiffness and other cardiometabolic risk factors (Huynh et al. 2014). Furthermore, Krause et al. (2000) have found that prolonged standing at work is correlated with the progression of atherosclerotic events in the carotid bifurcation, in terms of increase of IMT.
The effects of posture has been also investigated in the brachial and femoral arteries (Newcomer et al. 2008), showing that, comparing the standing and sitting positions, the heart rate and blood flow are higher and the mean arterial pressure (MAP) is lower in both arteries.
Although postural changes have been much investigated from clinical view point, no studies have been carried out regarding the hemodynamics. So, a detailed analysis is necessary.
The objective of this study was to examine the hemodynamic changes in the carotid bifurcation due to prolonged sitting and standing time (1 hour respectively) by means of the computational fluid dynamics (CFD). This numerical approach allows to study, in time and in space, the two hemodynamic variables - the pressure field and the velocity pattern- resolving the governing equations by means of a numerical approach (simulations) (Tu et al. 2007). In-vivo non-invasive pressure and velocity measurements (Van de Vosse and Stergiopulos 2011) were used as input for the simulations.

2. MATERIAL AND METHODS

2.1. Subjects

The subjects were 10 healthy volunteers, 5 men and 5 women, which didn't have cardiovascular diseases. Furthermore, the cohort has 29.3 ± 0.07 years and a BMI of 22.90 ± 2.72 kg/m^2.

2.2. In-vivo measurements

The caliber of vessel and the velocity profile after 1h of sitting (case A) and after 1h of standing (case B) were recorded in the common carotid artery (CCA) and internal carotid artery (ICA) by means of the Hitachi-Aloka ProSound F37 ultrasound system (Hitachi Aloka

Medical America, Inc.). Starting on these data, the flow profile was calculated.
An applanation tonometry was used to record the pressure in the external carotid artery (ECA).
In all cases, the mean value and the standard deviation were evaluated. The diameter and the velocity at peak systolic and end diastole in sitting time and in standing one are reported in Table 1, 2 and 3 respectively. Pressure values in systolic peak and at end diastole and the MAP in the two cases are reported in Table 4.

2.3. CFD model

2.3.1. Geometrical model

A carotid bifurcation was reconstructed by means of the segmentation process from CT images of a 30 years old man, done for clinical reasons, using Invesalius open source software. The geometry included the common carotid artery (CCA), the internal carotid artery (ICA) and the external carotid artery (ECA) (Figure 1). Starting from this 3D model, a new idealized model was reconstructed considering the centerlines of the patient-specific bifurcation in order to obtain the real bendings of the vessel. The diameter variation was modeled hypothesizing a circular shape. Furthermore, the mean value, obtained considered the 10 volunteer, was set for CCA and ICA caliber of the idealized model (Table 1). The ECA diameter value was chosen from the patient-specific model.

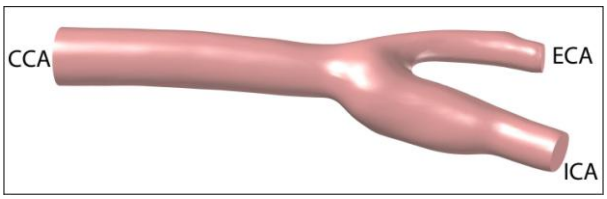

Figure 1: Geometrical idealized model of carotid bifurcation

Table 1: CCA and ICA diameter values for each volunteer, measured with the ultrasound system

Patient	Diameter [mm]	
	CCA	ICA
1	6.30	4.90
2	6.50	4.20
3	6.00	4.60
4	6.20	4.10
5	6.80	4.00
6	6.20	4.70
7	6.40	4.50
8	6.80	4.40
9	5.80	4.80
10	6.00	4.80
Mean	6.30	4.50
SD	0.33	0.32

Table 2: Velocity value in systolic peak for each patient in sitting position and in standing one.

Systolic Velocity [cm/s]				
Patient	Sitting		Standing	
	CCA	ICA	CCA	ICA
1	35	20	39	22
2	32	20	41	28
3	30	15	38	21
4	40	23	44	24
5	35	25	39	29
6	42	20	46	24
7	48	28	50	30
8	32	21	38	26
9	38	18	50	22
10	36	17	49	23
Mean	36.80	20.70	43.40	24.90
SD	5.41	3.83	5.04	3.18

Table 3: Velocity value at end diastole for each patient in sitting position and in standing one.

Diastolic Velocity [cm/s]				
Patient	Sitting		Standing	
	CCA	ICA	CCA	ICA
1	15	8	17	9
2	16	10	19	12
3	14	7	17	9
4	17	10	20	12
5	18	13	21	14
6	16	8	19	10
7	18	11	20	13
8	17	12	20	14
9	15	6	17	8
10	13	6	17	9
Mean	15.90	9.10	18.70	11.00
SD	1.66	2.47	1.57	2.26

2.3.2. Mathematical model of blood flow

To study the hemodynamics from a macroscopic point of view, the blood can be modeled as an incompressible fluid with a density of 1,060 kg/m^3 (Cutnell and Johnson 1998) and a Newtonian behavior, with viscosity equal to 0.0035 Pa·s (Yilmaz and Gundogdu 2008). Furthermore, blood flow was hypothesized as laminar and 3D Navier-Stokes equations were used as governing laws:

$$\nabla \cdot \mathbf{u} = 0 \quad (1)$$

$$\rho\,(\partial \mathbf{u}/\partial t) + \rho(\mathbf{u}\cdot\nabla)\mathbf{u} = \nabla\cdot[-p\mathbf{I} + \mu(\nabla\mathbf{u} + (\nabla\mathbf{u})^T] \quad (2)$$

Table 4: Pressure evaluated for each patient (P) in sitting and standing, considering the systolic peak (S), the end diastole (D). The mean arterial pressure (MAP) is also reported.

Pressure [mmHg]						
P	**Sitting**			**Standing**		
	S	**D**	**MAP**	**S**	**D**	**MAP**
1	110	75	86.67	95	70	78.33
2	130	80	96.67	120	75	90.00
3	110	75	86.67	95	65	75.00
4	120	70	86.67	100	65	76.67
5	120	95	103.33	110	75	86.67
6	110	70	83.33	95	65	75.00
7	120	80	93.33	105	70	81.67
8	125	80	95.00	115	70	85.00
9	120	70	86.67	110	60	76.67
10	120	85	96.67	105	70	81.67
Mean	118.50	78.00	91.50	105.00	68.50	80.67
SD	6.69	7.89	6.40	8.82	4.74	5.22

2.3.3. Boundary conditions

The CCA flow waveform was assumed as an inlet boundary condition, whereas the ICA flow waveform was set as an outlet boundary conditions, considering in both cases a fully developed steady profile (Poiseuille). Furthermore, the pressure waveform was applied as outlet boundary condition in ECA.

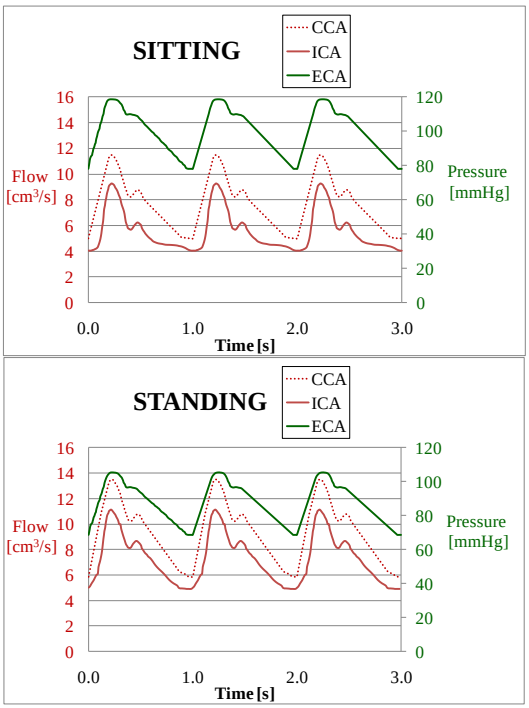

Figure 2: Boundary conditions in sitting position and in standing one.

2.3.4. Simulation details

The carotid bifurcation was discretized with tetrahedral, prism, triangular and quadrilateral elements. Moreover, in order to obtain accurate and grid independent solutions, the mesh was modeled so that the grid error - evaluated as:

$$e=|(Q_{in}-Q_{out})/Q_{in}|\cdot 100 \quad (3)$$

where Q_{in} is the mean flow in inlet (CCA) and Q_{out} is the mean flow in outlet (ECA+ICA) - was less than 1%. According to the continuity equation (2), $Q_{in} = Q_{out}$, so the error evaluated with (3) is correlated to the grid. Moreover, considering a mesh of 65,063 total elements, the flows are Q_{CCA}=7.69 cm^3/s, Q_{ICA}=5.59 cm^3/s, Q_{ECA}=2.09 cm^3/s, so e=0.13%.

The CFD analysis was carried out using COMSOL 5.0 (COMSOL Inc, Stockholm, Sweden), a finite-element-based commercial software package. In both situations, time-dependent simulations were implemented, considering a time step of 0.001 s and using the direct solver Pardiso and the BDF method for the time stepping. Furthermore, the elements used in the finite element formulation were linear for both the velocity components and the pressure field (P1+P1).

2.3.5. Atherosclerotic parameters

Atherosclerosis is highly influenced by shear stress generated at the interface between blood and artery wall (Malek et al. 1999), known as wall shear stress (WSS). It can be evaluated as:

$$WSS=\sqrt{[(\tau_x)^2+(\tau_y)^2+(\tau_z)^2]} \quad (4)$$

where τ_x, τ_y and τ_z are the viscous stress in x, y and z directions, respectively. WSS is a time-dependent parameter, so the average over one cardiac cycle (T) can be evaluated, known as time average WSS (TAWSS):

$$TAWSS=1/T\cdot\int_0^T |WSS|\, dt \quad (5)$$

Physiological level of TAWSS in arteries is in the range 1.5 - 2 Pa (Malek et al. 1999).

Another parameter linked to the shear stress is the oscillatory shear index (OSI), which reveals the overall WSS vector oscillation:

$$OSI=0.5\cdot\{1-[(|\int_0^T WSS\, dt|)/\int_0^T |WSS|\, dt]\} \quad (6)$$

It varies from 0 to 0.5 and it is a dimensionless measure: the zero value indicates that there is no WSS variation (orderly and unidirectional flow), while 0.5 indicates a variation of 180° accordingly to a purely unsteady and chaotic flow with zero WSS (Dong et al. 2013). Moreover, it was demonstrated that this mechanical indicator is a good predictive parameter of plaque site (Knight et al. 2010).

The values of TAWSS and OSI are combined in relative residence time (RRT) parameter, expressed as:

$$RRT=[(1-2\cdot OSI)\cdot TAWSS]^{-1} \quad (7)$$

that expresses the residence time of particles near the wall (Lee et al. 2009).

Atherosclerosis plaque can arise when the flow is disturbed and this area can be identified considering

WSS $\leq$ 0.481 Pa, OSI $\geq$ 0.145 and RRT $\geq$ 2.944 Pa^{-1} (Lee et al. 2008).

3. RESULTS AND DISCUSSION

3.1. Flow and pressure waveforms

The flow waveform in CCA, ECA and ICA in sitting and in standing time is shown in Figure 3. In standing position the CCA and ICA flows are higher than the flows in sitting situation, with a mean increase of about 17.50% and 21% respectively. Furthermore, since the ICA mean flow percentage in respect to the CCA flow is about 80% in sitting and about 82% in standing, the flow in ECA is similar after the two postural situations.
Regarding the pressure field, its distribution is similar in the three vessels (ICA, ECA and CCA) both in sitting and in standing situation (Figure 4) because the carotid bifurcation has a small length. Moreover, MAP is lower of about 11.84% in standing position respect to the sitting one.

3.2. Velocity pattern

To analyze in details the velocity pattern during sitting (A) and standing (B), the streamlines of the velocity magnitude in systolic peak and at end diastole are reported in Figure 5 and 6 respectively. Furthermore, two different views - frontal (1) and posterior (2) - are considered. In both postural positions, chaotic flow occurs in the ICA in correspondence of bifurcation (carotid bulb), both in systole and in diastole. This swirling pattern is more emphasized in sitting, where flows are lowest. Moreover, in this area of bifurcation, the velocity values are near 0 m/s. This suggests that blood stasis characterizes this region.

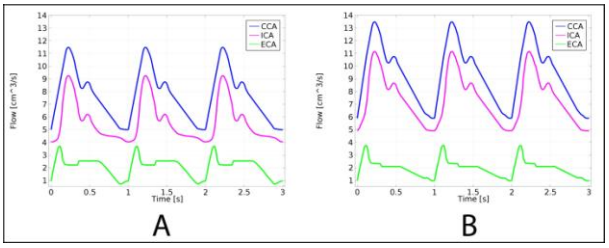

Figure 3: Flow waveforms in CCA, ICA and ECA during sitting (A) and standing (B)

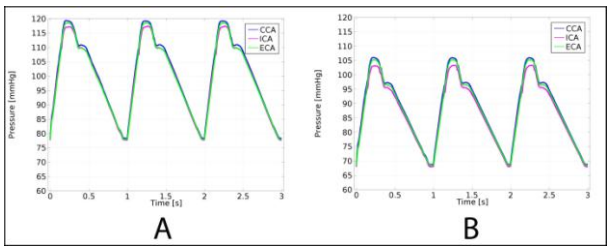

Figure 4: Pressure waveforms in CCA, ICA and ECA during sitting (A) and standing (B)

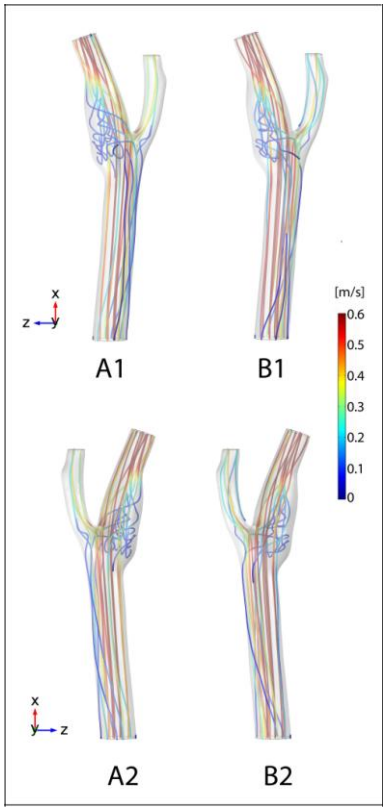

Figure 5: Streamlines of velocity magnitude at systolic peak during sitting (A) and standing (B), considering the frontal (1) and posterior (2) views.

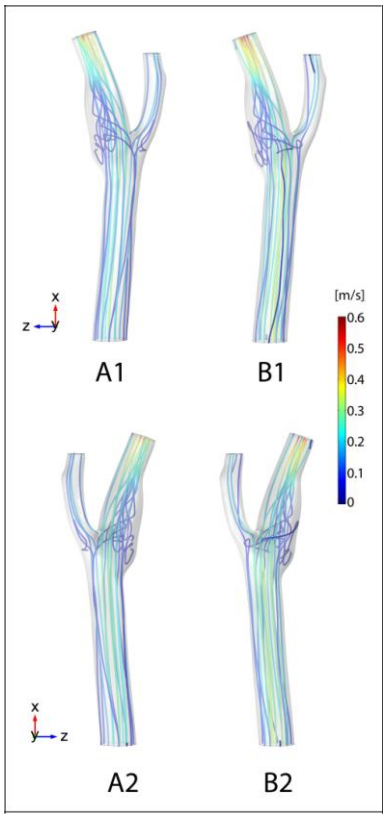

Figure 6: Streamlines of velocity magnitude at end diastole during sitting (A) and standing (B), considering the frontal (1) and posterior (2) views.

3.3. Hemodynamic parameters

The TAWSS distribution in sitting and standing is reported in Figure 7. Low WSS values are obtained in the bifurcation in correspondence of the carotid bulb, where stasis occurs. The worse TAWSS behavior happens in the sitting case, because a big area presents very low WSS, with zero value in some points (A1).

Moreover, WSS $\leq$ 0.4 Pa is associated with IMT (Glor et al. 2003), so in this case there is a high probability of wall thickening.

To investigate the flow pattern and its directionality, in terms of orderly or chaotic flow, unidirectional or retrograde flow and, consequently, WSS oscillation, the OSI pattern is illustrated in Figure 8. Common features among the two postural positions are that high values are recorded in the bifurcation in correspondence of the emergence of ECA and in the final area of carotid bulb, so the flow is swirling in all time of the cardiac cycle, and that 0 OSI characterized the remain areas, suggesting that orderly flow characterized these regions in the cardiac cycle. In sitting position the areas with OSI $\geq$ 0.145 are more extensive, so the carotid has a higher predisposition to endothelial dysfunction and atherogenesis (Ku et al. 1985) in this case.

Finally, the RRT was evaluated and its distribution considering 1 cardiac cycle is shown in Figure 9. During prolonged sitting, high time characterizes the bifurcation and the carotid bulb, whereas the remain regions of carotid artery is exposed to low RRT. On contrary, only few points present high RRT (10 Pa^{-1}) in standing position.

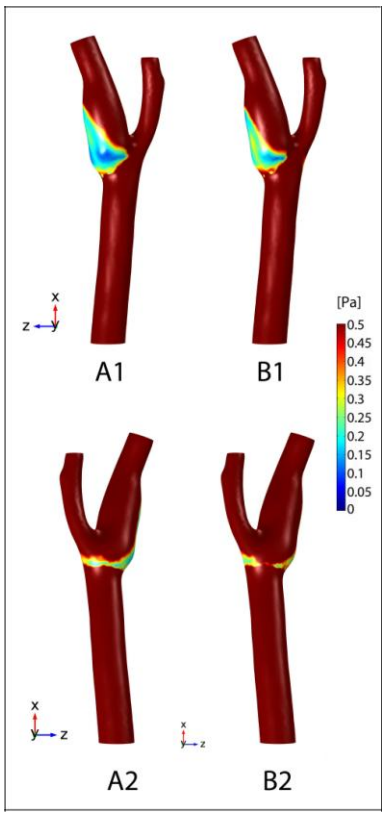

Figure 7: TAWSS during sitting (A) and standing (B), considering the frontal (1) and posterior (2) views.

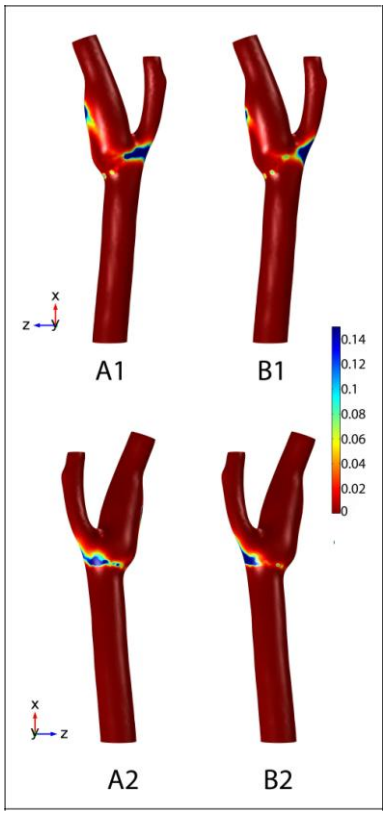

Figure 8: OSI during sitting (A) and standing (B), considering the frontal (1) and posterior (2) views.

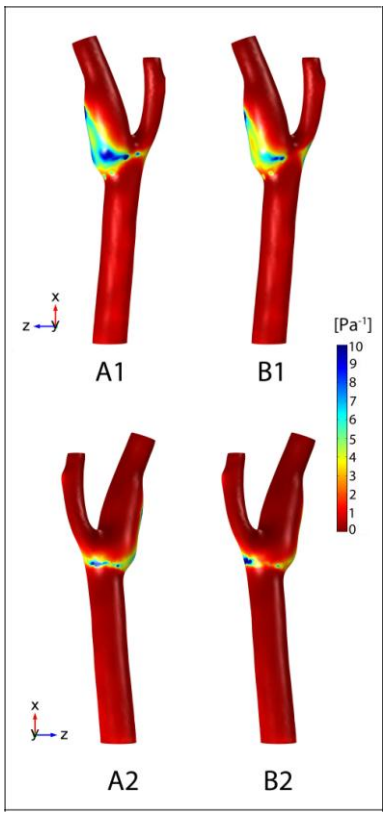

Figure 9: RRT during sitting (A) and standing (B), considering the frontal (1) and posterior (2) views.

Moreover, the atherogenic endothelial phenotype is promote in the areas with TAWSS $\leq$ 0.4 Pa and RRT $\geq$ 10 Pa^{-1} (Malek et al. 1999, Lee at al. 2009), so the worse situation occurs after prolonged sitting.

4. CONCLUSION

This computational study provides detailed information regarding the hemodynamic changes that occurred in the carotid bifurcation considering prolonged sitting and standing. The numerical results suggest that the carotid bulb is the most atherosclerosis susceptible location both for the sitting and the standing position. Furthermore, the worse hemodynamic profile is generated after prolonged sitting time, suggesting that a high risk of plaque formation and, consequently, of stenosis could happen.

REFERENCES

Azhim A., Katai M., Akutagawa M., Hirao Y., Yoshizaki K., Obara S., ... and Kinouchi, Y., 2007. Exercise improved age-associated changes in the carotid blood velocity waveforms. J. of Biomed. & Pharm. Eng, 1, 17-26.

Azhim A., Ueno A., Tanaka M., Akutagawa M. and Kinouchi Y., 2011. Evaluation of blood flow velocity envelope in common carotid artery for reference data. Biomedical Signal Processing and Control, 6(2), 209-215.

Cutnell J. D. and Johnson, K.W., 1998. Physics. Wiley, New York.

Dong J., Wong K. K. and Tu J., 2013. Hemodynamics analysis of patient-specific carotid bifurcation: A CFD model of downstream peripheral vascular impedance. International journal for numerical methods in biomedical engineering, 29(4), 476-491.

Dunstan D.W., Kingwell B.A., Larsen R., Healy G.N., Cerin E., Hamilton M. T., ... and Owen N., 2012. Breaking up prolonged sitting reduces postprandial glucose and insulin responses. Diabetes care, 35(5), 976-983.

Frostegard J., 2013. Immunity, atherosclerosis and cardiovascular disease. BMC medicine, 11(1), 117.

García-Hermoso A., Martínez-Vizcaíno V., Recio-Rodríguez J.I., Sánchez-López M., Gómez-Marcos M.Á., García-Ortiz L. and EVIDENT Group., 2015. Sedentary behaviour patterns and carotid intima-media thickness in Spanish healthy adult population. Atherosclerosis, 239(2), 571-576.

Glor F.P., Long Q., Hughes A.D., Augst A.D., Ariff B., Thom S.M., ... and Xu X.Y., 2003. Reproducibility study of magnetic resonance image-based computational fluid dynamics prediction of carotid bifurcation flow. Annals of Biomedical Engineering, 31(2), 142-151.

Huynh Q.L., Blizzard C.L., Sharman J.E., Magnussen C.G., Dwyer T. and Venn A.J., 2014. The cross-sectional association of sitting time with carotid artery stiffness in young adults. BMJ open, 4(3), e004384.

Knight J., Olgac U., Saur S.C., Poulikakos D., Marshall W., Cattin P.C., ... and Kurtcuoglu V., 2010. Choosing the optimal wall shear parameter for the prediction of plaque location—a patient-specific computational study in human right coronary arteries. Atherosclerosis, 211(2), 445-450.

Kozàkovà M., Palombo C., Morizzo C., Nolan J.J., Konrad T. and Balkau B., 2010. Effect of sedentary behaviour and vigorous physical activity on segment-specific carotid wall thickness and its progression in a healthy population. European heart journal, 31(12), 1511-1519.

Ku D.N., Giddens D.P., Zarins C.K. and Glagov S., 1985. Pulsatile flow and atherosclerosis in the human carotid bifurcation. Positive correlation between plaque location and low oscillating shear stress. Arteriosclerosis, thrombosis, and vascular biology, 5(3), 293-302.

Lee S.W., Antiga L., Spence J.D. and Steinman D.A. (2008). Geometry of the carotid bifurcation predicts its exposure to disturbed flow. Stroke, 39(8), 2341-2347.

Lee S.W., Antiga L. and Steinman D.A., 2009. Correlations among indicators of disturbed flow at the normal carotid bifurcation. Journal of biomechanical engineering, 131(6), 061013.

Malek A.M., Alper S.L. and Izumo S., 1999. Hemodynamic shear stress and its role in atherosclerosis. Jama, 282(21), 2035-2042.

Newcomer S.C., Sauder C.L., Kuipers N.T., Laughlin MH. and Ray C.A., 2008. Effects of posture on shear rates in human brachial and superficial femoral arteries. American Journal of Physiology-Heart and Circulatory Physiology, 294(4), H1833-H1839.

Owen N., Healy G.N., Matthews C.E. and Dunstan D.W., 2010. Too much sitting: the population-health science of sedentary behavior. Exercise and sport sciences reviews, 38(3), 105.

Tu J., Yeoh G.H. and Liu C., 2007. Computational fluid dynamics: a practical approach. Butterworth-Heinemann.

Van de Vosse F. N. and Stergiopulos N., 2011. Pulse wave propagation in the arterial tree. Annual Review of Fluid Mechanics, 43, 467-499.

Yilmaz F. and Gundogdu M.Y., 2008. A critical review on blood flow in large arteries; relevance to blood rheology, viscosity models, and physiologic conditions. Korea-Australia Rheology Journal, 20(4), 197-211.

AGENT-BASED MODELLING FOR RETHINKING THE SOCIOECONOMIC DETERMINANTS OF CHILD HEALTH IN SUB-SAHARAN AFRICA

Carine Van Malderen [(a)], Hedwig Deconinck [(b)], Niko Speybroeck [(c)], Jean-Christophe Chiem [(d)]

[(a),(b),(c),(d)] Institute of Health and Society (IRSS), Université catholique de Louvain, Brussels, Belgium

[(a)]carine.vanmalderen@uclouvain.be, [(b)]hedwig.deconinck@gmail.com, [(c)]niko.speybroeck@uclouvain.be, [(d)]jean-christophe.chiem@uclouvain.be

ABSTRACT

Socioeconomic factors play distal roles in shaping populations' health. In sub-Saharan Africa, these structural health determinants are strongly associated with intermediate determinants of under-5 mortality such as lifestyle factors, health seeking behaviour, or exposure to a health threat. The aim of the study was to use simulation tools for rethinking the dynamics between socioeconomic factors, preventive health measures, and child health. An agent-based model was developed, consisting of rules and equations based on data from four Demographic and Health Surveys conducted in sub-Saharan countries. The model, visualizing the impact of different factors and complex effects, enhanced the understanding and debate on causal pathways of socioeconomic inequalities in under-5 mortality.

Keywords: Socioeconomic, child health, agent-based modelling, population surveys

1. INTRODUCTION

The global under-5 mortality rate has dropped from 90 deaths per 1,000 live births in 1990 to 46 in 2013. The highest rates are in sub-Saharan Africa, with an under-5 mortality rate of 92 deaths per 1,000 live births in 2012. The leading causes of death among children under-5 include pneumonia, preterm birth complications, intrapartum-related complications, diarrhoea and malaria (UN Inter-agency Group for Child Mortality Estimation 2014). Even if under-5 mortality has declined in most sub-Saharan African countries, substantial inequalities exist between population sub-groups within countries (Boco 2010).

The emergence and evolution of socioeconomic inequalities in health involves multiple factors interacting with each other at different levels (individual, household and community). Regression models (such as generalized linear models and decomposition techniques) provided interesting insights on the contribution of different determinants to health and health inequality (Van Malderen C. et al. 2013). However, models incorporating complex and indirect health effects are needed to better understand causal pathways that produce health inequality over time. Simulation models, offering simplified representations of a certain real-life system (Galea et al. 2010; Kaplan et al. 2011; Lempert 2002), have the potential to integrate the growing knowledge about multilevel causes of health and their patterns of feedback and interaction. By mimicking the possible mechanisms responsible for the generation and maintenance of health inequalities, simulation models can also be used to inform how specific policy interventions could influence the health of populations (Auchincloss et al. 2011).

By using simulation modelling, we show a new approach to study socioeconomic determination of health with applying a complexity lens. We show how an agent-based simulation model based on population survey data can help visualizing and understanding the complex processes leading to health and health inequality. The model explores the following questions:

- How to imagine a dynamic population with cross-sectional data?
- Which socioeconomic determinant influences urban versus rural health inequalities the most?
- Why a same shock (or policy change) may have a different health impact depending on the respective country-context?
- How the degree of collectivism could influence a change in socioeconomic determinants?
- What if the association between education and use of preventive health measures was influenced by the level of education in the population?
- What would be the impact of a feedback loop of ill health on the distribution of future socioeconomic determinants?

2. METHODS

2.1. Conceptual framework

Socioeconomic determinants are described as the distal determinants of child mortality in the Mosley and Chen conceptual framework (Mosley and Chen 2003). In their framework, the authors distinguish the community level variables (ecological setting, political economy and health system), the household level

variables (income and wealth) and the individual variables (parents' education, time, health, traditions/norms/attitudes). For this simulation exercise and based on available data, the following variables were retained: mother's education, residence (urban or rural), housing, transport means, age of the child and use of preventive health interventions. These determinants are linked together (Figure 1).

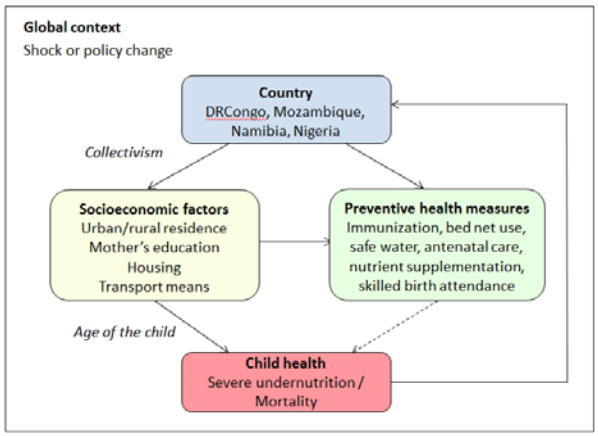

Figure 1: Conceptual framework of studied determinants and under-5 mortality (inspired by (Mosley and Chen 2003)

Dotted arrow: the relationship was not modelled because the cross-sectional data did not allow a reliable assessment of the impact of prevention score on child health.

2.2. Data

Data from Demographic and Health Surveys (DHS) were used. Four sub-Saharan African countries with a recent standard DHS were included: Democratic Republic of the Congo 2013, Mozambique 2011, Namibia 2013, and Nigeria 2013, representing Central, Eastern, Southern and Western Africa, respectively. The analysis was restricted to children under 5 years of age. Details on survey sampling, data collection and data processing can be found in the country reports, available from the Measure DHS website (Measure DHS 2015).

2.2.1. Child age and health

Age of children in months and under-5 (0-59 months) death were obtained from the birth history of interviewed females aged 15 to 49 years old. Weight of children born five years prior to the interview was measured during the survey and weight-for-age standard deviations (according to the World Health Organization 2006 Child Growth Standard) were used to assess undernutrition. Severe undernutrition was defined as weight-for-age less than -3 standard deviations. The health outcome (ill health) is a combination of severe undernutrition and mortality. The idea of combining these two outcomes was proposed by (Mosley and Chen 2003). The combination of the two indicators of ill health allowed a more robust assessment of the regression coefficients avoiding two common problems in regression analysis: the weak number of cases when studying mortality alone, and missing values when studying malnutrition alone.

2.2.2. Preventive health measures

Seven indicators of preventive health measures were gathered into a co-coverage indicator (Barros and Victora 2013): skilled antenatal care attendance (at least one visit with a doctor, midwife or nurse); skilled birth attendance (delivery assisted by a doctor, midwife or nurse); bednet use (whether children under-5 in the household slept under a bednet the night prior to the interview), vitamin A supplementation, BCG (tuberculosis) and DPT3 (diphtheria-tetanus-pertussis) immunization and improved drinking water. A high prevention score was defined as the use of at least four preventive health interventions reported by the mother.

2.2.3. Socioeconomic factors

Four socioeconomic factors were selected according to their reported association with severe undernutrition, mortality and preventive measures in children under 5 (Coleman et al. 2011; Van de Poel et al. 2007; Van de Poel et al. 2009; Van Malderen C. et al. 2013) and the availability of data: urban or rural residence, mother's education (primary education completed or not), quality housing (quality floor, roof and wall + improved toilet facility), and transport means (having a car or a motorbike).

2.3. Description of the model

Child

Health status	The child is healthy (0) or ill (1)
Age	Age of the child in months
Urban	The child lives in a urban residence or not
Education	The mother has a primary education level, or none
Housing	The child lives in a quality house or not
Transport	The child lives in a household having a moto or a car

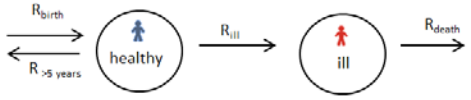

Parameter	Description
R_{birth}	Births (alive) in the population each month
$R_{>5\ years}$	Children older than 5 years old leave the population
R_{ill}	P(get ill) = f(urban, education, housing, transport)
R_{death}	Ill children leave the population

Figure 2: Model overview: agent, variables and health pathways

The population consists of children 0 to 59 months old characterized by the following variables: health status, age, urban residence, mother's primary education, quality housing, and transport means (Figure 2). DHS datasets were transferred to RGui (R version

3.1.1., The R foundation for Statistical Computing) for analysis. The distribution of children's socioeconomic data -urban residence, education, housing and transport- were transferred into Netlogo 5.2-RC3 using the R package "RNetLogo".

The time unit is one month. Each month, 1000 children are born and enter the population. Each created child receives the socioeconomic attributes of a child randomly selected from the survey data. Children may transit through two different states: healthy or ill health (severe undernutrition or death). Each month, new children are born, grow up, and have a R_{ill} probability to get ill. Children leave the population when they are ill or when they reach 60 months of age.

2.4. Regression equations

Equations for calculating probabilities of having a high prevention score and of child ill health (R_{ill}) given the observed values of the socioeconomic factors were obtained with logistic regression. The general formula was:

$$\text{Logit}(p) = \alpha + \beta_1 \text{ urban} + \beta_2 \text{ education} + \beta_3 \text{ housing} + \beta_4 \text{ transport}$$

In each country, the parameters α, β_1, β_2, β_3 and β_4 were assessed for three outcomes:

- having a high prevention score
- becoming ill if the child is less than 12 months old
- becoming ill if the child is 12-59 months old.

Regression coefficients were then transferred into Netlogo for the simulation. For a given child, the probability of having a high prevention score or becoming ill was derived from the logit(p) obtained with the aforementioned regression equations.

2.5. Outcomes

Two outcomes are compared between urban and rural areas:

- Proportion of high prevention score
- Incidence of ill health

2.6. Scenarios

After children are created according to the DHS values, a proportion of children either loses (shock: event of an environmental or man-made origin that impacts on socioeconomic determinants) or gain (policy change) one or several socioeconomic attributes.

2.7. Additional (optional) if-then rules

Several rules were added to the model to account for more complexity (Table 1). First, the possible effect of a country's degree of collectivism (collectivism, contrary to individualism, "pertains to societies in which people from birth onwards are integrated into strong, cohesive in-groups, which throughout people's lifetime continue to protect them in exchange for unquestioning loyalty" (Allik and Realo 2004)) was modelled. Second, the association between education and preventive health measures uptake (the higher the level of education in a population, the higher the association between health messages and preventive health measures uptake) was tested. This assumption integrates the idea that "campaign strategies may only be successful to the degree that they are backed by community education" (Saunders and Goddard 2015). Third, a feedback loop modelling the effect of child health on future socioeconomic determinants was introduced. The historical association between declines in child mortality, rising education and economic growth was modelled in (Azarnert 2005).

Table 1: Additional if/then rules

	Rule
High collectivism	If a child's education, housing, or transport is 0, then it becomes the average of his closest neighbours with a given probability. Rural and urban areas are separated in the simulation space.
Variable slope	The association between education and preventive health measures uptake is proportional to the level of education in the population; the slope, recalculated each month, is increased by the average education in a given subgroup.
Feedback loop	A monthly decrease in ill health is applied. Education, housing and transport in new children are increased by either the ratio or the difference between the baseline mortality and the actualized month's mortality level.

3. RESULTS

The six research questions listed in the introduction were explored using the basic simulation model and additional if-then rules. In this simulation we made the assumption that regression equations remain unchanged month after month. Results should not be interpreted as predictions. Units were expressly removed from plots so the reader can focus on behavior over time.

3.1. How to imagine a dynamic population with cross-sectional data?

3.1.1. Regression coefficients

Table 2: Regression coefficients from the multivariate regression models estimating the effect of socioeconomic determinants on a high prevention score and ill health, DHS 2011-2013

	Prevention	Ill health (<12 months)	Ill health (12-59 months)
DRCongo			
intercept	-1.14	-1.72	-1.05
urban	1.05	-0.37	-0.17
education	0.36	0.05	-0.26
housing	1.07	-0.71	-0.22
transport	0.13	0.34	-0.20
Mozambique			
intercept	-0.98	-2.01	-1.88
urban	1.30	0.15	-0.10
education	0.83	-0.92	-0.32
housing	0.95	-0.26	-0.10
transport	0.34	-0.36	-0.31
Namibia			
intercept	0.37	-1.36	-1.50
urban	0.56	0.00	0.20
education	0.70	-0.59	-0.11
housing	0.26	0.47	-0.58
transport	0.09	-0.32	-0.63
Nigeria			
intercept	-3.00	-1.31	-0.83
urban	0.93	-0.09	-0.14
education	2.10	-0.50	-0.75
housing	0.94	-0.07	-0.27
transport	0.03	-0.12	-0.06

In the four countries, all socioeconomic determinants were associated with a high prevention score (Table 2). In infants less than 12 months old, transport means, urban residence and quality housing were associated with higher odds of ill health in some countries. In children 12-59 months old, socioeconomic determinants were associated with lower odds of ill health, with the exception of urban residence in Namibia.

3.1.2. Simulated versus observed values

Table 3: Comparison between observed (DHS) and simulated values of socioeconomic determinants, preventive health measures uptake and ill health.

	DRCongo (N = 18446)		Mozambique (N = 10609)		Namibia (N = 4896)		Nigeria (N = 30959)	
	Obs.	Sim.	Obs.	Sim.	Obs.	Sim.	Obs.	Sim.
Urban	29	28-38	30	29-36	45	44-46	33	32-40
Education	44	44-48	19	20-31	75	76-82	47	48-59
Housing	7	8-12	9	9-13	31	27-31	28	28-35
Transport	6	6-7	9	9-13	20	20-25	46	46-51
Prevention*	31	23-35	47	27-43	77	47-67	28	17-30
Ill health	22	14-16	11	10-12	16	14-18	20	15-18

Obs.=observed value from DHS data; Sim. = minimum and maximum value obtained from a 100 months simulation. *For the observed values, DRCongo: N = 9995, Mozambique: N=6303, Namibia: N=2973, Nigeria: N=16871

At the first step of the simulation (setup), the distribution of socioeconomic attributes in the simulated population was similar to the distribution observed in the DHS data (Table 2).

After running the simulation, some socioeconomic determinants deviated from their initial values, because of a higher mortality in several socioeconomic sub-groups. For instance, in DRCongo, the proportion of children in urban areas increased from 28 to 38 because children in urban areas had a lower death probability (see regression equations in Table 2). Accordingly, as the socioeconomic determinants associated with better outcomes underwent a "natural selection", preventive health measures uptake and ill health also improved (simulated prevention scores were higher and simulated ill health values were lower) compared to observed values.

3.2. Which socioeconomic determinant influences urban-rural inequality in use of preventive measures and ill health outcome the most?

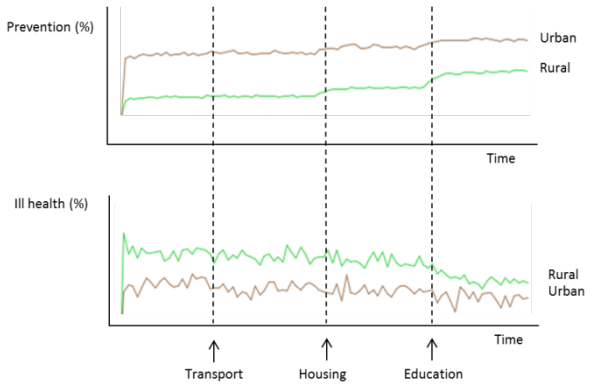

Figure 3: Impact of increased proportions of transport, housing and education on the prevention score and ill health by type of residence, Nigeria

The country with the highest absolute urban-rural inequality in ill health, Nigeria, was selected to illustrate how changing the proportion of socioeconomic determinants in the virtual population was expected to impact prevention and ill health outcomes.

Transport, housing and education increased by 25% in new children entering the model. Education had the strongest impact on both preventive health measures uptake and ill health. Indeed, education was positively associated with a high prevention score and negatively associated with ill health in both age groups (Table 2).

3.3. Why a same shock (or policy change) may have a different health impact depending on the respective country-context?

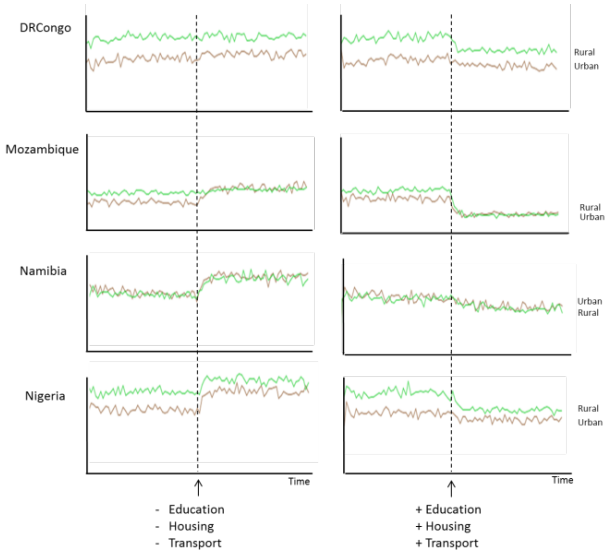

Figure 4: Impact of a shock and policy change targeting the three socioeconomic determinants on child ill health (%) in the four countries

In the four countries, after 45 simulation months, a shock lowering education, housing and transport by 25% in newborn children was applied (Figure 4, left). This simulation shows that the impact of a shock with a similar socioeconomic impact may differ according to the country-context.

In DRCongo, a shock did not result in a marked increase in ill health. Looking at the changes in the socioeconomic determinants, education initially at 44% showed a large decrease, whereas housing and transport that were low at baseline (8-12 and 6-7, respectively) remained low. Moreover, in this country, education was not negatively associated with ill health in infants less than 12 months old (Table 2).

In Mozambique, the shock resulted in an increase in ill health in urban areas. Indeed, urban residence is positively associated with ill health in infants less than 12 months old, and the effect of the induced shock could not be counteracted by the socioeconomic determinants (Table 2).

In Nigeria, where all socioeconomic determinants were associated with less ill health, the shock resulted in an increase in ill health for all children. A positive intervention that increases education, housing and transport by 25% (Figure 4, on the right) resulted in larger decreases of ill health in countries were the socioeconomic determinants were initially low, such as in DRCongo, Mozambique and rural Nigeria (Table 1).

3.4. How the degree of collectivism could influence a change in the socioeconomic determinants?

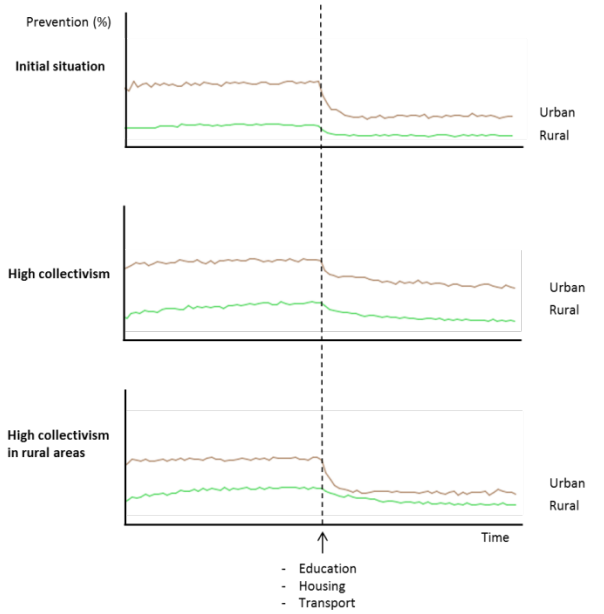

Figure 5: Impact of a shock affecting the three socioeconomic determinants on the prevention score and the role of collectivism, Nigeria

In this simulation, rural and urban areas were separated in the simulation space and children without education, housing or transport had a 50% probability to get these resources from their neighbours (Figure 5).

In the initial situation, the simulated shock (25% reduction in the three socioeconomic determinants) resulted in a large decrease in preventive measures use. In case of collectivism, this decrease was softened. When the collectivism rule was applied only in children from rural areas, the urban-rural inequality tended to be lower.

3.5. What if the association between education and use of preventive health measures was influenced by the mean of education in the population?

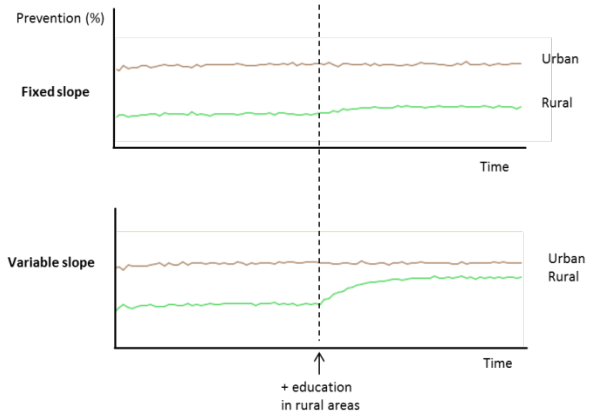

Figure 6: How changing the association (slope) between education and preventive measures use could improve the coverage of preventive health measures in rural areas, Mozambique

In the samples used, Mozambique showed the lowest coverage in education. In the first simulation (fixed slope obtained from the regression analysis), after 45 months education increased by 5% each month in rural areas (Figure 6). In the second simulation (variable slope), education also increased by 5% each month in rural areas. In addition, in rural areas the slope of education in the equation determining odds of having a high prevention score was proportionate to the level of education of rural areas. In urban areas no additional rule was applied.

The simulation illustrates that increasing education (literacy) and its association with increased uptake of preventive health measures (e.g., through information, education and communication activities) could result in a greater improvement in preventive health measures coverage than increasing education alone.

3.6. What would be the impact of a feedback loop of ill health on future socioeconomic determinants?

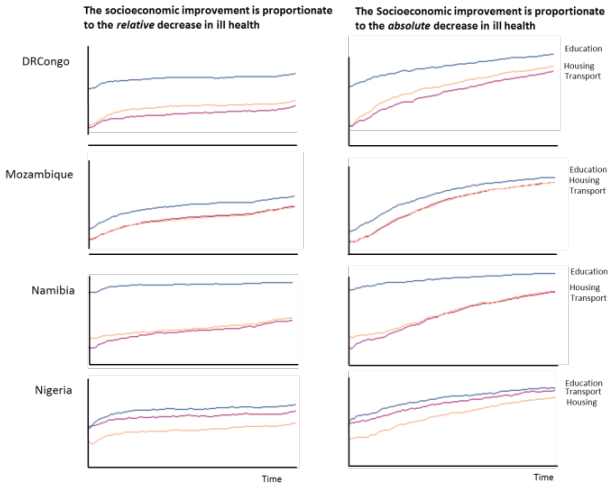

Figure 7: How a decrease in mortality could impact the socioeconomic determinants in the four countries

Here, a monthly decrease in ill health (the intercept) was applied and the impact of such a decrease on the socioeconomic determinants was simulated in two different ways. Education, housing and transport in new children were increased by (i) the ratio (Figure 7, left) and (ii) the difference (Figure 7, right) between the baseline mortality and the actualized month's mortality level.

This exercise illustrates that improvement in the socioeconomic determinants could be possible if the overall situation in the country would improve. The assumptions, though totally imaginary (how could this observation be ever tested in real-time?), raise the question on how this improvement could be obtained by a reduction in ill health. The improvement in socioeconomic resources resulted in an improvement in preventive health measures coverage and could have an accelerating effect on improved health outcomes (decreased ill health). Note that the accelerated decline was weak because a weak reduction in ill health (0.15% decline) was modelled.

4. DISCUSSION

The paper aimed at introducing a new approach for rethinking the socioeconomic determination of health and exploring complex features that go beyond the scope of what is usually studied.

4.1. Benefits

4.1.1. Imagine the impact of a change in a socioeconomic determinant on a population health and health inequality

In its most basic form, the model reproduces the patterns obtained from the regression equations assessed on the DHS data. Taking real combination of socioeconomic attributes and applying the regression equations obtained from the same DHS data allows having an idea of the possible impact of a determinant.

Interpreting the coefficient only does not directly inform on how a change in this determinant will affect the health of population and health distribution between urban and rural areas. Indeed, the improvement in outcomes may depend on the initial proportions of socioeconomic determinants. In DRCongo and Mozambique, the gain obtained from an increase in the three socioeconomic determinants was higher than in Namibia where the initial proportion of education was already high.

The effect of improvement in socioeconomic determinants on urban-rural inequalities in preventive health measures uptake and health depends on several elements: the proportion of children in urban and rural areas; the proportion of socioeconomic determinants in each area; the association of urban residence with preventive health measures uptake and health; having a global vision of the phenomenon is hard when considering each element separately. The simulation allowed first visualizing the situation and then trying to understand the observed patterns by looking at the possible effect of each element.

4.1.2. Taking an interaction into account: having a vision of under-five mortality knowing that the effects of socioeconomic determinants may differ according to age of the child

An important added value is to visualize simultaneously the effects of three different equations: prevention score, ill health in children <12 months and ill health in children 12-59 months according to the same socioeconomic determinants. When studying the effect of determinants of one outcome, it remains easy to understand the effect of each determinant included and the possible change in the outcome that could be induced if the determinant was changed. Determinants of child mortality may differ according to age of the child and studies usually focus either on the determinants of infant (<12 months) mortality (Drevenstedt et al. 2008; Hosseinpoor et al. 2006; Van de Poel et al. 2009) or child (0-59 months) (Ayotunde et al. 2009; Garenne and Gakusi 2006; Houweling et al.

2005) mortality. Distinguish the effects in both sub-groups keeping under-5 ill health as an outcome could be possible in this simulation.
In countries where some determinants were positively associated with ill health in one age group but negatively associated with ill health in the other age group, the simulation allowed visualizing what would be the total effect on the overall child health.

4.1.3. Visualize the production of two outcomes simultaneously

In this simulation, two outcomes were visualized simultaneously: the prevention score and ill health, according to the same socioeconomic determinants. Though the direct relation between preventive measures and child health could not be modelled, studying both simultaneously allowed observing how improvements in socioeconomic determinants directly improved either preventive health measures coverage or child health. The latter were usually less marked, and reasons are specific for each situation. Either association (coefficients) with the prevention score were higher than with ill health, or determinants were positively associated with ill health in one age group and negatively associated with ill health in the other age group (e.g., housing in Namibia).

4.1.4. Imagine the role of complex effects

Complex effects such as the role of social capital (Allik and Realo 2004) or the impact of ill health on socioeconomic resources (Azarnert 2005) are assumed but hardly quantifiable. In the simulation such complex effect were yet modelled. While the formulation of rules is arbitrary and does not pretend to explain what really happens, it attempts to imagine how complex and still unknown processes shape population health, and increase awareness of complex effects.

4.2. Limitations

Limitations are all the unavoidable analytical and interpretation errors that could occur at each step of the study, e.g.: data collection (including biases linked to interviews), use of preventive health measures and ill health scores, regression coefficient estimations, transformation of logit(p) into probabilities, choices of the rules. The only validation possible was comparing the simulated proportions of the selected variables with the DHS proportions. Moreover, the development of a dynamic vision (process-based) from cross-sectional data was a major challenge of the study. The aforementioned limitations do not allow the model to perform predictions.

4.3. Perspectives

Simulation modelling involves a lengthy process of combining data analysis, expert opinions, variables and equations selection and rules formulation, and exploring simulation outputs (Figure 8). Learning about the subject (here, socioeconomic determinants of child health) occurs at each step. The questions explored here, such as the role of social capital, interactions between education and preventive health measures and applying feedback loops, will stimulate new investigations. The discussion with experts initiated in the development of this initial model will be continued; simulation outputs will be confronted and variables, equations and rules could be further adapted.

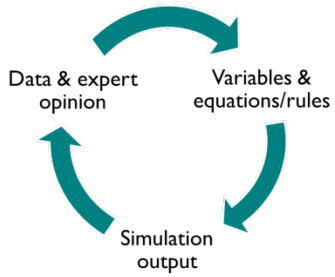

Figure 8: Process of learning about the mechanism of socioeconomic health determinants in children through simulation modelling

ACKNOWLEDGMENTS

We thank Cesar Victora and Aluisio Barros (International Center for Equity in Health, Pelotas, Brazil) for their contribution in the development of the conceptual framework and their advice in the development of the simulation model.

APPENDIX

1. OVERVIEW OF THE NETLOGO INTERFACE

2. R CODE (RNETLOGO): EXAMPLES

```
# a vector with total number of children
in each country
num<-c(18446,11377,30959, 4896, 10609 )

# Initialization in Netlogo
NLCommand("clear")

# put data into Netlogo :
# the « num » vector
```

```
NLDfToList(num)

# a dataframe with regression
coefficients for the three outcomes
NLDfToList(DRCglm[,2:4])

# the database with the four
socioeconomic variables
NLDfToList(DRCongo)

# specify the country in the Netlogo
chooser
NLCommand("set Country \"DRCongo\"")

# run the setup in Netlogo
NLCommand("setup")

# report the minimum and maximum
percentage of urban for 100 months
urbs <- NLDoReport(100, "go", "%urb")
min(unlist(urbs))
max(unlist(urbs))
```

3. NETLOGO CODE

The full model may be accessed on http://socioeconomicdeterminants.sourceforge.net .

The following lines show some extracts for illustration.

```
;*************************************
; globals
;*************************************
globals [
house urb ed transp ; socioeconomic
variables imported from R (Demographic
and Health Surveys) with RNetlogo. These
are list ranging from 0 to the total
number of individuals in the country.
X2 X3 X4 ; lists of regression
coefficients for ill health in children
<12 months old (R2), ill health in
children 12-59 months old (R3) and a high
prevention score (R4), imported from R
num ; a list containing the total number
of individuals for each country, imported
from R
mortality2 ; a list containing mortality
rates for each simulated month
Pfeed ]

;*************************************
; Children
;*************************************
breed [children child]
children-own [status age prevention
transport housing education urban]

to setup-children [num_children]
if ticks = 0 [ set mortality2 [  ] ]
set-default-shape children "person"
create-children num_children [ ; the
number of created children is given by
the slider "num_children"
set age random 0
set status 0
set color blue
let number 0
let ncountry 0
if Country = "DRCongo" [set ncountry 0]
if Country = "Ethiopia" [set ncountry 1]
if Country = "Nigeria" [set ncountry 2]
if Country = "Namibia" [set ncountry 3]
if Country = "Mozambique" [set ncountry
4]
set number random item ncountry num ; a
number between 0 and the total number of
individuals in the country is randomly
selected
set transport item number transp ; each
created child receives attributes from
the child randomly selected in the list
(at the position defined by the number
selected in the line above)
set education item number ed
set housing item number house
set urban item number urb]

; optional if-then rules
if intervention-onebyone [
if ticks = 18 [ ask children with
[education = 0] [if random 100 < 25 [set
education 1]]]
    if ticks = 42 [ ask children with
[transport = 0] [if random 100 < 25 [set
transport 1]]]
    if ticks = 66 [ ask children with
[housing = 0] [if random 100 < 25 [set
housing 1]]]]

if shock [ if ticks > 50 [
ask children with [education = 1] [if
random 100 < 25 [set education 0]]
ask children with [transport = 1] [if
random 100 < 25 [set transport 0]]
ask children with [housing = 1] [if
random 100 < 25 [set housing 0]]]]

if policy-change [ if ticks > 50 [
ask children with [education = 0 ] [if
random 100 < 25 [set education 1]]
ask children with [transport = 0] [if
random 100 < 25 [set transport 1]]
ask children with [housing = 0] [if
random 100 < 25 [set housing 1]]]]

if feedback [ if ticks > 1 [
set Pfeed (( item 1 mortality2 - item
(ticks - 1 ) mortality2))
ask children with [education = 0] [if
random 100 < Pfeed [set education 1]]
ask children  with [transport = 0] [if
random 100 < Pfeed [set transport 1]]
ask children with [housing = 0] [if
random 100 < Pfeed [set housing 1]]]]

; separate children from urban and rural
area for the collectivism rule
ask children with [urban = 1] [set xcor
random-float -16 set ycor random-ycor]
ask children with [urban = 0] [set xcor
random-float 16 set ycor random-ycor]
end

;*************************************
```

```
; children actions (every month)
;*************************************
to old
ask children [ set age age + 1  if age >
59 [die]]
end

to become-wastedordead
let logitdead 0
let Pdead 0
ask children with [status = 0] [
let intercept1 0
let intercept2 0
set intercept1 item 0 x2
set intercept2 item 0 x3
if feedback [set intercept1 intercept1 -
ticks * 0.01]
if feedback [set intercept2 intercept2 -
ticks * 0.01]
ifelse age < 12
[set logitdead intercept1 + (item 1 X2 *
transport) + (item 2 X2  * housing) + (
item 3 X2 * education) + (item 4 X2 *
urban)]
 [set logitdead intercept2  + (item 1 X3
* transport) + ( item 2 X3 * housing) +
(item 3 X3 * education)+ (item 4 X3 *
urban)]
set Pdead (exp (logitdead) )/ ((1 +
exp(logitdead))) * 100
if random 100 < Pdead [set status 1 set
color red]]
end

to compute-prevention
  ask children [
    let logitprevent 0
    let Pprevent 0
    let slope 0
ifelse variable-slope
[   ifelse urban = 1
    [set slope item 3 X4]
    [set slope item 3 X4 + %ed-urban]]
[ set slope item 3 X4]
    set logitprevent  item 0 X4 + (item 1
X4   * transport ) + ( item 2 X4  *
housing ) + ( slope   * education) +
(item 4 X4 * urban)
    set Pprevent exp (logitprevent) / (1
+ exp(logitprevent)) * 100
    ifelse random-float 100 < Pprevent
    [set prevention 1]
    [set prevention 0]]
end

; collectivism if-then rule
to get-transport
  if collectivism = "high"  [
  ask children with [transport = 0 and
urban = 0] [if any? turtles-on neighbors
and random 100 < 50 [set transport mean
[transport] of turtles-on neighbors]]]
end

to get-education
  if collectivism = "high" [
  ask children with [education = 0 and
urban = 0] [if any? turtles-on neighbors
and random 100 < 50 [set education mean
[education] of turtles-on neighbors]]]
end

to get-housing
  if collectivism = "high"  [
  ask children with [housing = 0 and
urban = 0] [if any? turtles-on neighbors
and random 100 < 50 [set housing mean
[housing] of turtles-on neighbors]]]
end

;*************************************
; setup
;*************************************
to setup
  setup-children num_children_init
  reset-ticks
end


;*************************************
; go
;*************************************
to go
 get-transport
 get-education
 get-housing
 compute-prevention
 become-wastedordead
 set mortality2 lput mortality mortality2
 tick
 old
 setup-children num_children_init
 ask children with [status = 1] [die]
end


;*************************************
; clear
;*************************************
to clear
    __clear-all-and-reset-ticks
    set num_children_init 1000

    set collectivism "low"

end
```

REFERENCES

Allik, J. & Realo, A. 2004. Individualism-collectivism and social capital. Journal of Cross-cultural Psychology, 31, (1) 29-49

Auchincloss, A.H., Riolo, R.L., Brown, D.G., Cook, J., & Roux, A.V.D. 2011. An Agent-Based Model of Income Inequalities in Diet in the Context of Residential Segregation. American Journal of Preventive Medicine, 40, (3) 303-311

Ayotunde, T., Mary, O., Melvin, A.O., & Faniyi, F.F. 2009. Maternal age at birth and under-5 mortality in Nigeria. East Afr.J Public Health, 6, (1) 11-14

Azarnert, L.V. 2005. Child mortality, fertility, and human capital accumulation. J Popul Econ

Barros, A.J. & Victora, C.G. 2013. Measuring coverage in MNCH: determining and interpreting inequalities in coverage of maternal, newborn, and child health interventions. PLoS Med, 10, (5) e1001390

Boco, AG. 2010. Individual and community level effects on child mortality: an analysis of 28 demographic and health surveys in sub-Saharan Africa. DHS working papers MEASURE DHS

Coleman, B.J., Howard, E., & Jenkinson, A. 2011. The difference transport makes to child mortality and preventive healthcare efforts: Riders for Health. Arch.Dis.Child, 96, (2) 197-199

Drevenstedt, G.L., Crimmins, E.M., Vasunilashorn, S., & Finch, C.E. 2008. The rise and fall of excess male infant mortality. Proc.Natl.Acad.Sci.U.S A, 105, (13) 5016-5021

Galea, S., Riddle, M., & Kaplan, G.A. 2010. Causal thinking and complex system approaches in epidemiology. Int J Epidemiol., 39, (1) 97-106

Garenne, M. & Gakusi, A.E. 2006. Vulnerability and resilience: Determinants of under-five mortality changes in Zambia. World Development, 34, (10) 1765-1787

Hosseinpoor, A.R., van Doorslaer, E., Speybroeck, N., Naghavi, M., Mohammad, K., Majdzadeh, R., Delavar, B., Jamshidi, H., & Vega, J. 2006. Decomposing socioeconomic inequality in infant mortality in Iran. International Journal of Epidemiology, 35, (5) 1211-1219

Houweling, T.A., Caspar, A.E., Looman, W.N., & Mackenbach, J.P. 2005. Determinants of under-5 mortality among the poor and the rich: a cross-national analysis of 43 developing countries. Int J Epidemiol, 34, (6) 1257-1265

Kaplan, G., Galea, S., & Riddle, M. 2011. Complexity, Epidemiology and the Understanding of "What If". Journal of Epidemiology and Community Health, 65, A41

Lempert, R. 2002. Agent-based modeling as organizational and public policy simulators. Proceedings of the National Academy of Sciences of the United States of America, 99, 7195-7196

Measure DHS 2015. The Demographic and Health Surveys program. <http://www.dhsprogram.com>. (accessed 08/06/2015)

Mosley, W.H. & Chen, L.C. 2003. An analytical framework for the study of child survival in developing countries. 1984. Bull.World Health Organ, 81, (2) 140-145

Saunders, B.J. & Goddard, C. 2015. The role of mass media in facilitatingcommunity education and childabuse prevention strategies. The Australian Institute of Family Studies

UN Inter-agency Group for Child Mortality Estimation 2014. Levels & Trends in Child Mortality. Report 2014 (Estimates Developed by the UN Inter-agency Group for Child Mortality Estimation). United Nations Children's Fund

Van de Poel, E., Hosseinpoor, A.R., Jehu-Appiah, C., Vega, J., & Speybroeck, N. 2007. Malnutrition and the disproportional burden on the poor: the case of Ghana. International Journal for Equity in Health, 6, (21)

Van de Poel, E., O'Donnell, O., & van, D.E. 2009. What explains the rural-urban gap in infant mortality: household or community characteristics? Demography, 46, (4) 827-850

Van Malderen C., Van Oyen H., & Speybroeck, N. 2013. Contributing determinants of overall and wealth-related inequality in under-5 mortality in 13 African countries. J Epidemiol Community Health

ROTATED PRINCIPAL COMPONENTS FOR FUZZY SEGMENTATION SZINITIGGRAPHIC TIME SERIES IN INDIVIDUAL DOSE PLANING

Werner Backfrieder [(a)], Gerald Zwettler [(b)]

[(a)]Dept. Biomedical Informatics, University of Applied Sciences Upper Austria, Hagenberg, Austria
[(b)] Research Department, University of Applied Sciences Upper Austria, Hagenberg, Austria

[(a)]Werner.Backfrieder, [(b)]Gerald.Zwettler@fh-hagenberg.at

ABSTRACT
Time activity curves are assessed from whole body szintigraphic time series for individual dose estimation to limit the applicable therapeutic dose, preventing critical organs from substantial damage during radiation therapy. Whole body scans are projective images, thus organ ROIs may overlap. After careful image registration rotated principal components analysis is applied to the time series, identifying image parts with similar dynamics. This method allows the separation of overlapping structures providing fuzzy regions, where fractions of the pixel counts are assigned to the respective accumulating morphology. The summed counts from theses fuzzy regions are modified with the physical decay constant of the considered therapeutic isotope, providing the correct time samples for further dose calculation. Mono- or bi-exponential regression yields the time activity curves for the respective morphologies, passed to a standard dose calculation program. The newly developed method allows the fuzzy separation of overlapping structures in projective planar imaging series, yielding more accurate dose calculation in individual radiation therapy.

Keywords: factor analysis, image registration, dose planning, regression

1. INTRODUCTION

The internal application of radioactive elements for therapy has long tradition in oncology. The specific bindings of a radiopharmaceutical to tumor tissue or accumulation in glands are utilized to concentrate therapeutic dosage in the target region. But radioactive dose is not only focused there and collateral damage has to be generally avoided or minimized. For risk assessment of other organs, Monte-Carlo dose calculations for standardized phantom geometries are done. The effective dose per administered activity is calculated based on simple geometric modeling of the human morphology; there exist dose calculations for pediatric, female, pregnant, and male models. Results for all relevant body compartments are published in the ICRP reports. The principles are implemented in the software package MIRDOSE (Stabin 1996), the clinical standard until 2004, before OLINDA was deployed (Stabin and Siegel 2004).

With the further development of imaging modalities anthropomorphic models were further refined towards realistically shaped organs, segmented in 3D from real model 3D data sets.

Individual dose planning focuses on the assessment of pharmacokinetics and accumulation of the radioactive isotope in every single patient. Most therapeutic radiopharmaceuticals are mainly beta emitters and have no or only weak gamma lines in their emission spectra, thus assessment of the pharmaceutical local distribution is not possible. A common method is the use of an imaging isotope for assessment, i.e. an isotope with the same pharmacokinetics as the therapeutic isotope, but with sufficient gamma-emission to observe the metabolism of significant organs and the accumulation in lesions. The assessment of the organ specific time activity curves, the main information for the subsequent dose calculation, is based on the cumulative counts within the image regions, drawn manually on the whole body images, acquired at different points in time. To correct for the latter applied therapeutic isotope the summed counts are modified, reflecting the physical half-life-time of the therapeutic isotope (Mizarei et al 2013).

More recent approaches for individual dose planning are based on hybrid data SPECT-CT or PET-CT in combination with whole body data series for estimation of temporal evolution dose distribution (Lee 2014).

In the current approach specific tracer dynamics of metabolism, subject to dose calculation, is utilized to distinguish between organs and accumulating pathologies, even allowing the segregation of overlapping compartments. This method may potentially extract accurate dose information from simple whole body studies with its projective acquisition geometry. This information is only accessible from more costly 3D whole body tomographic studies.

2. MATERIALS

Time activity series from 6 patients were analyzed, four male and two female studies. Their age ranges from 53 to 72 years. After administration of 60 MBq In-111 whole body scans were acquired 20 min, 90 min, 24h, 48h, 72h, and 96 h after injection. Image data were acquired with a double headed gamma-camera system, Philips BrightView, the heads in 180 degree position. Anterior and posterior data stored in a 1024x512 image matrix, 2.8mm pixel-size and scan-speed 10cm/min.

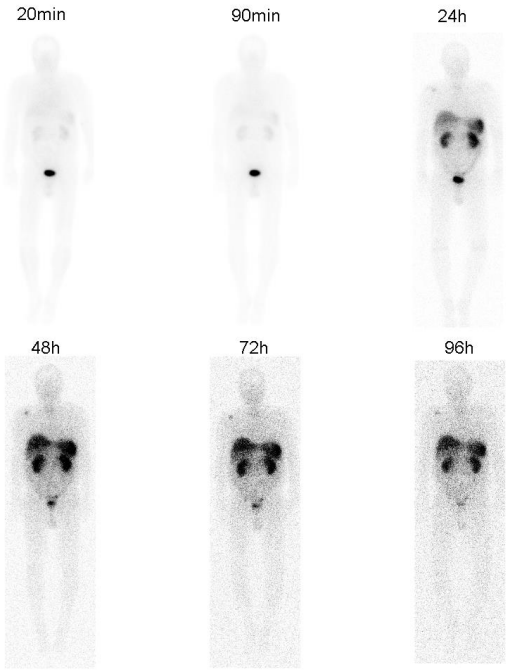

Figure 1: Anterior projection of the whole body time-activity study, i.e. six scans over a period of 96 hours. Projection images are acquired on a 1024 by 512 matrix, with 10cm/min scan speed. The intensity window is scaled to 45% of the maximum in each individual frame.

3. METHODS

Data analysis, i.e. dose assessment, comprises several steps, image registration, region drawing, factor analysis for automated separation of overlapping structures in projections, organ sampling and fitting of decay curves for each organ.

Each time activity series comprises 6 studies with simultaneously acquired anterior and posterior projections over a period of 96 hours, acquired in different scanning sessions. During each scan the patient-position may slightly differ, for meaningful data analysis careful image registration is required. Since the uptake and the subsequent decay of the radiopharmaceutical have locally different characteristics and organ specific visibility changes dramatically, a more sophisticated registration method is implemented. Surface oriented methods like chamfer matching are hardly applicable, since low contrast in late studies, i.e. 72 and 96 hours, allow no reliable extraction of outer body contours. It is aimed to utilize maximal available information provided by images, thus a pixel oriented approach is adapted for whole body image alignment.

Mutual information is a statistical measure from information theory; it describes the relation of symbols in two coherent data sets, respective tissues or morphologies. It is extensively used in image registration of multimodal data, where correlation methods are not applicable to modality specific manifestation of tissue. In perfectly registered images mutual information is maximized (Studholme et al. 1996, Hill et al. 1998, Crum et al. 2003).

For alignment of two-dimensional images the global maximum in a three-dimensional variable space, one rotational and two translational degrees of freedom, is determined. The solution space is searched with a steepest gradient algorithm, evaluating the mutual information equation

$$MI(X;Y) = \sum_{y \in Y} \sum_{x \in X} p(x,y) \log\left(\frac{p(x,y)}{p(x)\,p(y)} \right), \quad (1)$$

dependent on the joint probability $p(x,y)$ of images X and Y and the probabilities of both single images $p(x)$ and $p(y)$.

With the standard approach for dose assessment, regions are drawn manually over the essential organs and body parts, i.e. kidneys, liver, spleen, bladder, total body, background and reference. Typical regions are shown in Fig. 2.

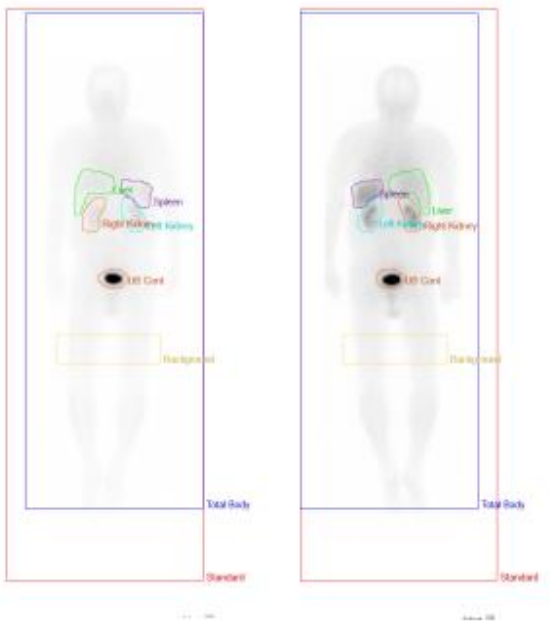

Figure 2: Manually drawn regions used in the standard approach for dose calculation. Regions may be drawn and displayed on, both, the anterior and posterior projection: kidneys (brown, cyan), liver (green), spleen (purple), bladder (ocher), body background (gold), total body (blue), and the reference standard (orange).

In many cases projections of kidneys overlap liver or spleen. A factor analysis approach was developed to separate those structures relying only on the projected images. Data from a rectangular region covering left and right kidney, liver and spleen are cut at each acquisition time, both from the anterior and posterior

image. Image sections are individually normalized to mean zero ($\mu=0$) and standard-deviation one ($\sigma=1$). ROI image data are reorganized from matrix to vector form and principal components analysis (PCA) is performed.

$$X = \begin{pmatrix} x_{11} & x_{12} & \cdots & x_{1m} \\ x_{21} & x_{22} & \cdots & x_{2m} \\ \vdots & \vdots & \ddots & \vdots \\ x_{N1} & x_{N2} & \cdots & x_{Nm} \end{pmatrix} \quad (2)$$

This is the normalized matrix of region of interest (ROI) image data. Each column contains the image data from a region, *m* is the number of analyzed ROIs and *N* is the number of pixels, each.

The correlation matrix *COR* is built

$$COR = X^T \cdot X, \quad (3)$$

and Eigenvectors C of the correlation matrix allow for decomposition of the image matrix X

$$X = I \cdot C^T + E, \quad (4)$$

Where *C* is a *p* by *m* matrix and *I* is a *p* by *N* matrix. The number of principal components *p* is assessed from the Eigenvalues, since the trace of the correlation matrix is the total variance of the data set, reflected by the sum of the Eigenvalues. Principal component images (PCI) are assessed by regression from image data and Eigenvectors. The context of time activity curves leads to the interpretation of the Eigenvalue matrix *C* as temporal evolution of radiopharmaceutical dynamics in accordingly to static morphological structures. These structures are represented by the PCIs and each observed image at each point in time is the weighted sum of these images, with the column of *C* associated with this time sample.

Principal components are not sufficient to reflect real physical properties of the analyzed regions; they are still orthogonal and provide an artificial decomposition of observed data. PCA itself explains the decomposition in terms of total variance and this is a proper unsupervised approach to separate noise from real dynamics in data. Neglecting the components higher than a certain threshold of cumulated Eigenvalues is a proper way to suppress the ambiguity component *E* from further analysis and leads to the number *p* of components

$$\sum_{i=1}^{p} \lambda_i \geq t, \quad (5)$$

where *t* is the desired fraction of the total variance, and λ_i are decreasingly sorted Eigenvalues.

To achieve accurate modelling of physiological processes, the arbitrariness of factorization is utilized

$$I \cdot C^T = IRR^{-1}C^T = F \cdot C^T, \quad (6)$$

where *R* is a *(p,p)* transformation matrix (*TT-1=1*). In principal components and factor analysis the matrices *F* and *C* represent the so called 'rotated' principal components, underlying certain optimization criteria, e.g. maximization of variance in Varimax rotation (Jackson 1991). In these transforms the components are kept mutually independent, i.e. the transformation matrix is orthonormal and its geometrical interpretation is a rotation. In our work we adapted that transform to oblique rotation, knowing a sufficient number of pixels of factor structures in advance, and then the transform matrix *R* can be estimated from

$$\begin{aligned} F_k &= I_k \cdot R \\ R &= (I_k^T I_k)^{-1} I_k^T F_k \end{aligned}, \quad (7)$$

where F_k is the part of the factor region known *a priori* and U_k is the respective amount of pixels in the PC images (Šámal et al 1987, 1989) .

In this approach the assumption of not totally overlapping structures leads to zero valued regions in the resulting factor images *F* providing the boundary condition for the transform matrix *R* (Backfrieder et al.1996).

The factor images provide fuzzy regions allowing the separation of overlapping organ structures in projection images of whole body scans. Based on this fuzzy segmentation more accurate time sampling of the organ specific tracer distribution is achieved. Summed counts are corrected for the decay constant of the therapeutic isotope and finally time activity curves for dose calculation are obtained by supervised mono- or bi-exponential regression of summed activities in the regions over time.

4. RESULTS

Registration of planar whole body projections in 2D provides accurate results. The images of the time series are registered to a single reference frame, generally the frame 90 minutes after injection, were all relevant morphologies are clearly manifested. An example for registration is shown with the linked display tool of the AnalyzeAVW software package (Biomedical Image

Resource, Mayo Clinic, Rochester, MN), cf. Figure 3. The reference (base) frame is displayed at the upper left, the matching frame on the bottom row; a weighted sum of both images is shown at the upper right. The tools allows for individual contrast enhancement of frames and provides a linked cursor to check accuracy.

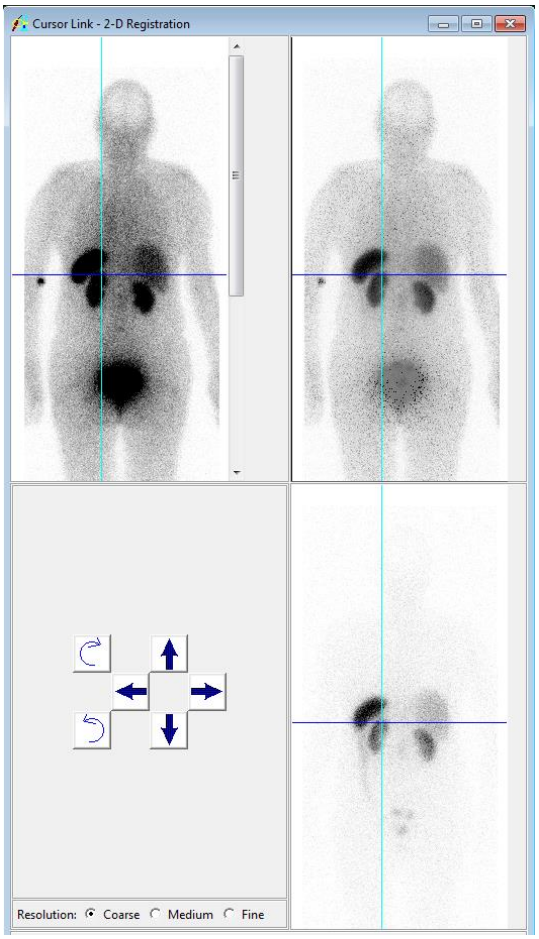

Figure 3: Cursor link tool for display of aligned images after mutual information registration. The upper left and the lower right image display the reference (base) frame and the matched frame. On the upper right a weighted overlay of both frames is shown. In this example tracer distributions 90 minutes (frame 2) and 48 hours (frame 4) after application are registered. The tool allows individual intensity scaling and weighting of each frame.

Separation of kidney and spleen was achieved by rotated principal components. The cumulated counts of all acquired projection image with overlapping regions is shown in Figure 4. The proper segmentation into a kidney region and a region containing the spleen with fuzzy parts in the overlapping area was accurately achieved, cf. Figure 5.

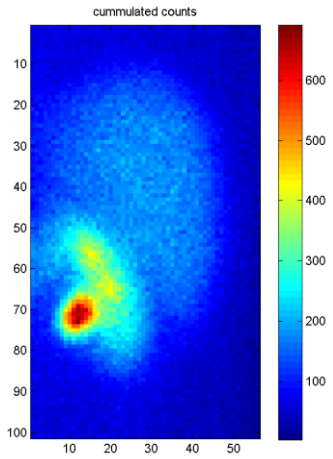

Figure 4: Cumulated counts of left kidney and spleen

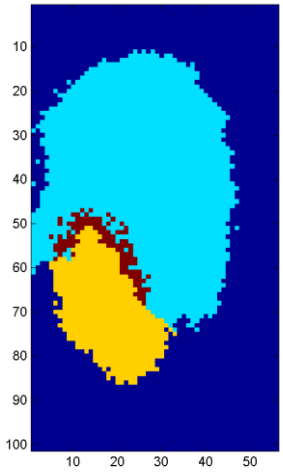

Figure 5: Overlapping regions calculated for liver and spleen. The kidney is marked ocher, the spleen is colored light blue, and areas belonging to both structures are marked dark brown.

5. DISCUSSION

The application of rotated principal components to time series for in vivo radioactive dose calculation allows the accurate segmentation of even overlapping structures in projection images. The method is an alternative to manual segmentation and an exploits whole available data, furthermore the application of an unsupervised method from multivariate statistics encourages to explore even non typical dynamic processes in time activity series. The rotation principle relies on *a priori* known parts of the image data, i.e. mutually non overlapping parts, where the respective structures are expected to be zero valued.

The method will be accurately tested with detailed mathematical phantom studies and a hybrid phantom, comprising known temporal tracer distribution and segmented morphologies from a 3D SPECT scan.

After careful clinical evaluation and comparison to results of standard whole body dosimetry, this method may be a further step toward accurate individual dosimetry based on organ specific time activity curves.

Even overlapping compartments may be accurately separated in the projective whole body scans. Alternatively this is only possible processing tomographic 3D image series, but low activity and long acquisition time are major drawbacks of these methods for use in dosimetry.

ACKNOWLEDGEMENTS

Authors would like to thank Univ.-Prof. Dr. Michael Gabriel and the clinical staff of the Institute of Nuclear Medicine and Endocrinology of the General Hospital of Linz, Austria, for providing in-vivo data and medical expertise.

REFERENCES

Backfrieder W, Baumgartner R, Sámal M, Moser E, Bergmann H, 1996. Quantification of intensity variations in functional MR images using rotated principal components. *Phys Med Biol.* 1996 Aug; 41(8): 1425-38.

Crum WR, Hill DL, Hawkes DJ, Information theoretic similarity measures in non-rigid registration. *Inf Process Med Imaging*. 2003 Jul; 18: 378-87.

Hill DL, Maurer CR , Jr, Studholme C, Fitzpatrick JM, Hawkes DJ, 1998. Correcting scaling errors in tomographic images using a nine degree of freedom registration algorithm. *J Comput Assist Tomogr*. 1998 Mar-Apr; 22(2): 317-23.

Jackson JE, 1991. *A users guide to principal components*. New York, Willey.

Mirzaei S, Sohlberg A, Knoll P, Zakavi R, Diemling M, 2013. Easy-to-use online software package for internal dose assessment after radionuclide treatment in clinical routine. *Clin Nucl Med*. 2013 Sep; 38(9): 686-90.

Lee JA, Ahn YC, Lim DH, Park HC, Asranbaeva MS, 2014. Dosimetric and clinical influence of 3D versus 2D planning in postoperative radiation therapy for gastric cancer. *Cancer Res Treat*. 2014 Dec 2, to be published. Available from: http://dx.doi.org/10.4143/crt.2014.018

Sámal M, Kárný M, Sůrová H, Maríková E, Dienstbier Z, 1987. Rotation to simple structure in factor analysis of dynamic radionuclide studies. *Phys Med Biol.* 1987 Mar; 32(3): 371-82.

Sámal M, Kárný M, Sůrová H, Pěnicka P, Maríková E, Dienstbier Z, 1989. On the existence of an unambiguous solution in factor analysis of dynamic studies. *Phys Med Biol*. 1989 Feb; 34(2): 223-8.

Stabin JA, 1996. MIRDOSE: personal computer software for internal dose assessment in nuclear medicine. *J Nucl. Med*. 1996, Mar, 37(3): 538-46.

Stabin JA, Siegel MG, 2003. Physical models and dose factors for use in internal dose assessment. *Health Physics*, 2003, Sep; 85(3): 294-310

Studholme C, Hill DL, Hawkes DJ, 1996. Automated 3-D registration of MR and CT images of the head. *Med Image Anal.* 1996 Jun; 1(2): 163-75.

AUTHORS BIOGRAPHY

Werner Backfrieder received his degree in technical physics at the Vienna University of Technology in 1992. Then he was with the Department of Biomedical Engineering and Physics of the Medical University of Vienna, where he reached a tenure position in 2002. Since 2002 he is with the University of Applied Sciences Upper Austria at the division of Biomedical Informatics. His research focus is on Medical Physics and Medical Image Processing in Nuclear Medicine and Radiology with emphasis to high performance computing. Recently research efforts are laid on virtual reality techniques in the context of surgical planning and navigation.

Gerald A. Zwettler was born in Wels, Austria and attended the Upper Austrian University of Applied Sciences, Campus Hagenberg where he studied software engineering for medicine and graduated Dipl.-Ing.(FH) in 2005 and the follow up master studies in software engineering in 2009. In 2010 he has started his PhD studies at the University of Vienna at the Institute of Scientific Computing, where he received his degree in December 2014. Since 2005 he is working as research and teaching assistant at the Upper Austrian University of Applied Sciences at the school of informatics, communications and media at the Campus Hagenberg in the field of medical image analysis and software engineering with focus on computer-based diagnostics support and medical applications.

SIMULATION-BASED FRAMEWORK TO COMPUTE POPULATION RISK RELATED TO TRAFFIC ACCIDENTS

FJ Otamendi[(a)], D Garcia-Heredia[(b)]

[(a),(b)]Universidad Rey Juan Carlos

[(a)]franciscojavier.otamendi@urjc.es, [(b)] d.garciahe@alumnos.urjc.es

ABSTRACT

A new family of indicators for the assessment of the risk of not being properly attended after a traffic accident has been defined. Its name is Dynamic Population Risk (DPR) and it is based on the dynamic behaviour of the traffic system (weather, congestions, population) and not just on the static location of the ambulances at the hub. Its development has been verified and validated using a simulation-based framework. Possible uses for policy development are mentioned.

1. INTRODUCTION

There is an increasing need in health systems to develop and quantify indicators that may be used for policy development. Indicators of efficiency and efficacy should help in compensating the economic investment and the return via improved public health (Ministerio de Sanidad 2010). In other words, there has to be a balance in the staffing of resources assigned to an activity and the level of service that wants to be achieved.

In this case, the system to be simulated is the assistance of victims of traffic accidents by ambulances or special mobile units where the quickness of the reaction is critical (Sánchez-Mangas et al., 2010), especially in rural areas (Muelleman a Mueller, 1996). The response time should obviously be as short as possible since it is well known that "the quicker the rescue, the higher the possibility of the patient recovering". The Golden Hour principle is widely accepted as a requisite for public health, that is, the probability of recovering greatly decreases if a traffic victim is not properly assisted within one hour.

This system of assisting traffic accidents is known as EMS, Emergency Medical System. The system works as follows. The ambulances are located at the base or hub. If an accident occurs, the ambulance is occupied (not available for another call) during a certain time period which covers the following tasks:

1. Preparation of the assistance: before leaving the base, the staff needs to prepare matters.
2. Travelling to location: the ambulance moves towards the location of the accident
3. At the accident site: the staff actuates to assist and pick the injured up
4. Travelling to hospital: the ambulance moves from the site towards a medical centre.
5. At the hospital: the staff actuates to drop the injured off
6. Travelling back towards the base to report and be ready for a new call.

A complete survey of applications of simulation to EMS was published in 2013 (Aboueljinane et al., 2013). It divides the types of decisions into long-term (potential bases location, dimensioning of resources), mid-term (deployment problem, shift scheduling) and short term (resource dispatching, destination hospital selection, redeployment problems). A simulation optimization framework may become necessary to address the corresponding optimization problem (Zhen et al, 2014) in any of the above situations.

For decision making, two types of indicators have been used in the past to quantify the level of service in EMS deployment. (Aboueljinane et al., 2013): time/distance (average response time, coverage within a standard time T, coverage within a time greater than T, round trip time, service time, vehicle utilization rate, # of calls served per vehicle/base, dispatching time, travel time to scene, waiting time, size of queue, loss ratio, overtime, total mileage) and survival cost (survival rate, cost effectiveness).

The most common one is the response time (for example, Aboueljinane, Sahin, Jemai and Marty, 2014), which is usually calculated as the average time that the resources take to arrive to the scene of the accident. This indicator is related to the proportion of time the response time is within the Recommended Safety Time Threshold (Ramirez-Nafarrete, Baykal, Gel and Fowler 2014). This second indicator sometimes is called "Maximal Expected Coverage", the measure that is complementary to the risk (Gendreau, Laport and Semet, 2006).

In terms of survival, or at least potential survival, we can mention the population risk, which is frequently stated as "the percentage of the population that lives outside a given time threshold from the hub of resources" (Ministerio de Sanidad 2010). It represents the percentage of population covered within the given subjective time threshold.

All the indicators are of course related and based on the response time (and hence the adequacy of using simulation as the modelling tool), but the computation of the response time has to rely on historic data and is dynamic in nature, whereas the quantification of the population at risk is based on static population and location data and the response time is just the subjective threshold.

That is the reason why in many places, Spain in particular, mid-term and long-term planning of resources is based on static population risk. There is no need to have real data other than population to establish the number of resources that should be installed at each response hub. For example, in Spain (Ministerio de Sanidad 2010), following international principles, there is a rule-of-thumb that determines that there should be an emergency unit per 50000 habitants.

The objective of this article is to keep on defining new indicators that could be used for policy development in EMS systems. This article proposes a set of survival indicators that combine the individual indicators that have already been mentioned. These new indicators will be classified as dynamic population risk indicators, in the sense that the value of the risk (or coverage) will not be constant over time to overcome the problems of the static risk indicator but it will still be based on the correct quantification of the response time.

Using as the initial measure the static population risk, the new idea is to incorporate dynamic conditions to its calculation. The proposed indicator accounts for unexpected conditions that might increase the response time: weather and traffic conditions or road maintenance. It also takes into account the variation in population and the related accident rate, for example during the weekends or holiday periods. As a result of the time penalties associated to these sources of variation, the availability of resources changes and the potential survival rate may decrease significantly over certain periods of time.

The proposed dynamic population risk indicator (DPR) will be then calculated as the time-weighted average of the static population risk (SPR). As long as there are units outside the hub, the DPR will be different to the SPR: if the units are available, they may be spread out in such a way that DPR is momentarily smaller than the SPR; if they are not available at all, the SPR will be lower than the DPR.

Both the DPR and SPR will depend on the time threshold that wants to be subjectively set. For that reason, there is a value of the indicator for each threshold K. The specific indicators therefore should be referred as DPR (K) and SPR (K), leaving DPR and SPR for the specification of the set or family of indicators.

The development of this new family of indicators, DPR and SPR, is the core of this article. We build a simulation model to verify its robustness and validate its use in a real problem. We first embed their calculation in a MsExcel framework, and finally we show their application in a traditional EMS setting in which the optimum number of ambulances is determined after taking into account dynamic conditions..

2. THE EMS SIMULATION MODEL

The aim is therefore to derive and quantify robust indicators, using a simulation model that can represent the system under study. A researcher must then choose a tool that conveniently fulfils this objective.

In this case, the model is going to be set in MsExcel because it is a perfect tool to implement easy routines that help define, verify and validate any decision making framework with the required level of detail. Then, if the model wants to be implemented for ad-hoc utilization, the model may be updated accordingly with the necessary complexity.

The abstraction process of the EMS starts with the definition of the **map** that represents the region that is going to be analysed with its roads. The map is easily represented with a grid composed of cells (i,j) that cover the whole region. One of those cells holds the base.

The **population** at each cell (i,j) is f_{ij} (absolute frequency), with the relative percentage of the population being defined as:

$$\Psi_{ij} = \frac{f_{ij}}{\sum_i \sum_j f_{ij}}$$

The roads are represented as **travel times** d_{ij}^{t}, which are the travel times from the current position at the current time from where the ambulance is to the cell (i,j) in the spreadsheet grid. It is calculated by adding time jumps to adjacent cells with the jump being defined as a random variable, ξ. Perfect or static conditions are set when there are no congestions at any road and the weather does not affect the driving behaviours.

This variable is adjusted with a factor δ that accounts for the **time penalties** that may be incurred due to imperfect traffic conditions. δ is a non-negative value that adds to the static times under perfect conditions. It is worth mentioning that the way this matrix of time distances is defined and modelled is based on the underlying assumption that the resources are intelligent and always select the shortest route in terms of the response time.

The **movement** of the ambulances are the key of the model. The base receives a call and then a free ambulance drives towards the location of the accident, assists the injured people, moves then to the hospital and back to the base. It is very important to note that the ambulance that leaves the base is not available to give service to any other accident until reaching the base again. In other words, any ambulance is unavailable during a period of time. In the case of a given region staffed with just one ambulance, the whole population is at risk whenever that lonely ambulance is not at the base. Moreover, only ambulances at the base count since those are the only ones that can immediately react to incoming calls. This reasoning is critical for understanding the system and for the development of the model and calculation of the indicator.

We have opted not to model the movement of the ambulance but instead calculate the availability of the ambulances at regular intervals of time. Indeed, for any instance, we determine if there is at least one ambulance at the base. At each instance that we simulate, we use a binomial distribution ρ to represent the **availability** of the ambulances. If the count of ambulances in the system is c, then ρ = B(c, p), where p is the probability of each ambulance being available, and therefore, the availability of at least one ambulance is:

Availability $\alpha = 1 - P(\rho = 0)$.

The **location** at any instance of the ambulance is modelled with a bi-dimensional random variable (βx, βy).

The execution of the model is performed as follows:

1. Definition of the maps
    a. Population
    b. Time distances
    c. Hub location
2. At each instance:
    a. Location of ambulance within the map
    b. Availability (or not) of ambulance
    c. Recalculation of time distances
    d. Calculation of instantaneous population risk
3. At the end of the simulation
    a. Calculation of SPR and DPR
    b. Drawing of functions

The model is run to cover a total number of instances T (t=0, 1, … ,T).

3. POPULATION RISK INDICATORS

The calculation of the indicators and the drawing of their corresponding functions is therefore the key of article.

Population risk is defined as the percentage of the population that lies outside a given subjective time threshold. We can differentiate between static or perfect conditions with full availability of ambulances and no time penalties, and dynamic conditions. In the first case, the SPR, static population risk indicator, is defined and, in the second case, the DPR, dynamic population risk indicator, is defined.

The population risk depends on the time threshold that is subjectively and a priori established. For generality, we define K thresholds and calculate the population risk, each with a different value k. Therefore, we define two families of indicators, SPR (K) and DPR (K).

Both families are based on the following definition of the coverage of population based on the k[th] threshold at time t, Π_k^t:

$$\Pi_k^t = \frac{\Sigma_i \ \Sigma_j \ \phi_{ijk}^t \Psi_{ij}}{IJ}$$

where

$$\phi_{ijk}^t = \alpha * \begin{cases} 1, if\ d_{ij}^t \leq \Omega_k, \\ 0, if\ d_{ij}^t > \Omega_k \end{cases}$$

is the indicator of coverage of cell (i,j) at time t. If the travel time from the current position at the current time d_{ij}^t is less than the threshold time Ω_k that corresponds to the k[th] threshold, the instantaneous coverage is calculated to 1, and 0 otherwise. The coverage is further multiplied by the availability of the set of ambulances for the final calculation of the indicator at time t corresponding to the k[th] threshold.

The static indicator of population risk is then:

$$SPR(k)=1-\Pi^0{}_k$$

and it is just the sum of population outside the threshold, since α=1.

The dynamic population is therefore the average over the total number of samples obtained at regular intervals of time:

$$DPR(k)=1-\Pi_k = \frac{\Sigma_k \ \Pi_k^t}{T}$$

4. THE SOFTWARE

In this section, the adequacy of the MsExcel software that has been developed is shown with a simple example. As input, the software asks for several data. Figure 1 shows the population percentage at each of the cells (i,j) of the map which in this case is a matrix of 10x10.

0.5%	1.1%	1.0%	1.7%	1.6%	1.4%	1.6%	2.0%	0.7%	0.5%
0.1%	0.4%	0.7%	0.8%	1.2%	0.9%	1.7%	1.9%	0.4%	0.1%
1.1%	1.3%	0.3%	1.9%	2.1%	0.1%	0.1%	2.0%	0.4%	0.9%
0.3%	0.4%	1.3%	0.9%	1.7%	0.2%	0.0%	0.6%	0.0%	0.1%
0.2%	1.7%	0.2%	1.9%	2.0%	0.8%	0.6%	0.4%	0.8%	1.9%
2.1%	0.3%	0.8%	1.0%	1.4%	1.6%	0.6%	1.5%	1.8%	1.3%
1.9%	1.0%	0.8%	1.6%	0.6%	1.4%	0.8%	1.1%	0.1%	0.3%
2.1%	0.3%	1.0%	0.3%	0.4%	1.6%	2.0%	1.5%	1.1%	1.3%
0.8%	1.0%	1.0%	1.3%	1.3%	1.2%	1.4%	1.4%	0.8%	1.2%
0.5%	0.8%	1.3%	1.3%	1.5%	1.2%	0.5%	0.6%	0.3%	0.4%

Figure 1: Software input: population

The colour coding is such that the darkness increases with the population. Cell (5,5) is where the base is located, cell that is indicated by a dark border.

Figure 2 includes the time distances from the base in static conditions.

9.7	8.2	6.3	4.5	4.5	4.9	6.5	8.2	8.6	9.0
6.1	4.4	3.5	3.4	3.4	5.3	6.0	7.6	8.5	9.3
8.4	6.8	4.9	3.4	2.2	3.1	3.6	5.1	6.2	6.4
5.1	3.9	3.3	2.9	1.1	1.5	3.5	5.3	5.7	7.6
5.7	4.5	2.5	1.2	0.0	2.0	2.9	3.1	4.0	5.0
6.0	5.4	4.0	3.0	1.2	2.4	2.6	4.2	4.8	6.5
7.8	7.0	5.0	3.2	1.9	2.1	2.8	4.0	4.2	4.2
8.3	6.8	5.5	3.8	2.8	4.3	4.9	6.4	7.9	8.2
8.4	6.9	6.9	5.0	3.4	3.8	5.0	5.8	7.6	8.5
9.1	7.3	7.3	6.6	5.0	7.0	9.0	10.2	10.7	12.4

Figure 2: Software input: time distances

The rest of the necessary input values are:

- The number of ambulances, c=1
- Availability of each ambulance, p=0.9
- Time penalty = 2

As output, the software shows a calculation of both the SPR(K) and the DPR(K) for easy comparison. Graphically, the calculations are shown as a function of different time thresholds K, which could be also specified a priori. In this case, K = 0, 2, 4, …, 18, 20.

Figure 3 shows that the static risk is 0, SPR(12) = 0, if the time threshold is 12 minutes or more. In other words, all the population is within 12 minutes of the hub. However, 4% is at risk if the threshold is set to 10 minutes, SPR(10) = 4%.

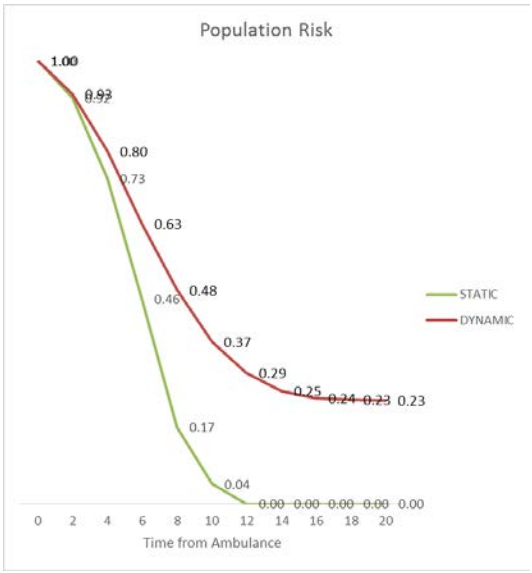

Figure 3: Software output: Static vs Dynamic Population Risk

If penalties are included in the calculation of the new dynamic indicator, then 23% of the population is on average outside the 20 minute mark and 29% outside 12 minutes, DPR (20)=23% and DPR (12) = 29%.

The time distances from the dynamic location of the units are also shown over the region that is being analysed using a heat map. Figure 4 depicts the situation under static conditions, or time distances from the hub. The map is arranged in cell format for easiness of representation. Almost all of the population is within 10 minutes, expect for 4 cells at the right corners.

8	8	8	8	6	8	10	12	12	12
8	6	6	4	4	6	8	8	10	10
8	8	6	4	4	4	6	6	8	8
8	6	6	4	2	4	4	4	6	6
4	2	2	2	2	2	4	6	6	8
6	4	4	2	2	4	6	6	8	10
8	6	6	4	4	4	4	6	6	8
10	8	8	6	6	6	6	8	8	10
10	8	8	6	6	6	6	8	10	10
10	10	8	8	8	8	8	10	10	12

Figure 4: Software output: Time distances from hub under static conditions

Figure 5 shows dynamic conditions, indicating the average time distance from the location of the closest unit. In the average dynamic map, there is only one cell in the grid which is covered on average within 6 minutes. The corners are on average at a distance of 14 minutes.

14	12	12	10	10	10	12	12	12	14
12	12	10	10	10	10	10	12	12	14
12	10	8	8	8	10	10	10	12	14
10	10	8	8	6	8	10	10	10	12
10	10	8	8	8	8	10	10	10	10
10	10	8	8	8	8	8	8	10	10
10	10	8	8	8	10	8	10	10	12
12	10	10	10	10	10	10	10	12	14
12	12	10	10	10	10	10	12	12	12
14	12	12	10	10	12	12	12	12	14

Figure 5: Software output: Time distances from random location of ambulances

5. EMS SIMULATION OPTIMIZATION FRAMEWORK

If using this software for a real application in which decisions might be taken by varying the values of the input parameters, a simulation optimization framework may become necessary to address the corresponding optimization problem (Zhen et al, 2014). Therefore, an additional output of our work is a simulation-optimization framework to test the new family of indicators within real applications.

5.1. Definition

The decision problems faced in industry, commerce, public administration, and the society in general keep growing in size and complexity. For the study of these decision problems, it is necessary to develop efficient methodologies and tools, so it is possible to try and evaluate many different alternatives and to take the correct decision in a reasonable amount of time. One of the main example problems of this complex type that a manager faces is that of deployment of the EMS (the real system in our case, Fig. 6).

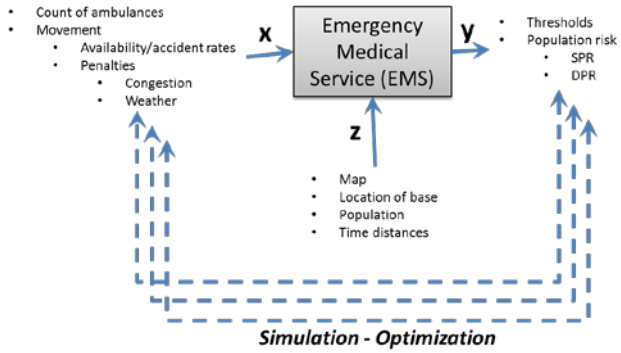

Fig. 6. Description of the EMS optimization framework.

The first source of complexity is the number of decision variables (or control parameters or input variables, x), or to be more precise, the number of different alternatives that a manager faces in the process. The total number (n) is the multiplication of the feasible values for each of the variables (n_c *n_a*n_p):

- Count of ambulances (c): from a minimum to a maximum value for a total of n_c.
- Accident rate (a): at least, base and peak for a total of n_a.
- Penalties (p): at least with no penalties and with a penalty, for a total of n_p.

The number of different criteria (or output variables or objectives, y) also adds to the complexity of the analysis, mainly because usually they independently work in opposite directions. At least a measure of cost and another of level of service are usually included in any study. Then, if the level of resources is increased to improve the level of service, the cost criterion will pay the price, and vice versa. In this case we will concentrate just of the new family of survival indicators, SPR(K) and DPR(K).

The third source of increased complexity is the volume of available data (z). Not only that, the data is available at a much quicker pace that the manager can handle. The improvement in online information systems has called for shorter decision making periods.

Fortunately, some of the complexity of these studies has been diminished by the improvement not only of the solution techniques but also of the information technology. These improvements call these days for the experimentation with models instead of with the real system, models which are embedded in the information systems of the company. Among these models, simulation has grown as one of the most reliable abstraction tools due to its very good compromise between the level of detail in the representation of the real system and the execution time of the model, which calls for an appropriate experimentation and decision making.

On that regard, computer simulation has received a lot of attention in the last decades to model complex systems under uncertainty, in many areas but specifically in traffic (Ingolfsson et al., 2003). Its success does not rely mainly upon improvements in theoretical aspects but in hardware and software, especially in terms of efficiency, allowing for the study of even more complex, uncertain systems within the allotted analysis time. The use of simulation opens the possibilities of further research into decision processes which are specific to this tool.

To study a given system via simulation, the first step is to formulate the problem and to develop the model that represents the system. The model will simultaneously include the mathematical and logical relations between the elements of the system as well as random variables for the necessary data (for example, travel times or location of bases). The data must be easily read into the

model. The next step is to build credibility. The model is executed repetitively to confirm that it has sound foundations. For each run, a different set of values is taken from each random variable to verify that the model works correctly. At the same time, a different combination of values for the decision variables is used so that the objectives are not only calculated but compared numerically.

Different alternatives are tried, the objectives quantified and the best alternative is chosen for implementation. This step is usually carried out using a user-friendly interface that automatically tries many different alternatives, performing also the comparison and the selection step for the manager. During implementation, this interface is also used to see the results for the selected alternative.

Therefore, in this final step of the analysis process, the desire is to obtain information about the values of the input or decision variables that improve the values obtained for the objective function. In the EMS example, the objective may be to calculate the optimum number of EMS units according to reasonable values of the new family of indicators.

5.2. Experimenter

The developed software also includes an experimenter that will help with the trial of different possibilities automatically (by pressing the button "EXECUTE") (Figure 7) by trying each and every combination of feasible values for the different variables. We run a test case with the following settings:

- Count of ambulances, c={1,2,3,4,5}
- Availability, α={0, 0.1, 0.2, …, 0.9, 1}
- Time penalty, δ ={0, 0.5, 1, …, 3.5, 4}

The total count of scenarios is calculated as the product of the feasible levels (Fig. 4: 5*11*9=495 scenarios). 100 runs are executed of each scenario, for a total of 49500 runs.

A pivot table as well as a pivot figure summarize the result for both SPR(10), SPR(20), DPR(10) and DPR(20) for each variable independently.

6. AN APPLICATION: THE PROBLEM OF DEPLOYMENT

The problem addressed in this article as a test-bench is that of deployment, or to correctly staff the EMS with ambulances or emergency units. More specifically, the number of ambulances has to be enough to guarantee that those involved in an accident receive attention quickly, but not so many so as to incur in excessive costs.

Deployment has been addressed in the literature in recent years due to the importance of designing correctly the rescue service and of staffing properly the resources. For example, a simulation tool is used to measure the "time to rescue" in the Val-de-Marne department in France (Aboueljinane et. al, 2014). The time is translated into coverage, defined as the percentage of calls that are attended within a 20 minutes threshold. This service indicator in decision making is then used to propose the level of resources as well as the location of the base.

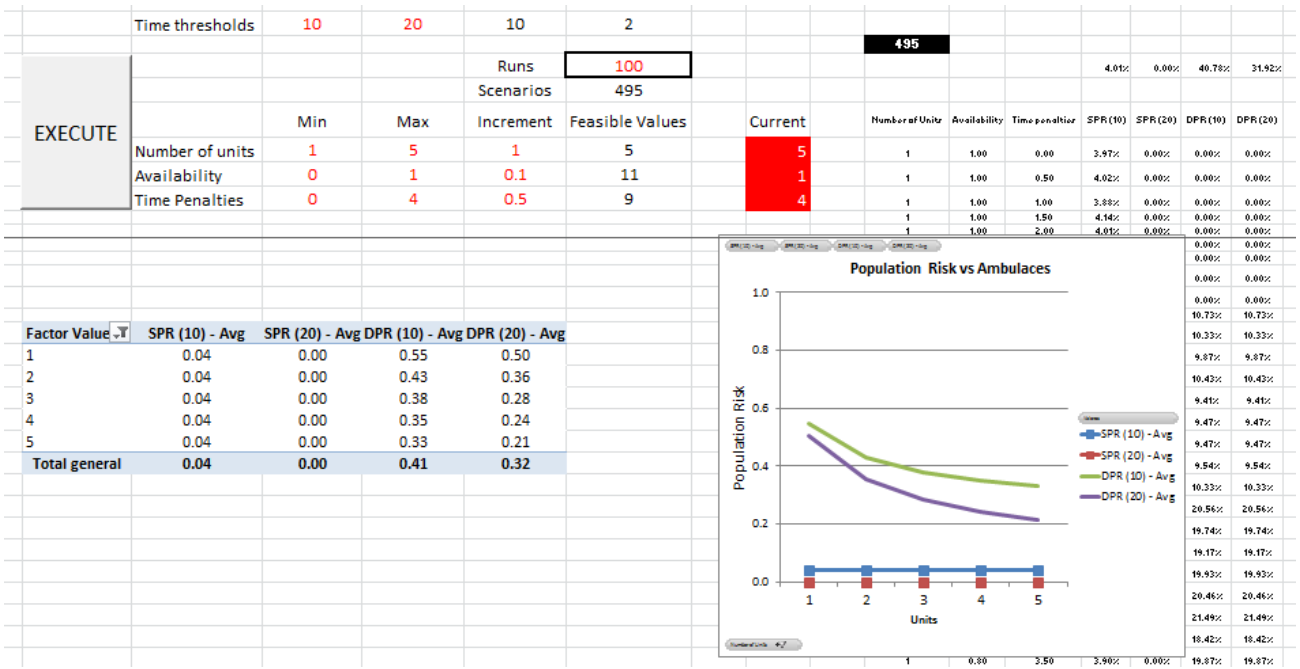

Figure 7: Experimenter screen

The experimenter is run using the setting included in section 5.2., varying the number of ambulances between 1 and 5. Figure 8 depicts the results as a function of the number of ambulances. The x-axis represents the ambulances and the y-axis the risk. The whole population is within 20 minutes (SPR (20)=0) and 96% within 10 minutes (SPR (10)=0.04).

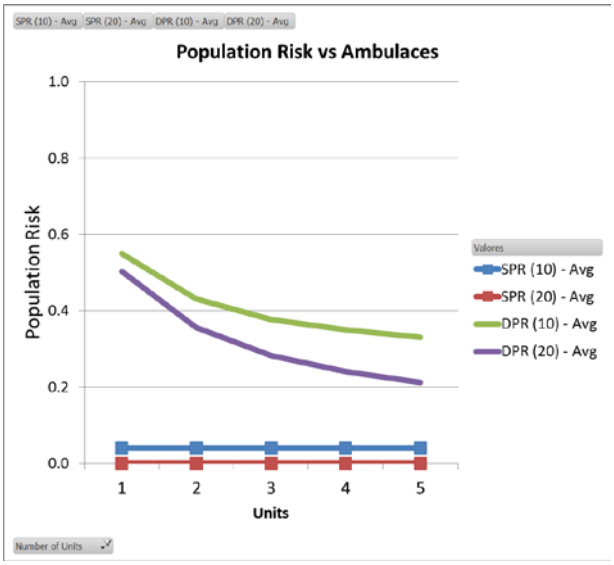

Figure 8: Experimenter output for the count of ambulances

The dynamic values are obviously much worse, with population risk as high as 20% even with 5 ambulances and a 20-minute threshold. With only 1 ambulance, the risk is above 50%.

The analysis shows that most probably the appropriate number of rescue units should be 3. The risk functions start to flatten down at 25%.

We have also performed a sensitivity analysis on each factor. The availability of at least one ambulance greatly influences the risk (Figure 9). The EMS requires that the accident rate is such that the availability is at least 0.6 so that the risk is controlled below 20%.

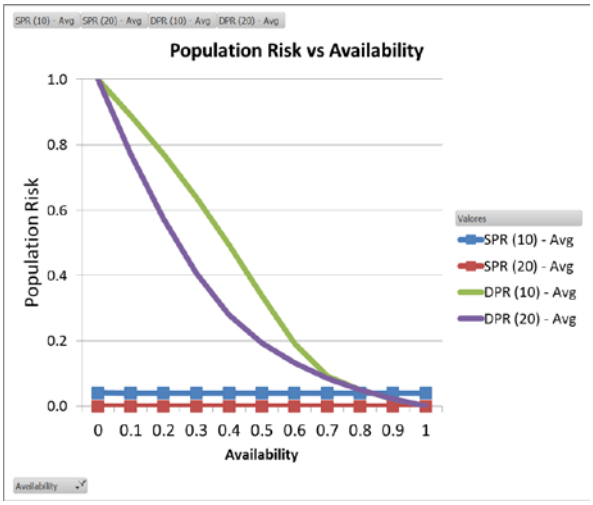

Figure 9: Experimenter output for the Availability of ambulances

Finally, it looks like size of the time penalty does not have an effect on the risk (Figure 10). The graphs are flat throughout the whole range of penalty values.

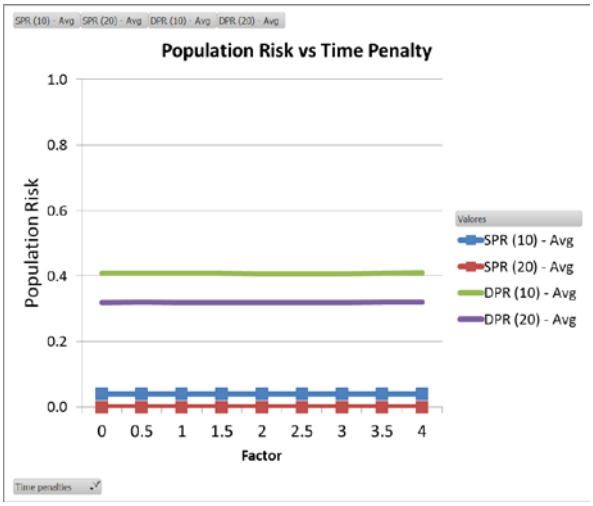

Figure 10: Experimenter output for time penalties

7. DISCUSSION

We have designed a simulation-optimization framework to represent the EMS and validate our proposal of a new family of indicator to measure the potential risk of the population.

A simplistic model in MsExcel has allowed for the proper definition and testing of the indicators. Most of time, the model should be a means to an end, so the level of detail is critical while developing a credible, reliable and usable tool for decision making. In this setting, it was not necessary to model the movement of the ambulances in detail in order to develop robust indicators of survival in dynamic traffic conditions.

It is our aim to further develop and apply the framework to real situations. On that regard, we are developing a model in C++ to fully represent the movement of the ambulances so the analysis of real EMSs over a given region can be carried out. It will include travelling times both under normal conditions or under changing weather (fog (Mueller and Trick, 2012) or snow (Kunkel and McLay, 2013)) and traffic conditions.

Then, the framework could have more uses within decision simulation support systems (DSSS) related toemergency situations.

Online dynamic assignment of ambulances to accidents and the redeployment of ambulances (Maleki and Majlesinasab, 2014) or the analysis of the so-called diversion problem (allocation of ambulances to hospitals) (Lin et al., 2015) are types of situations that

could be addresses via modifications of the current framework.

ACKNOWLEDGMENTS

This research has been funded by Research Grant SPIP2014-01358, Proyectos en Materia de Tráfico, Movilidad y Seguridad Vial (Traffic, Mobility and Road Safety), Dirección General de Tráfico, Ministerio del Interior.

REFERENCES

Aboueljinane L., Sahin E., Jemai Z., 2013. A review on simulation models applied to emergency medical service operations. Computers and Industrial Engineering, 66, 734-750.

Aboueljinane L., Sahin E., Jemai Z., Marty J., 2014. A simulation study to improve the performance of an emergency medical service: Application to the French Val-de-Marne department. Simulation Modelling Practice and Theory, 47, 46–59.

Gendreau M., Laporte G., Semet F., 2006. The maximal expected coverage relocation problem for emergency vehicles. Journal of the Operational Research Society, 57, 22-28.

Ingolfsson A., Erkut E., Budge S., 2003. Simulation of Single Start Station for Edmonton. The Journal of the Operational Research Society, 54, 736–746.

Kunkel, A., McLay, L.A., 2013. Determining minimum staffing levels during snowstorms using an integrated simulation, regression and reliability model. Health Care Management Science, 16, 14--26.

Lin, C.H., Kao, C.Y., Huang, C.Y., 2015. Managing emergency department overcrowding via ambulance diversion: A discrete event simulation model. Journal of the Formosan Medical Association, 114, 64-71.

Maleki, M., Majlesinasab, N., 2014. Two new models for redeployment of ambulances. Computers & Industrial Engineering, 78, 271-284.

Ministerio de Sanidad, 2010. Protocolo de actuación y buenas prácticas en la atención sanitaria inicial al accidentado de tráfico.

Muelleman, R.L., Mueller, K., 1996. Fatal motor vehicle crashes: variation of crash characteristics within rural regions of different population densities. The Journal of Trauma: Injury, Infection and Critical Care, 41, 315-320.

Mueller, A.S., Trick, L.M., 2012. Driving in fog: The effects of driving experience and visibility on speed compensation and hazard avoidance. Accident Analysis and Prevention, 48, 472-479.

Ramirez-Nafarrate A., Baykal A., Gel E.S., Fowler J.W., 2014. Optimal control policies for ambulance diversion. European Journal of Operational Research, 236, 298-312.

Sánchez-Mangas R., García-Ferrrer, A., de Juan, A,; Martín Arroyo, A., 2010. The probability of death in road traffic accidents. How important is a quick medical response?. Accident Analysis and Prevention, 42, 1048-1056.

Zhen, L., Wang, K., Hu, H., Chang, D., 2014. A simulation optimization framework for ambulance deployment and relocation problems. Computers & Industrial Engineering, 72, 12-23.

BIOSIGNAL ACQUISITION SYSTEM FOR PROSTHESIS CONTROL AND REHABILITATION MONITORING

Volkhard Klinger

Department of Embedded Systems
FHDW Hannover
30173 Hannover, Germany

volkhard.klinger@fhdw.de

ABSTRACT
Simulation, modelling and verification are powerful methods in computer aided therapy, rehabilitation monitoring, identification and control. They are major prerequisites to face great challenges in medical technology. To realize tasks and services like an on-line data monitoring or a nerve signal based prosthesis control, smart, intelligent and mobile systems are required. Here we present data acquisition and learning systems providing methods and techniques to acquire electromyogram (EMG)- and electroneurogram (ENG)-based data for the evaluation and identification of biosignals. We focus on the development, integration and verification of platform technologies which support this entire data processing. Simulation and verification approaches are integrated to evaluate causal relationships between physiological and bioinformatics processes. Based on this we are stepping up efforts to develop substitute methods and computer-aided simulation models with the objective of reducing experiments on animals. This work continues the former work about system identification and biosignal acquisition and verification systems presented in (Bohlmann, Klinger, and Szczerbicka 2010; Klinger and Klauke 2013; Klinger 2014).
This paper focuses on the next generation of an embedded data acquisition and identification system and its flexible platform architecture. We present results of the enhanced closed-loop verification approach and of the signal quality using the Cuff-electrode-based ENG-data acquisition system.

Keywords: ENG-based prosthesis control, rehabilitation monitoring, system identification, system verification, simulation framework, simulation and modelling in computer aided therapy, robot-manipulators

1. INTRODUCTION

The use of electrical biosignals, like electro-encephalogram (EEG), electromyogram (EMG) and electroneurogram (ENG), gains a lot of importance for the assessment of functions in the human body. These signals are used as major indicators which provide medical professionals, patients or professional athletes during diagnostic and monitoring processes. In particular EMG and ENG are used to get information about the peripheral nerve system including information transfer due to sensual data and motion control by peripheral nerves. Based on these signals a multitude of applications is existing; they range from the achievement of a therapeutic goal up to prosthesis control, for example, to operate an artificial hand or an artificial forearm. There are several requirements existing to realize such these functionalities:

- Data acquisition and stimulation

The EEG, EMG or ENG data has to be acquired and sampled according their signal characteristics, given in Table I. In particular applications stimulation is necessary, for example for the measurement of the nerve conduction velocity.

- Data processing

The acquired data (action potentials) are disturbed by intrinsic noise. In addition they are overlaid by a substantial extrinsic noise, originated for example by EMG from surrounding muscles. Therefore we have to filter the recorded data with integrated analogue filter and additional digital filter. There are several specific high-pass, low-pass, band-pass and notch filter available. A further data processing is necessary, on the one hand to improve the data condition due to asynchronous and aperiodic samples, and on the other hand to generate events from the action potentials like the activity level of a muscle group or the detection of an exposure scenario.

Table 1: Biosignal Characteristics

Signal types	Amplitude range	Frequency range
EEG	$(100 - 1000)\ \mu V$	$(0.5 - 100)$ Hz
EMG	$(100 - 5000)\ \mu V$	$(0 - 8)$ kHz
ENG	$(1 - 400)\ \mu V$	$(0 - 12)$ kHz

- Identification

The identification feature is required for prosthesis control or any type of high level signal evaluation. The identification is based on machine learning and recognizes movement commands and feedback

signals. The identification method and the corresponding verification scenario has been introduced in (Klinger and Klauke 2013; Klinger 2014) based on results in (Bohlmann, Klinger, and Szczerbicka 2010; Bohlmann, Klauke, Klinger, and Szczerbicka 2011).

- Data archiving

After data acquisition and data processing the results has to be saved locally if there is no direct data transmission for an evaluation possible or desirable due to an offline analysis. Furthermore for identification a certain data amount is necessary to apply the identification algorithms during the operating phase (Klinger and Klauke 2013).

- Data interfacing

The data has to be transmitted for evaluation or monitoring purposes to a host system.

- User Interfacing

To select and execute certain functionalities and for online information an user interface must be available.

- Configuration

Due to the different application scenarios and system functions a configuration is necessary.

With regard to many different application scenarios and the corresponding requirements, the embedded system architecture is based on a modular hardware and software platform. We will present the system architecture and its characteristics including data acquisition, identification and data exchange in section 2. In section 3 we will discuss two specific applications to illustrate the platform character of the system. The results given in section 4 focus on the enhanced overall verification method, using modelling and simulation techniques and the verification of the data acquisition for ENG-based data.

2. SYSTEM ARCHITECTURE

In Figure 1 the overall concept is shown in a block diagram. Two central components are to be recognized in this level: The data acquisition and signal conditioning in the analog frontend as well as the data evaluation and identification (Signal Processing, Learning). In the data acquisition block the action potentials of the nerves are captured by a so called Cuff-electrode (Klinger 2014; Klinger and Klauke 2013). Following this, the analog signals are being amplified and digitalized. Afterwards there occurs a two-stage evaluation and identification step of the data (Bohlmann, Klauke, Klinger, and Szczerbicka 2011; Bohlmann, Klinger, and Szczerbicka 2009; Bohlmann, Klinger, and Szczerbicka 2010).

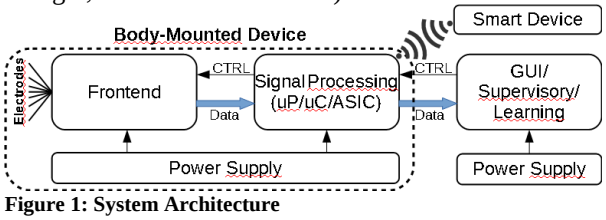

Figure 1: System Architecture

This subdivision in two phases is necessary to allow a learning phase and an operation phase. In the learning phase the base identification which allows a correlation between nerve signal and movement is carried out. The operation phase is using the identification results of the learning phase to realize a customization and adjustment due to parameter drift or electrode movement and to control the exoprosthesis. Therefore the base identification from the learning phase is used by a mobile processing device, which supports continuous learning.

Based on the overall system concept the system is designed as a platform providing a modular hardware and software architecture. The different modules, like analog frontend, analog digital converter (ADC), processing elements, application specific integrated circuits (ASICs), interface solutions or memory devices are important for specific use cases, like the operating mode, an online data evaluation, a long-term data archiving, etc.. The complexity of the hardware platform requires lots of software features, e.g. for the data management, the system configuration, the system programming, the development and for the graphical user interface. In addition, several use cases are existing with regard to different areas of operation, like medical test, the clinical application, the use by patients, long term or short term signal evaluation. To be able to fit all these requirements and constraints, the platform paradigm is valid for the hardware domain as well as for the software domain. Here a software platform is conceived which is based on the RichClient-Platform of Eclipse and uses the capabilities of the open system gateway initiative (OSGI).

In this paper, however, we would like to focus on the flexibility of the platform based architecture. To improve the first design we have taken several aspects into consideration. At first the system has been shrinked to realize a body-mounted system. Figure 2 shows the 1st and 2nd generation of the smart modular biosignal acquisition, identification and control system (SMoBAICS). Our first prototype has been used for the examination of the platform architecture and of the module design. Besides, the modules, in particular the analog frontend module, were subdivided in several submodules to be able to learn from the measuring campaigns efficiently. Here we have used a backplane architecture for the whole system to realize a fast and easy module replacement of the ADC, the amplifier, etc.. In addition, most of the components are configurable by software to guarantee high flexibility. With the help of this first prototype platform important knowledge about the signal characteristic features was obtained. The second platform approach reduces the system dimensions; now the area per module is 33x60 mm^2. The height per module ranges from amounts from 5.4 mm to 6.4 mm. Using a system configuration consisting of 5 modules, the overall volume is less than 80 cm^3, compared to the old system platform with $\approx$ 1750 cm^3. The next step will be the system in package platform (SIP) to realize an implant-

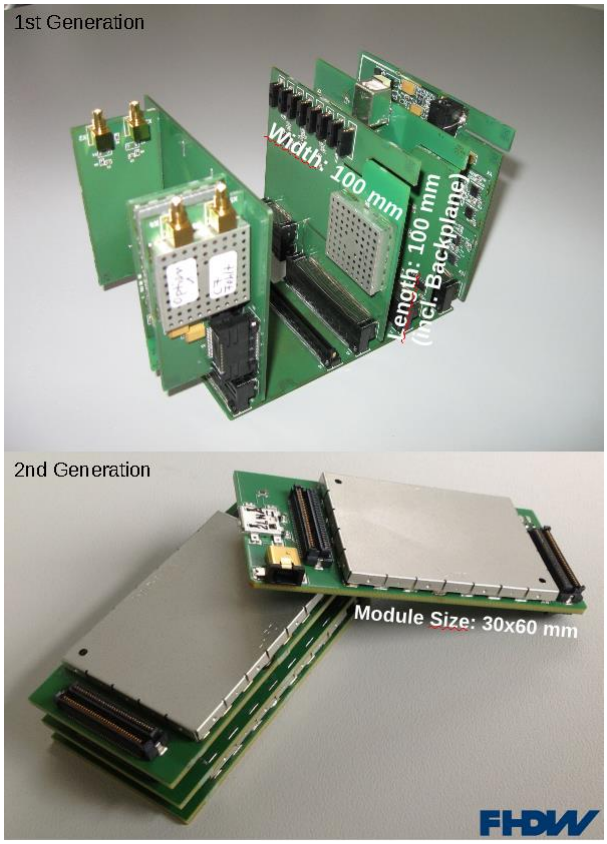

Figure 2: System evolution

table medical device. The additional design specifications for the new system are:

- Mobility

  The measurement period of the EMG- or ENG-based biosignals and an optional stimulation has to be several hours to integrate the monitoring process into the user's life and satisfy long-term measurements.

- Considerable Improvement in Communication Options

  The system has to realize a communication channel to medical staff informing about critical situations or therapy-relevant events. This communication channel has to be established using a smart phone which is connected via Bluetooth or Wi-Fi to the system.

- Local Intelligence

  To trigger the measurements and to realize an event based communication with the user or external staff, local processing power is necessary. In addition, the local identification, used in the operation and mobile mode, needs local intelligence for event and pattern matching.

In the following text we present the design of the new CPU-module extending the system capabilities. This CPU-module provides a better local data management and more computing power for the online identification algorithms during mobile operation and the ongoing system evolution. In addition, the connectivity of the

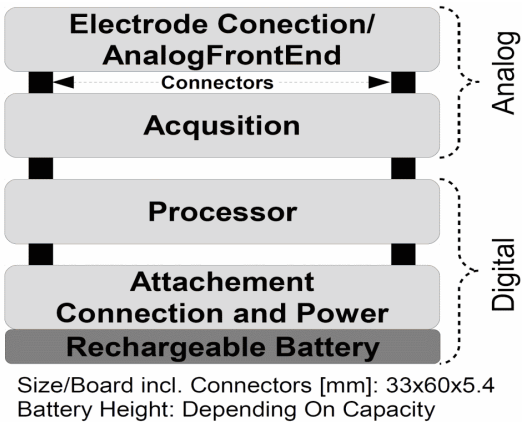

Figure 3: Module stack of the embedded data acquisition and identification module

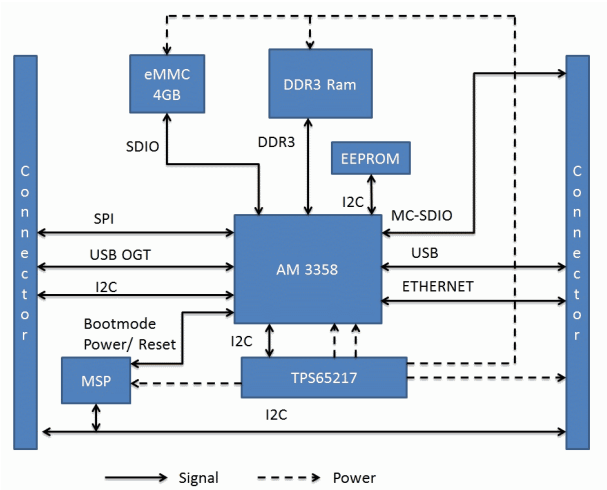

Figure 4: CPU-Module: Processor Board

system can be improved using for example the full Bluetooth/Wi-Fi stack based on Linux operating systems. The overall module stack of the system is shown in Figure 3. This module stack contains the whole functionality of the block diagram in Figure 1 including power supply by a rechargeable battery. The new CPU-module has been developed according the platform design guidelines. Using a high performance microprocessor (Sitara AM3358), the system capabilities, in particular the communication can be improved considerably. This board takes the data from the Acquisition Board, processes the data and either sends the data via communication channel. The CPU-module is split into two modules due to design considerations. The first module contains the ARM Cortex A8 processor along with the RAM, ROM as well as the power management chip. In Figure 4 the block diagram of the board is shown. The system is based on the AM3358 processor which is capable of running at 1GHz speed, along with support from a DDR3 RAM and a flash memory system. The AM3358 is best to be paired with the TPS65217 Power Management IC which provides all the supply voltages that are needed for operating the processor as well as the peripherals. The support for the USB, SPI and the

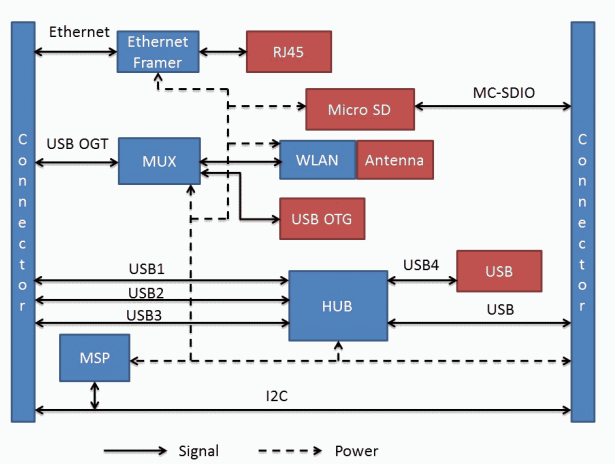

Figure 5: CPU-Module: Attachment Board

Ethernet ports are fed to the stack connectors as the ports are located on the Attachment Board along with the Memory Card slot. In addition, the board level controller (MSP430) is integrated, acting as the board identification and overall control system. Using the I2C protocol the various boards are able to identify and configure themselves accordingly. On the Processor Board, the MSP430 microcontroller also serves as a secondary control device with regard to low power operation. On the Attachment Board all peripherals are combined that are connected to the Processor Board, like USB ports, Ethernet port and also a micro SD card slot which can be used to store the data that is processed by the Processor Board. The overview of the Attachment Board is seen in Figure 5. The Attachment Board interfaces to the processor board through the stack connectors. It provides all external connectivity and the base plate for the rechargeable battery.

3. APPLICATION FIELDS

There are numerous applications in the field of biosignal measurement and signal processing. We will focus on two specific examples, demonstrating the flexibility of the platform concept.

3.1. Rehabilitation and Long-term Treatment Monitoring

There appears a whole array of diseases where it is necessary to monitor specific parameters for a long term treatment, for recovery from illness or for rehabilitation. Several reasons for such a decrease in nerve conduction are well known but not understood, like demyelinating or axonal injury. Neurophysiological measurements and tests are available to improve the knowledge and to improve the curing prospects. But in most cases these measurements are used rarely, once a week some even less often. It is necessary to provide a continuous

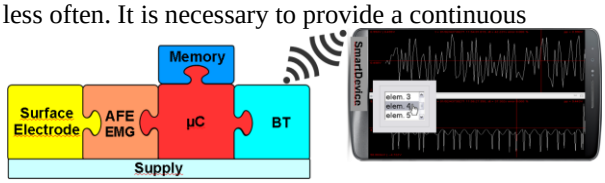

Figure 6: System for NCV (AFE: AnalogFrontend; µC: Microcontroller; BT: Bluetooth)

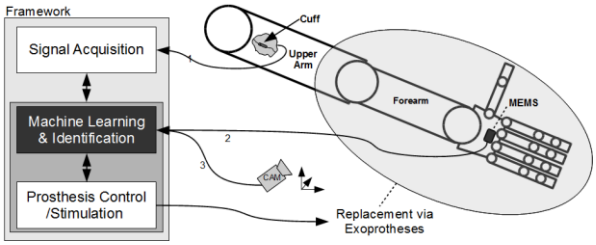

Figure 7: SMoBAICS Appplication

monitoring to get a better understanding of the interference of other parameters, like temperature, time of day, state of exhaustion, etc.. To fit all these requirements, a mobile system is necessary which provides the key functions described in section 1. One common examination is the measurement of nerve conduction velocity (NCV) in which impairments can be identified. While determining the nerve conduction, the nerve to be examined will be electrically stimulated at least at two places in its course. In Figure 6 the adequate system configuration is shown. It combines from surface electrode up to Bluetooth interface all modules to acquire and save data and to connect to a widely used smart device.

3.2. Prosthesis Control

Today prosthesis is even more than only easy spare parts for the human body. From the simple wooden butts of the past ingenious high-tech constructions have become. However, the modern medicine can substitute even more than only arms and legs. The main problem is the human machine interface of prosthesis and its movement control. The objective is to use biosignals for the information transfer between human being and prosthesis. Several possibilities are existing to realize such an interface. Our approach is the direct use of the action potentials of peripheral neural bundles via an ENG (Gold, Henze, and Koch 2007; Neymotin, Lytton, Olypher, and Fenton 2011). Based on these signals, a prosthesis, for example, an artificial hand or an artificial forearm, can be controlled specifically. In addition, by using a direct nerve interface it is possible to realize a bidirectional interface, not only for the actuatory data but for the reactuatory and sensory signals. The acquisition and interpretation of nerve signals is one key challenge to realize an intelligent control of prostheses or handicapped limbs. The interpretation is one central aspect due to the high information density within a nerve. In Figure 7 overall flow of motion control including the feedback loop is shown. Part of the system is camera and micro-electro-mechanical system (MEMS) support to improve the movement identification by methods of inverse and forward kinematics. The system configuration to fit this scenario contains:

- Cuff-electrode

  Using a special type of electrode, a Cuff-Electrode, the electrical potentials are recorded. The Cuff-electrode has been chosen for minimally invasive

surgical and therapeutic applications (Klinger and Klauke 2013).

- Analog frontend for ENG

To record the very small signals, which are only of the order of a few microvolts, we have designed a special front-end hardware (Klinger and Klauke 2013).

- Microprocessor
  - System and data management

    The AM3358 processor provides data management and configuration from the analog sampling module and data preprocessing for identification and archiving.
  - Identification

    The information taken from the Cuff-electrode contains a superposition from all action potentials of all single axons within the selected nerve bundle. Therefore an identification process is necessary to extract the trajectory information and to build up a model of the nerve bundle due to its axon configuration. The AM3358 provides enough computing power for the evaluation of the online identification.
  - Connectivity

    The Am3358 provides the full driver and communication stacks to enable seamless integration into the communication environment.
- Wi-Fi or Bluetooth interface to host

  Necessary hardware and antenna for establishing the wireless or Ethernet interface.

Figure 8 shows the scenario related system configuration. The Cuff-electrode is connected via cable.

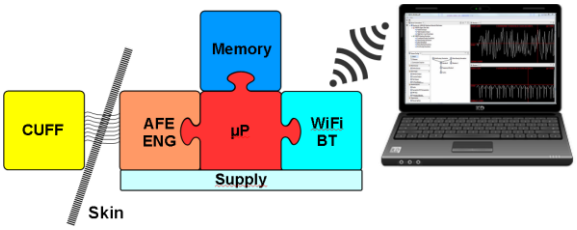

Figure 8: System for Prosthesis Control (AFE: AnalogFrontend; µP: Microprocessor; BT: Bluetooth)

4. RESULTS

In this paper two different aspects are in the focus due to the results. In subsection 4.1 we will present the enhanced verification method providing an all-level verification for the identification method. In subsection 4.2 we will focus on signal quality and interference ratio of the ENG-based analog frontend. The signal quality and accuracy is one of the key factors for the data based identification.

4.1. Enhanced Verification Method

The verification of the identification method is based on physiological data (Kandel, Schwartz, and Jessell 2000), and simulation knowledge (Law and Kelton 2000; Zeigler, Praehofer, and Kim 2000; Carnevale and Hines 2006). The new closed-loop verification provides an efficient and transparent verification process for the identification method. Causes and effects of certain sequence of motions can be investigated in detail. The used verification method allows different loops to check different characteristics using different levels of the identification method. In Figure 9 three different loops are shown taken the generated or motion-based generation of certain stimulation vectors and simulated action potentials into consideration.

- Verification of cluster assignment and physiological parameters (1)

The first option verifies the disposition of the clusters or anatomic fascicles of the nerve bundles. Using certain stimulation vectors this verification approach is used to optimize the parameters of the identification method. Using real data, recorded with an analogue front-end system, it can be used to evaluate inter- or intra-individual differences of human beings to optimize the identification method with regard to adaptability. This verification step is based on the NEURON simulator modelling the intra- and extracellular nerve bundle (Carnevale and Hines 2006).

- Verification of action potential sequences (2)

This verification approach can be used either to improve the identification method towards better action potential disintegration or to enhance the knowledge base regarding the peripheral nerve-muscle interface. The generation of certain stimulation vectors itself can be used to adapt the abstraction level and complexity of the identification task. This verification step is based on the NEURON simulator, Java Framework and Matlab (Carnevale and Hines 2006; Corke 2011). The stimulation vectors (StimVectors) are generated based on simulated movements data.

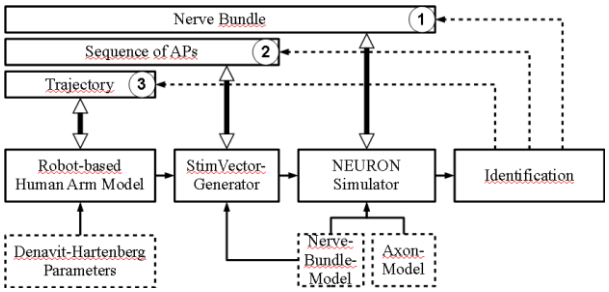

Figure 9: Verification architecture of SMoBAICS

- Trajectory verification (3)

The trajectory verification is the most sophisticated verification approach. Starting with the sequence of motion the verification consists of the comparison of the initial sequence of motion (start trajectory) and the identified sequence of motion (result trajectory). The comparison between both trajectories allows a qualitative and quantitative evaluation of the whole identification loop. This

trajectory verification includes the integration of camera- or MEMS-data within the identification method for the learning and the operating phase if there are no encoder data from prosthesis are available. It is well known that the human arm or total or partial prostheses are redundant manipulators therefore we have to use more than information from actions potentials to identify the position of the end-effector. During the operating phase we have to use MEMS, but it lacks in bias stability compared to the camera system. So we have to take this into account integrating the inertial navigation into the identification method (Woodman 2007). To evaluate a closed-loop verification system further, a robot-manipulator like a human arm (Denavit-Hartenberg parameters) including an MEMS device provides real movement data including real MEMS parameters. Closed loop verification consists of the causal chain:

1. Generating movement data using a robot-manipulator (Corke 2011)
2. StimVector generation based on the movement data and anatomical data (the calculated parameters are Denavit-Hartenberg parameters of the robot model according e.g. an anatomical data of an human arm.).
3. Simulation by NEURON simulator and extracting the data of the simulated Cuff-electrode.
4. Identification
5. Identification-based trajectory processing
6. Comparison of robot-manipulator movement and identified trajectory.

This verification step is based on the NEURON simulator, Java Framework and Matlab, too. It uses in addition inverse/forward kinematic algorithms (Craig 2004; Khalil and Dombre 2002).

4.2. Results from the Acquisition System

Focusing on the second application scenario (see subsection 3.2), the entire system uses data-based methods where the data are acquired by the Cuff-electrode; therefore data quality is one key parameter. In this subsection we present measurement data taken by the analog frontend (ENG) and a Cuff-electrode (Klinger and Klauke 2013) to evaluate the signal quality. The results were determined in an animal experiment with rats, carried out at the Medical School Hannover (MHH). All information in the following diagrams is scaled as follows:

- Abscissa: Time
  Relative timeline, corresponding to the number of cycles of the analog-digital converter, sample rate: 4 kHz.
- Ordinate: Amplitude
  All values are given in µV .

In Figure 10 one single impulse measured by the Cuff-electrode is shown. This impulse, a classical All-or-None-impulse, shows from the amplitude heave as well as from the temporal expiry the course to be expected for a capacitive electrode. Helpfully with this measurement are the appraisals which can be won with regard to the nerve isolating qualities by Epineuria as well as Perineuria and Endoneuria.

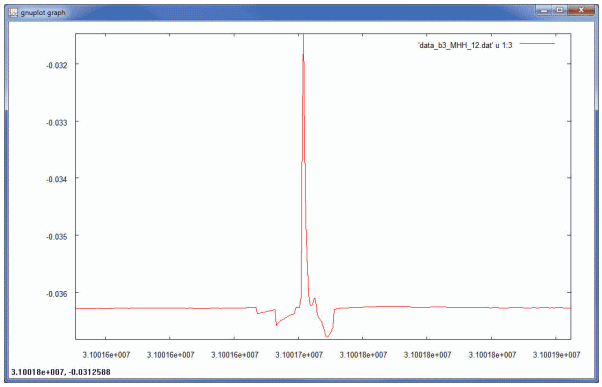

Figure 10: Measurement of a classical All-or- None-impulse with the capacitive Cuff-electrode

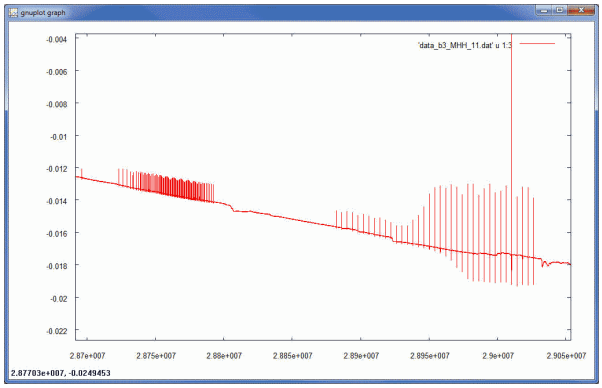

Figure 11: Measurement of the nerve activities due to stimulations with varying frequency

In Figure 11 the nerve activities on stimulation with different frequency are shown. On the left there is a faster stimulation (20 Hz) with an uniform electrical stimulation. On the right there is a slower stimulation (3 Hz) where the electrical stimulation is increased by scaling the stimulation current. The measured signals agree with the relative stimulation voltage and stimulation frequency. In the amplitude certain changes are recognizable; these changes appear on the basis of superposition of action impulses generated by a number of axons. The spatial resolution within the fascicle is up to now not possible because the used Cuff provides only 2 sensors which are used to check different amplifier configurations and reference potential configurations. On the reason for the increase in activity can be speculated here, meaning the certain fascicle activity of the whole nerve fiber. According the expectations, the total number of axons which are active is increased. The superposition of axon activities inside one nerve fiber related to a complex sequence of muscle contractions is due to a simple correlation. Thus, for example, the

overall muscle contraction is controlled according the force required for a movement. Two different mechanisms are well known: To get more overall moving force

- the frequency of axon impulses controlling some muscle fibers has to be increased, and
- the number of active axons has to be increased to control more and more muscle fibers.

This effect can be also observed in Figure 12. There a sequence of action potentials is shown on account of a more complicated stimulation, triggered through a real leg movement during the animal experiment. Here a number of axons within the taken nerve bundle are firing action potentials according the triggered muscle activity. The different amplitudes are composed by the superposition of the sequences of action potentials formed by All-or-None single impulses. The superposition of several All-or-None action potentials can be measured outside the nerve bundle by the Cuff electrode.

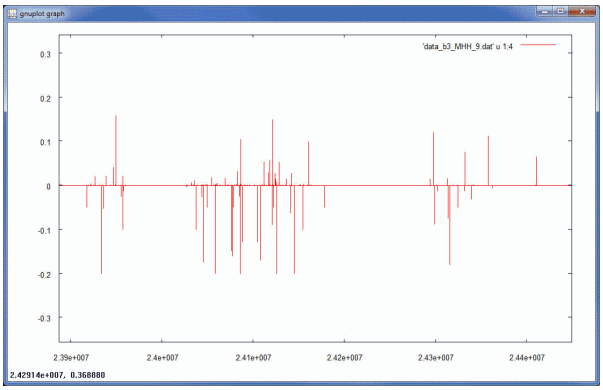

Figure 12: Measurement of the superposition of action potentials from the taken nerve bundle by the Cuff-electrode

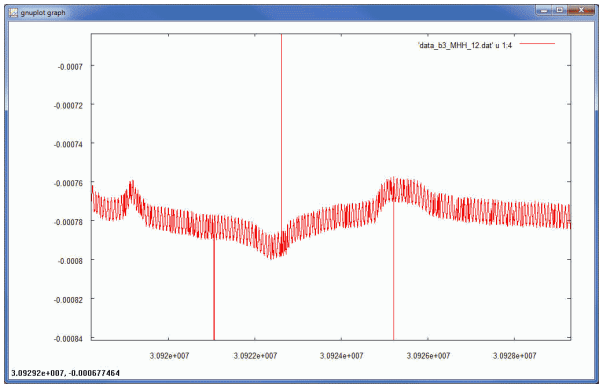

Figure 13: Resolution and noise amplitude

These results are important to receive data from the possible amplitude area and to get information about the whole signal path and its proper configuration parameters. For the improvement of the signal-to-noise ratio the analog front-end module has been optimized, especially for the measurement of ENG data. In Figure 13 there is the noise on an input signal shown. The noise amplitude is less than 20 nV. Compared to the action potentials measured by the Cuff-electrode the signal to noise ration fulfils the requirements. On account of the very good low-noise specification and large amplitude range, the sensor signal can be used at a very high-resolution. Its properties for extracellular recording measurements could be confirmed. The three outliers in the measured signal are uncritical; the software bug has been tracked for fixing.

5. SUMMARY AND FURTHER WORK

The presented approach for a platform-based embedded biosignal acquisition and identification system offers a wide range of medical applications. The modular system character provides adaptability to different diagnostic, rehabilitation monitoring and control scenarios with regard to computing power, connectivity and analog frontend characteristics. To emphasize this key feature beyond the presented application scenarios in section 3, in Figure 14 a possible next system generation for the prosthesis control application based on an integrated system-in-package (SIP)-solution is shown. The communication between SIP-based implant and the body-mounted system is connected for example via medical-implant- communication-service (MICS).

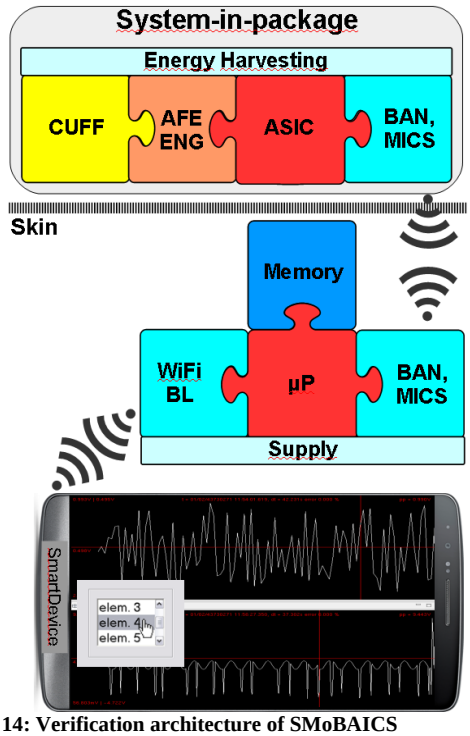

Figure 14: Verification architecture of SMoBAICS

The simulation-based closed-loop verification, presented in subsection IV-A, provides an efficient and transparent verification. Using the NEURON simulator and forward/inverse kinematic it allows a large test depth including anatomical and physiological parameters, like nerve bundle configuration and electrical parameters of peripheral nerves. The identification method helps to understand and to evaluate the correlation between movement and peripheral nerve information, including the actoric and the related sensoric feedback information flow. The

results related to the ENG-based data acquisition system, introduced in subsection 4.2, show the technical feasibility and establishes the basis for the data-based identification. All results help to reduce the number of animal experiments using simulation and closed-loop verification methods.

The embedded EMG- and ENG-based biosignal data acquisition and identification system using a flexible hardware and software-platform offers considerable potential. Additional tests and clinical applications will follow to improve the system characteristics and the identification further.

6. ACKNOWLEDGEMENT

All in-vivo experiments are performed in collaboration with the Clinic for Neurosurgery at the MHH.

REFERENCES

Sebastian Bohlmann, Arne Klauke, Volkhard Klinger, and Helena Szczerbicka. Model synthesis using a multi-agent learning strategy. In The 23rd European Modeling & Simulation Symposium (Simulation in Industry), Rome, Italy, September 2011.

Sebastian Bohlmann, Volkhard Klinger, and Helena Szczerbicka. HPNS - a Hybrid Process Net Simulation Environment Executing Online Dynamic Models of Industrial Manufacturing Systems. In Proceedings of the 2009 Winter Simulation Conference M. D. Rossetti, R. R. Hill, B. Johansson, A. Dunkin, and R. G. Ingalls, eds., 2009.

Sebastian Bohlmann, Volkhard Klinger, and Helena Szczerbicka. System Identification with Multi-Agent-based Evolutionary Computation Using a Local Optimization Kernel. In The Ninth International Conference on Machine Learning and Applications, pages 840–845, 2010.

Nicholas T. Carnevale and Michael L. Hines. The NEURON Book. Cambridge Univ. Press, New York, NY, USA, 2006.

Peter Corke. Robotics, Vision and Control – Fundamental Algorithms in MATLAB R , volume 73 of Springer Tracts in Advanced Robotics. Springer, 2011.

J.J. Craig. Introduction to Robotics: Mechanics and Control. Prentice Hall, New Jersey, USA, 2004.

Carl Gold, Darrell A. Henze, and Christof Koch. Using extracellular action potential recordings to constrain compartmental models. Journal of Computational Neuroscience, 23(1):39–58, 2007.

Eric R. Kandel, James H. Schwartz, and Thomas M. Jessell. Principles of Neural Science. Elsevier, New York, fourth edition, 2000.

W. Khalil and E. Dombre. Modeling, Identification & Control of Robots. Routledge, New York, USA, 2002.

Volkhard Klinger. Verification concept for an electroneurogram based prosthesis control. In Agostino Bruzzone, Marco Frascio, Vera Novak, Francesco Longo, Yuri Merkuryev, and Vera Novak, editors, 3nd International Workshop on Innovative Simulation for Health Care (IWISH 2014), 2014.

Volkhard Klinger and Arne Klauke. Identification of motion-based action potentials in neural bundles using an algorithm with multi-agent technology. In Werner Backfrieder, Marco Frascio, Vera Novak, Agostino Bruzzone, and Francesco Longo, editors, 2nd International Workshop on Innovative Simulation for Health Care (IWISH 2013), 2013.

Averill M. Law and W. David Kelton. Simulation Modeling and Analysis. McGraw-Hill, 2000.

S.A. Neymotin, W.W. Lytton, A.V. Olypher, and A.A. Fenton. Measuring the quality of neuronal identification in ensemble recordings. J Neurosci, 31(45):16398–409, 2011.

Oliver J. Woodman. An introduction to inertial navigation. Technical Report UCAM-CL-TR-696, University of Cambridge, Computer Laboratory, August 2007.

Bernard P. Zeigler, Herbert Praehofer, and Tag Gon Kim. Theory of Modeling and Simulation: Integrating Discrete Event and Continuous Complex Dynamic Systems. Academic Press, San Diego, USA, 2 edition, 2000.

AUTHOR BIOGRAPHY

VOLKHARD KLINGER has been a full time professor for embedded systems and computer science at the University of Applied Sciences FHDW in Hannover since 2002. After his academic studies at the RWTH Aachen he received his Ph.D. in Electrical Engineering from Technische Universitaet Hamburg-Harburg. He teaches courses in computer science, embedded systems, electrical engineering and ASIC/system design.

His email address is: <Volkhard.Klinger@fhdw.de>.

USING THE OSCE METHOD IN A SIMULATION CENTRE TO ENSURE EQUITY AND OBJECTIVITY IN ASSESSING THE COMMUNICATION AND RELATIONAL SKILLS IN A LARGE OF STUDENT NURSES DURING A LONG EXAMINATION SESSION

Annamaria Bagnasco[(a)], Angela Tolotti[(b)], Giancarlo Torre[(c)], Loredana Sasso[(d)]

[(a),(b),(d)] Department of Health Sciences, University of Genoa, Via Pastore 1, I-16132 Genoa, Italy
[(c)] Centre of Simulation, School of Medical and Pharmaceutical Sciences, University of Genoa, Via Pastore 1, I-16132 Genoa, Italy.

[(a)]annamaria.bagnasco@unige.it, [(b)] angela.tolotti@unipv.it , [(c)] gctorre@unige.it , [(d)] l.sasso@unige.it

ABSTRACT

There is little known about OSCE use in European countries such as Italy, where other than cost analysis, there is little reporting of OSCE use or validation.
This paper reports on one Italian initiative, which evaluated the equity and objectivity of the OSCE method of assessing communication skills.
An OSCE method was used to assess the communication and relational skills of first-year students of the Degree Course in Nursing. A method of simulation was implemented through role-playing with standardized patients.
The study confirmed the validity of the OSCE method in ensuring equity and objectivity of communication skills assessment in a large population of nursing students for the purpose of certification throughout the duration of the examination. This has important implications for nurse education and practice as it is not clear the extent to which OSCE approaches are culturally sensitive, or valid and reliable across cultures.

Keywords: OSCE, Simulation, communications skills, Inter-rater evaluation.

1. INTRODUCTION

One of the problems connected with assessment efficacy often lies in the incongruence among training objectives, teaching methods and the instruments used to measure the outcomes of learning. While many methods are used to measure student performance, their choice must be guided chiefly by two criteria: appropriateness to the outcomes of learning and the objectivity of their assessments. In the international literature, numerous studies have reported that the application of the Objective Structured Clinical Evaluation (OSCE) methodology in the assessment of training and the certification of clinical and relational skills is a guarantee of objectivity and equity. Some studies have described the use of the OSCE methodology in the certification of large numbers of students belonging to healthcare professions (Newbel, 2004) OSCE is a method of assessment that enables relational skills to be measured on the basis of the performances displayed by the students over a range of clinical behaviors with standardized patients. The prime objective is to assess the student's ability to implement theoretical knowledge in a simulated practical situation (Mc William & Botwinski, 2010). The OSCE examination is conducted in settings that are equipped to measure a set of clinical skills in a realistic manner through simulated clinical scenarios involving standardized patients. While the measurement of non-technical skills has been the subject of much debate the use of standardized patients and scales of observation for the assessment of communication skills has proved efficacious.

2. AIM

The aim of the present study was to evaluate the equity and objectivity of the OSCE method of assessing clinical learning with regard to communicative/relational skills among a large population of students over a long period of examination.

3. METHODS

The OSCE methodology was adopted to assess the communicative and relational skills of first-year students of the Degree Course in Nursing. To this end, an examination environment was specially designed, which reproduced the characteristics of a room in a hospital ward.

During examinations, a method of simulation was implemented through role-playing with standardized patients.
Examinations were conducted by following eight scripts structured in accordance with core competence. The scenarios were based on the phases of information and communication with patients undergoing diuresis monitoring and subjects with problems of mobility, hygiene, alimentation, hydration and arterial hypertension.
The objectives that students were expected to achieve concerned five observable behaviors regarding the communication of relevant information, the use of language appropriate to the patient, verification that information had been understood, active listening and reassurance of the individual through advice on the clinical situation. Student performance was evaluated by means of validated assessment tables (Guilbert, 2002); these covered four variables and were broken down into five levels of expected, observable communicative behaviour. To evaluate performance, an assessment scale indicating values between -2 and +2 was used, and a score was attributed to each communicative behaviour with respect to the variable in question. The variables referred to terminology, listening, attention and clarity. (Table 1)

Score	Terminology	Listening	Attention	Clarity
-2	Too detailed – not appropriate	Hears but does not listen	Pays no verbal or behavioral attention	Communication is not clear and information is not precise
-1	Too detailed – appropriate	Listens but does not re-state	Verbal and behavioral attention are inconsistent	Communication is not clear and information is not very precise
0	Appropriate – Not very precise	Listens and re-states but not always correctly	Pays verbal attention	Communication is not always clear and information is not always precise
+1	Appropriate but does not answer questions immediately	Listens and re-states correctly	Pays verbal and behavioral attention	Information is precise but communication is not always clear
+2	Answers questions Immediately	Checks whether SP has understood	Gives feedback to SP	Information is correctly understood

Table 1. Guilbert's Evaluation Grid used to score the students' communication skills during the OSCE examination

4. RESULTS

All first-year students of the Degree Course in Nursing undergoing examination for clinical training certification (n=421) took part in the study. Ten examination sessions were conducted, the mean daily number of students examine being 42.1 (SD). With regard to the equity of the examinations, calculation of the daily pass rate indicated a random distribution over time.
The students from the 8 Training Centres were subdivided as follows: Center A 19%, Center B 12%, Center C 14%, Center D 10%, Center E 14%, Center F 17%, Center G 7% and Center H 7%.
For the Concordance of the scores and of the evaluations assigned by the examiners during the examination, Lin's Concordance Coefficient (CC) was calculated. The CC of the scores proved to be 0.993 (95% CI: 0.992-0.995, P<0.001).
With regard to the concordance of the marks assigned by each examiner, the CC proved to be 0.992 (95% CI: 0.991-0.994, P<0.001).
Regarding the concordance in the outcome of the final examination, Cohen's k index between the pass marks assigned by the two examiners proved to be 0.989 (95% CI 0.986-0.999, p<0.001).

5. CONCLUSIONS

The study confirmed the validity of the OSCE method in ensuring equity and objectivity of communication skills assessment in a large population of nursing students for the purpose of certification throughout the duration of the examination.

The objectiveness of the results obtained can be ascribed to the preparation of the examiners. Indeed, the role of the examiners in ensuring the validity of the assessment is fundamental. Furthermore, to guarantee objectivity, it is essential that the examination, the assessment tools and the conduct to be adopted during the examination be agreed upon. In this regard, much attention was devoted to the issue of communication with the examinee, which must be limited to explaining the necessary instructions. Indeed, during the examination, the examiners were not allowed to communicate with the student. This becomes particularly important when students conclude their performance before the allotted time. Indeed, during the test of the relational skills, examiners had a neutral position, behind the student, to avoid any contact or interference with the examinee. The possibility of placing the examiners in another room from where they could observe the student's performance directly (through a one-way mirror) may be helpful. Nevertheless, all of the above-mentioned aspects were monitored through audiovisual recording, and

everything happening in the examination room was viewed in real time on a screen.

REFERENCES

Guilbert J.J. 2002. Guida pedagogica per il personale sanitario. WHO, Publication offset n.35. Edizioni del Sud, Bari.

Mc William P., Botwinski, C. 2012. Identifying strengths and weaknesses in the utilization of Objective Structured Clinical Examination (OSCE) in a nursing program. Nurse Education Perceptive 33(1), 35-39.

Newbel, D. 2004. Techniques for measuring clinical competence: objective structured clinical examinations. Medical Education 38, 199-203

THE INTERPROFESSIONAL SKILL LAB IN THE SIMULATION CENTRE: AN EXPERIENCE OF COMMUNICATION BETWEEN THE MEDICAL-NURSING TEAM AND FAMILY MEMBERS

Annamaria Bagnasco[(a)], Sue-Anne Maruffi[(b)], Gianluca Catania [(c)], Giancarlo Torre[(d)], Loredana Sasso[(e)]

[(a),(c),(e)] Department of Health Sciences, University of Genoa, Via Pastore 1, I-16132 Genoa, Italy
[(d)] Centre of Simulation, School of Medical and Pharmaceutical Sciences, University of Genoa, Via Pastore 1, I-16132 Genoa, Italy.
[(b)] School of Nursing, University of Genoa, Via Pastore 1, I-16132 Genoa, Italy.

[(a)]annamaria.bagnasco@unige.it, [(b)] smaruffi@ospedale.al.it , [(c)]gianluca.catania@edu.unige.it
[(d)]gctorre@unige.it , [(e)] l.sasso@unige.it

ABSTRACT

During daily clinical practice, health professionals spend most of their time interacting with each other. Nevertheless, at university they are educated and trained separately and rarely have the opportunity to learn how to work as a team. In our center of simulation we organized an interdisciplinary education session with nursing and medical students to improve their interprofessional team behaviours and competences.
The students became more aware of the four domains of interprofessional competence (values/ethics, role and responsibility, interprofessional communication, teams and teamwork) and about the need to learn how to integrate with each other to work in synergy as an interprofessional team to meet people's healthcare needs, which are becoming increasingly complex.

Keywords: Center of Simulation, Interprofessional competence, behaviours, skills, teamwork, added value.

1. INTRODUCTION

Several studies have shown that care provided by interprofessional teams produce better outcomes for patients, compared to traditional methods. In 2002, interprofessional education was defined by the Centre for the Advancement of Interprofessional Education (CAIPE) a "occasions in which two or more professions learn *with, from* and *about* one another, in order to improve collaboration and the quality of care". In 2009, the American Association of Colleges of Pharmacy (AACP) expanded this definition: "Interprofessional education includes educators and students belonging to two or more healthcare professions and jointly taught disciplines promote a collaborative learning environment. The purpose of this endeavour is to develop knowledge, skills, and attitudes that translate into interprofessional team behaviours and competences.
Ideally, interprofessional education is vertically and horizontally embedded throughout the curriculum." Figure 1.

Figure 1. The relevance of interprofessional education

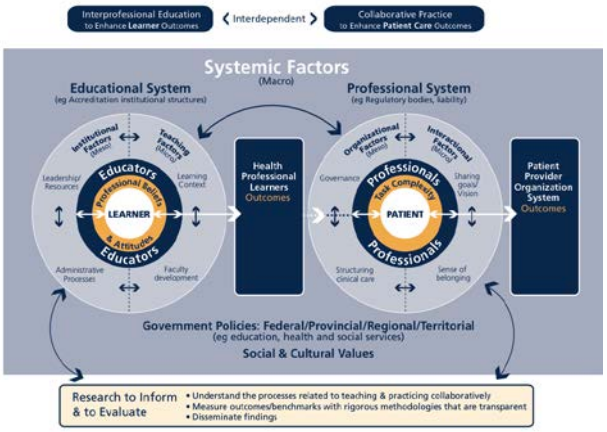

Reprinted with permission from *D'Amour, D. & Oandasan, I. (2005). Interprofessionality as the field of interprofessional practice and interprofessional education: An emerging concept. Journal of Interprofessional Care, Supplement 1, 8-20.*

Jean-Jacques Gilbert (2002) stated that being a collaborative worker requires both the transformation of the personal perspective and of the professional identity. Interprofessional competency or capability, consists of 4 domains: values/ethics, role and responsibility, interprofessional communication, teams and teamwork.

2. AIM

To implement and test the effectiveness of an interdisciplinary educational session with nursing and medical students in a centre of simulation at the University of Genoa.

3. METHODS

To build the contents of the interprofessional educational session, we adopted the Integrated course design methods, which included:

- Role play (to develop relational competences);
- Briefing & debriefing (to share information about the event);
- Semi-structured interview including 6 questions based on the literature and the role-play script;
- Guided reflection (to analyse the contents of this experience).

The title of the interprofessional educational event was: "Family and child centred care: The role of communication". The educational session was recorded and verbatim transcribed to extract the main concepts and constructs from what the students said. Informed consent was obtained and anonymity ensured.
The setting was the Centre of Simulation of The School of Medical and Pharmaceutical Sciences at the University of Genoa.
The sample was a non-probabilistic convenience sample including 11 nursing students and 8 medical students.

4. RESULTS

After analysing the data collected through the modified evaluation grid called "Clinical skill laboratory questionnaire", we can affirm that the interprofessional educational event was rated positively in terms of a) teaching method; b) educational materials; and c) educators.
The main concepts and constructs drawn from the questions the students asked and the aggregated response data were:

- Meaning of interprofessional team;
- Different and reciprocally-completing roles; physician/nurse *primus inter pares*;
- Things done at different moments;
- Feeling of 'loss' in terms of quality of care for patients when interventions are not jointly agreed;
- Recognise that there is the need for specific training in terms of interprofessional teamwork;
- Need to be educated for integration: knowing one another, share, and cooperate;
- Having a common vision that is centred on the patient.

These concepts confirmed that the interprofessional educational session was correctly designed and conducted.

5. CONCLUSIONS

On the basis of our results, the purpose of this study was achieved. The mix of teaching methods selected for out interprofessional education session in the Centre of Simulation were effective in launching a course of interprofessional education, which will enable to implement knowledge and awareness about the competences required to work in an interprofessional team, as well as the need to reflect on this topic.
The students became more aware of the four domains of interprofessional competence (values/ethics, role and responsibility, interprofessional communication, teams and teamwork) and about the need to learn how to integrate with each other to be able to work as an interprofessional team in the future, and in synergy meet people's healthcare needs and improve their outcomes. In addition, good interprofessional teamwork can produce a very positive impact in terms of quality of care, patient safety, healthcare outcomes, and better satisfaction both for patients and health professionals themselves.
It would be important to conduct further investigations to understand how to better integrate interprofessional education throughout the students' curricula, through practical joint learning sessions, as the students themselves suggested. Therefore, as Aristotle said: "The whole is greater than the sum of its parts", which in our case is the added value for the patient.

REFERENCES

Guilbert J.J., 2002. Guida pedagogica per il personale sanitario. WHO, Publication offset n.35. Edizioni del Sud, Bari.

AN ADVANCED CENTRE OF SIMULATION TO SUPPORT CAREGIVERS PROVIDING HOME CARE TO CHRONICALLY ILL PATIENTS, PATIENTS WITH RARE DISEASES, AND END OF LIFE CARE

Annamaria Bagnasco[(a)], Giancarlo Torre[(b)], Roberta Centanaro[(c)], Lucia Bacigalupo[(d)], Loredana Sasso[(e)]

[(a),(e),] Department of Health Sciences, University of Genoa, Via Pastore 1, I-16132 Genoa, Italy
[(b)] Centre of Simulation, School of Medical and Pharmaceutical Sciences, University of Genoa, Via Pastore 1, I-16132 Genoa, Italy.
[(c), (d)] School of Nursing, University of Genoa, Via Pastore 1, I-16132 Genoa, Italy.

[(a)] annamaria.bagnasco@unige.it , [(b)] gctorre@unige.it, [(c)] Roberta.centanaro@hsanmartino.it , [(d)] lucia.bacigalupo@hsanmartino.it, [(e)] l.sasso@unige.it

ABSTRACT

Due to the ageing of the population, informal caregivers are being challenged by having to take care for a rapidly increasing number of patients living with complex conditions at home. Informal caregivers are often overwhelmed by the increasing number of duties and responsibility in dealing with issued and fears related to taking care of patients with complex disorders. Health professional need to take action to respond to informal caregivers' training needs. For this reason, the University of Genoa has organized specific skill labs specially designed for informal caregivers, so that they may routinely receive adequate information and support to deal with complex patients.

Keywords: caregivers, complex patients, skill lab, center of simulation, training, support

1. INTRODUCTION

A number of international studies have shown that laboratory training is an effective means of developing the communication and gestural skills in healthcare workers. Simulation is a training method that represents certain aspects of clinical care in a lifelike manner, integrating them into an effective training environment (Patrick, 1992). Simulators have been part of simulation and clinical education since the 1950s. The first type of simulators consisted of static models that were used to learn basic skills, such as intravenous and urinary catheter insertion and medical training in mouth-to-mouth resuscitation. As simulation technology evolved the models were able to more closely mimic physiological states. High-fidelity human patient simulators (HPS) include software within the mannequin that can be accessed and manipulated with a laptop or desktop computer. Nowadays, high-fidelity HPS provide the most advanced simulation training in nursing and medicine (Laschinger, 2008). Progress in training methods has introduced the conceptual model of critical and creative thinking in learning communication and gestural skills, and many reports have shown how this model fosters the development of cognitive, strategic and planning skills.

The Clinical Skill Laboratory is a "facility whose purpose is to support the acquisition, maintenance and enhancement of the clinical skills. Clinical, communication and information technology skills can be acquired to update new competencies during professional life.

High fidelity simulation environments provide participants with the opportunity to generate, develop and enhance their communication skills and confidence in their own abilities without worrying about compromising patient safety; they also provide participants with the chance to practice and correct their mistakes in real time. It has also been clearly shown to improve team behaviours in a wide variety of clinical contexts and clinical personnel, associated with improved team performance in crisis situations (Lewis, 2012).

At the University of Genoa, a project geared towards training of informal caregivers has been initiated in a simulation center.

2. OBJECTIVES

The learning objectives for the informal caregivers were: provide hygienic care, inserting a catheter, moving a partially and totally dependent patient, managing a Percutaneous Endoscopic Gastrostomy (PEG), providing stoma care, managing mechanical ventilation, managing a tracheal cannula.

3. METHODS

After analyzing the specific aims of the informal caregivers, we identified the topics for the laboratory sessions that would contribute to the development of their communication and gestural skills.

Once all the laboratory sessions had taken place, the caregivers were asked to fill out an anonymous questionnaire about their education experience in the

Simulation Centre. The first section of the questionnaire focused on the perceptions of how important the topic of each laboratory session was; the second section focused on the quality of training methods, and the materials used during the laboratory sessions and the trainers, who were physicians and nurses. The third section focused on the assessment of their decision to take part in the training course at the Simulation Centre. A six-point Likert scale was used to measure satisfaction.

4. RESULTS

The respondents were 99.
High scores were obtained in relation to the quality of the education provided, underlining the relevance and the appropriateness of the teaching activities, the materials, and of the simulation technological support.
Also teaching effectiveness scored positively, and this confirmed the appropriateness of the methodology used to achieve the training levels required by informal caregivers.
Finally, the high scores related to their decision to take part in this course confirmed that the caregivers were very satisfied and that the course met their expectations and the educational needs.

Quality of education and training	Module 1		Module 2		Module 3		Module 4	
	N	%	N	%	N	%	N	%
Blank	11	9	5	3	0	0	1	1
Score 0	0	0	0	0	0	0	0	0
Score 1	0	0	0	0	0	0	0	0
Score 2	0	0	0	0	0	0	0	0
Score 3	4	3	3	2	0	0	2	2
Score 4	**17**	**14**	**21**	**19**	**2**	**2**	**39**	**24**
Score 5	**93**	**74**	**86**	**77**	**103**	**98**	**108**	**73**
Total	125	100	115	100	105	100	150	100

5. CONCLUSIONS

The Clinical Skill Laboratory is a "facility whose purpose is to support the acquisition, maintenance and enhancement of the clinical skills. Clinical, communication and information technology skills can be acquired to update new competencies during professional life (Rees & Jolly, 1998).

The results of our study showed that the informal caregivers were very satisfied with the clinical skill laboratory sessions, and were interested in participating in similar activities in the future. These findings suggest that simulation laboratory sessions should be provided to all informal caregivers on a routine basis.

The participants were also very satisfied with the trainers' expertise, approachability and communicativeness.
The importance of this study is related to the fact that informal caregivers will be those who will carry a large portion of the burden of care in patients' homes due to the ageing of the population. Therefore, health professional need to be aware of this situation and provide all the necessary support to informal caregivers, especially through simulated educational interventions like the one described in this study. We therefore reckon that in the near future the centers of simulation will be a source of instrumental support for all informal caregivers, and not only for health professionals and students.

REFERENCES

Laschinger S., Medves J., Pulling C., McGraw R., Waytuck B., Harrison M., Gambeta K., 2008. Effectiveness of simulation on health profession students' knowledge, skills, confidence and satisfaction. International Journal of evidence based healthcare, 6, 278–302

Lewis R., Strachan A., McKenzie Smith M., 2012. Is High Fidelity Simulation the Most Effective Method for the Development of Non-Technical Skills in Nursing? A Review of the Current Evidence. The open nursing journal, 6, 82-89

Patrick J., 1992. Training: Research and Practice. London: Academic Press Limited.

A SIMULATION TOOL TO PLAN DAILY NURSE REQUIREMENTS

Paolo Barone[(a)], Francesco Imbimbo[(b)], Rosa Napoletano[(c)], Stefano Riemma[(d)], Debora Sarno[(e)]

[(a),(c)]Neuroscience Department, University Hospital "S. Giovanni di Dio e Ruggi d'Aragona", Salerno, Italy
[(b),(d),(e)]Department of Industrial Engineering, University of Salerno, Fisciano, Italy

[(a)] pbarone@unisa.it, [(b)]f.imbimbo@hotmail.it, [(c)]napoletanorosa10@tiscali.it, [(d)]riemma@unisa.it,
[(e)] *corresponding author*: desarno@unisa.it

ABSTRACT
The economic cost crisis and the need for reducing costs while assuring a high service level to patients are the drivers of the introduction of operations management tools in the hospital environment. With the premise of flexible shifts schedules, the assessment of the actual nursing time can enable a wise resource planning, balancing the efficiency in resource usage (avoiding overstaffing) with the quality of care (assuring the presence of an adequate number of nurses to care patients). This paper proposes an innovative simulation method to plan daily nurse requirements in which the best number of nurses for each shift according to a desired service level is defined taking into account real requirements of hospitalized patients. In particular, patient dependence from nurses has been correlated to the time needed to perform nurse tasks deduced from the clinical pathway of patients. The validation and verification of the proposal have been assessed in a stroke unit.

Keywords: nurse requirements planning; patient dependency; healthcare operations management; patient flow simulation.

1. INTRODUCTION AND LITERATURE REVIEW

The economic cost crisis and the need for reducing costs and assuring a high service level to patients are the drivers of the introduction of operations management tools in the hospital environment (Iannone et al., 2011-2015; Guida et al., 2012). The huge impact of personnel (mainly nurses) cost on budgets and the relevance of the nurse involvement in the process of care of patients, make the nurse staff an interesting test-bed for such innovative tools. The adoption of flexible shifts schedules and the assessment of the actual nursing time can enable a wise resource planning, balancing the efficiency in resource usage with the quality of care.
The Nurse Requirements Planning (NRP) issue can be contextualized in the wider framework of "Nurse capacity planning and scheduling" (Punnakitikashem & Rosenberger, 2008) and (Siferd & Benton, 1994), ranging from the staffing in the long time horizon (Villarreal & Keskinocak, 2014) to the scheduling in the medium time horizon (Constantino et al., 2014), till the daily rescheduling and assignation of patients to specific nurses (Naidu, Sullivan, Wang, & Yang, 2000). Methods to determine the nurse requirements (from staffing to rescheduling) have been developed since the eighties' and range from consensus approaches to top-down management approaches (Naidu, Sullivan, Wang, & Yang, 2000). They can be grouped into 5 categories ordered from the simplest to the complex one (Keith, 2003) and, in particular:

- *Expert judgment*, in which the number of nurses per shit is subjectively defined by nurses;
- *Number of nurse per occupied bed*, taking into account the statistics about the number of nurses attributed to beds of a certain ward;
- *Acuity-quality methods*, in which the time needed to give assistance to patients is proportional to their dependency on nurses (expressed by a patient dependency category) or patient acuity (Ernst, Krishnamoorthy, & Sier 2004), and changes from ward to ward. An interesting example of day-to-day nurse scheduling based on patient acuity has been reported by (Siferd & Benton, 1994) who, given a mean patient acuity for all patients, expressed in terms of number of nurses required, considered a mean rate of change in patient condition over the shift, assuming that new patients have higher acuity than the hospitalized ones. Then, they carried out a number of simulations to assess the impact of size of unit, acuity and number of admits and discharges on the number of nurses needed. Another case comes from (Liang & Turkcan, 2015), who presented a multi-objective optimization model for determining the number of nurses and the schedule of patients (minimizing waiting time) in an outpatient oncology clinic. The sum of patient acuities was matched with the maximum acuity manageable by a nurse to make assignments.

Nurse direct workload, instead, was concentrated in the first 30 minutes after each patient treatment start time (later, the nurse has to monitor contemporary patients' infusions). Both acuities and nurse workload for the treatment (excluding the other activities of the patient pathway) were assumed deterministic;

- *Time-task activity methods*, based on the concept that the type and frequency of nursing interventions on patients are good predictors of nursing time. To apply the models it is required to define a duration for each possible activity and then constructing the care plan for each patient. The ward overhead time has to be added to the total direct care time.
- *Statistics-based methods*, regression methods relying on the specific ward under analysis.

Methodological approaches to implement these methods range from subjective deduction to heuristic algorithms, simulation models or operational research.

This paper proposes an innovative daily NRP method which summarizes the best features of both acuity-quality and time-task activity techniques in a easy-to-use solution that is based on the concepts of:

- tasks of the patient clinical pathway (Bhattacharjee & Ray, 2014), that is the "standard" sequence of diagnostic, therapeutic and care activities a patient, with certain pathology and according to medical guidelines and resources availability, should undertake in a hospital;
- patient dependence on nurses in the activities of day living (Kaliszer, 1976), which is correlated to the time needed to perform each nurse' task.

Because of both concepts involve probabilistic evaluations related to task occurrence and task durations for each patient, and considering that patients number and characteristics change also over a day due to new accesses, discharges and status variance, the nursing time and, consequently, the number of nurses required to meet patient's demand, have a stochastic behaviour. Then, the service level offered to patient (that is the probability to meet the total patient's demand) is stochastically dependent on the number of planned nurses.
A simulation tool has been used to simulate each patient flow and find the cumulated probability distribution function of the number of nurses required for each shift.
This distribution can be finally used by management to choose the right number of nurses for the real patient requirements according to the desired service level, avoiding of time consuming data entry for NRP calculation, thanks to the automatic retrieval of data from Electronic Medical Records and database of clinical pathways belonging to hospital's Information Systems.
The paper is structured as follows: Section 2 deals with the description of the proposed method and Section 3 regards with the case study chosen to assess the usability of the proposal (a stroke unit). Data collection and analysis, simulation, validation and verification are provided. The conclusions follow.

2. MODEL DESCRIPTION

As recognized by many authors, due the patient pathway complexity, simulation is the best modelling solution to take into account task time, routing probabilities, and facilities integration (Bhattacharjee & Ray, 2014); (Cardoen & Demeulemeester, 2008). The proposed NRP method is based on a Monte Carlo Simulation (MSC), a very common numeric simulation used to randomly generate a set of events of a stochastic variable according to its Probability Distribution Function (PDF). By means of MCS, the stochastic behaviour of patient accesses, characteristics, clinical activities of the pathway and the related duration are reproduced over the shifts to estimate the total nursing time in different scenarios and determine the nurse service level in dependence on the number of nurses.

Some medical unit data are needed:

- database of the pathway activities with the maximum and minimum duration;
- expected duration of the indirect activities for each shifts;
- duration and time schedule of the shifts;
- maximum availability of the nurse staff;
- PDFs of patient inter-arrival time, duration of the emergency activities, Barthel values assigned;
- probabilities of occurrence and assignation to a nurse for each activity.

In the daily operations, the following data should be collected for each hospitalized patient:

- day of the clinical pathway;
- possible modification in the pathway (patient flow routing definition);
- dependence from nurses, Barthel scale value, An extensive survey on English stroke units (Rudd, 2009.) demonstrated that patient dependency, expressed by the Barthel scale value, has a correlation with nurse direct workload (Spearman's correlation coefficient being -0.5); with nurse direct workload (Spearman's correlation coefficient being -0.5);
- planned discharge or transfer;
- time of the access to the medical unit.

The simulation steps are the following:

1. Simulation of incoming patients'. Patients inter-arrival is simulated based on the related PDF. This time is added to the last accesses in order to find the next entries of new patients.
2. Simulation of patients' requirements. While for the hospitalized patients the Barthel scale is attributed by nurses, for incoming patient this value is simulated according to the occurred PDF. The nursing time (duration) of each caring activity is assumed to be a linear function of the Barthel scale) (Fig. 1) that can range from 0 (complete dependency of patient from nurses) to 20 (the opposite).

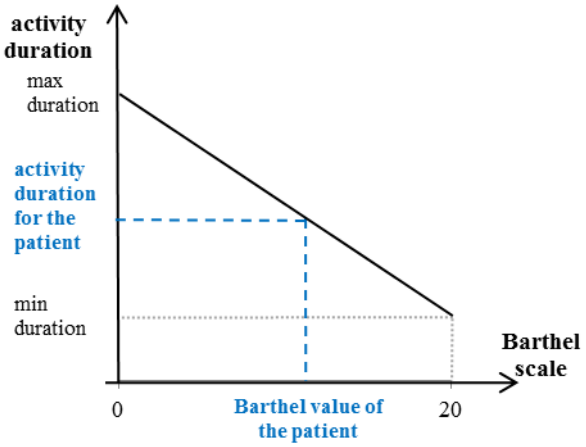

Figure 1: Activity duration for a patient in dependence on the Barthel value assigned to the patient.

The occurrence of each activity for the patient and the task assignation to nurses are taken into account based on its probability and, finally, the total duration of the nurses' activities for each shift is found.

3. Calculation of nurse requirement. The number of nurses required for each shift is found dividing the total duration of nurse activities by the time available by a single nurse during the shift and rounding this value to the highest integer.
4. Definition of the nurse requirement planning. The simulation from step 1 to 3 is repeated many times to reproduce the stochasticity of the variables involved. Finally, the cumulated probability distribution function of the number of nurses required for each shift is calculated, in which each number of nurses corresponds to a service level that can be probabilistically offered to patients. With this information the nurse manager or another decision maker are enabled to choose the best nurse sizing for the following day taking into account resource cost and service level to patients.

3. CASE STUDY: THE STROKE UNIT

3.1. Data collection

In order to validate and verify the proposed model, it has been implemented in a real environment. The case study under analysis is a stroke unit, a particular segment of the neurology medical unit dealing with stroke patients. Stroke is the second leading cause of disability in Europe and the reason of 10% of death worldwide (Wittenauer & Smit, 2013) and its clinical pathway is very expensive for healthcare systems (it is responsible for 7% of the UK NHS budget (Gillespie, McClean, Scotney, Garg, & Fullerton, 2011).

In the hospital environment, due to the high number of stroke cases and the relevant hospital cost, such patient pathway is well known: clinical process flow chart and task durations are standardized and shared among actors (emergency department, medical units' physicians and nurses) in order to efficiently manage patient care.

The stroke unit under study belongs to a medium-sized Italian acute university hospital of 1500 beds. It is devoted to the care of ischemic stroke (classified as DRG 014) and it is provided with 8 beds for inpatients and 1 room for incoming cases transferred from the Emergency Department.

The values of the model inputs have been collected in the stroke unit by means of semi-structured interviews, time measurements and data retrieval from hospital information systems. In order to share the pathway model with physician and nurses and enable them to make suggestions to improve its design, a 3D simulation was developed by using the software FlexSim Healthcare (Fig. 2).

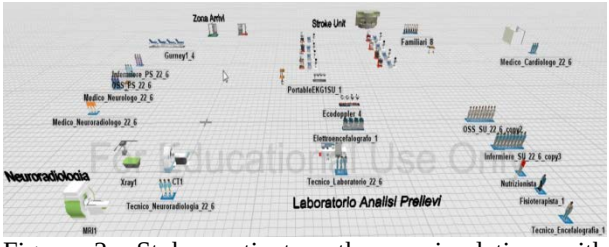

Figure 2: Stoke patient pathway simulation with FlexSim Healthcare software.

3.2. Model validation and simulation

Validation. The first validation of the model was carried out comparing the total nursing direct care time calculated by the model to the one experienced by nurses over a week and recorded by them in provided forms. The proposed model resulted to be a good predictor of reality (the error, with a confidence level of 95%, was 15%).

Case study simulation. Using the daily patient characteristics of Table 1 and implementing the model in a simple Microsoft Excel Spreadsheet, the resulting cumulated distribution function of the number of nurses required for a shift over 500 simulation replications is shown in Table 2. By this, the decision maker is enabled to make decisions about the number of nurses

to possibly re-schedule for the day. For example, for the first shift, 6 nurses are required to assure 99,9% service level to patients, while with 5 nurses, the probability of satisfying the patient needs is equal to 87,1%. In the second shift, instead, given the hospitalized patients and their needs that are evaluated by the simulation, the assignation of 4 nurses or more would be a waste.

Table 1: Patient data of 1 day of the case study

Patient	Barthel scale	Day of the pathway	Time of patient entry	Presence of patient for shift		
				1	2	3
1	0	1	01/01/2015 16:00	1	1	1
2	2	2		1	1	1
3	5	2		1	1	1
4	7	3		1	1	1
5	8	3		1	1	1
6	13	5		1	1	1
7	10	8		1	1	1
8	20	9		1	1	1

Table 2: Patient service level in dependence on the number of nurses required per shift

	Service level achievable with number of nurses for each shift		
Number of nurses	Shift 1	Shift 2	Shift 3
1	0,0%	0,0%	96,6%
2	0,0%	39,0%	100,0%
3	0,0%	99,1%	100,0%
4	12,1%	100,0%	100,0%
5	87,1%	100,0%	100,0%
6	99,9%	100,0%	100,0%
7	100,0%	100,0%	100,0%

Moreover, for each number of nurses per shift, the probability of the nurse saturation can be calculated (Figure 3), providing the decision maker with information about possible negative effect on stress. In the example, choosing 4 nurses for the first shift will imply a significant saturation (always more that 70% of nurse time will be used).

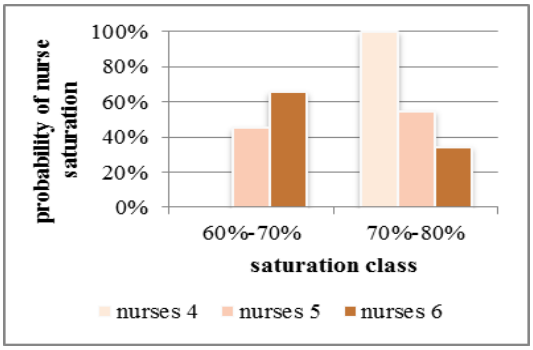

Figure 3: Nurse saturation probability in the shift 1

4. CONCLUSIONS

This study copes with the proposal of a daily Nurse Requirements Planning (NRP) method based on simulation of patient flow, which takes into account real patient needs considering both the variability of clinical pathways and of the duration of care activities. The method summarizes the best features of both time-task activity methods (because single tasks of the clinical pathway and the related occurrence probability are taken into account) and acuity-quality methods (because patient dependency from nurses is used to estimate single task duration). For the sake of simplicity, the model has been formalized considering the activities of one clinical pathway carried out in one medical unit. Anyway, it can be easily extended to many pathways, many medical units and many resources. Given the probabilistic dimension of the results, both in terms of service level and personnel saturation, it can be a valid support for management in nurse rescheduling decisions, being a daily support system in finding the trade-off between costs (dependent on the number of nurses) and service level offered to patient. The approach is based on patient clinical data collected in Electronic Medical Records and hospital information systems and it is suitable to work without any human intervention. The first results of the proposal have been assessed in a stroke unit of a medium-sized acute university hospital. The ongoing activities are aimed at refining the relation between activity duration and patient dependency on nurses by means of an extensive time and methods study on the field. Moreover, a cost analysis will be performed in order to quantitatively assess the impact of the NRP decisions on the medical unit budget.

REFERENCES

Bhattacharje P., Ray P. K., 2014. Patient flow modelling and performance analysis of healthcare delivery processes in hospitals: A review and reflections. Computers & Industrial Engineering, 78, 299-312.

Cardoen B., Demeulemeester E., 2008. Capacity of clinical pathways - a strategic multi-level evaluation tool. J Med Syst, 32 (6), 443–452.

Constantino A. A., Landa-Silva D., de Melo E. L., de Mendonça C. F. X, Rizzato D. B. and Romão W., 2013. A heuristic algorithm based on multi-assignment procedures for nurse scheduling. Annals Operations Research, 218 (1),165–183.

Ernst A.T., Jiang H., Krishnamoorthy M. and Sier D., 2004. Staff scheduling and rostering: A review of applications, methods and models. European Journal of Operational Research, 153 (1), 3–27.

Gillespie J., McClean S., Scotney B., Garg L., Barton M. and Fullerton K., 2011. Costing hospital resources for stroke patients using phase-type models. Health Care Management Science, 14 (3), 279–291.

Guida R., Iannone R., Miranda S., Riemma S.and Sarno D., 2012. From patients' needs to hospital pharmacy management: An holistic approach to the process modelling. 1st International Workshop on Innovative Simulation for Health Care, IWISH 2012, International Multidisciplinary Modeling and Simulation Multiconference, I3M 2012, 1, 56-62

Iannone R., Miranda S., Riemma S. and Sarno D., 2011. Proposal of a conceptual framework to optimise drug management in healthcare systems. IADIS, International Conference e-Health,.215–220., July 20-22, Rome (Italy).

Iannone R., Lambiase A., Miranda S., Riemma S. and Sarno D., 2013. Modelling hospital materials management processes. International Journal of Engineering Business and Management, 5(15) : 1-12.

Iannone R., Lambiase A., Miranda S., Riemma S. and Sarno D., 2014. Pulling drugs along the supply chain: Centralization of hospitals' inventory. International Journal of Engineering Business Management, 6 (1), 1-11.

Iannone R., Lambiase A., Miranda S., Riemma S. and Sarno D., 2015. Cost savings in hospital materials management: look-back versus look-ahead inventory policies. International Journal of Services and Operations Management. In press.

Kaliszer. J. S. M., 1976. A survey of patient-nurse dependency. Irish medical journal,.69(18), 488–492.

Keith H., 2003. Selecting and applying methods for estimating the size and mix of nursing teams: a systematic review of the literature commissioned by the department of health. Nuffield institute for health.

Liang B., Turkcan A., 2015. Acuity-based nurse assignment and patient scheduling in oncology clinics. Health Care Management Science, jan 2015

Naidu K., Sullivan KM., Wang PP. and Yang Y., 2000. Managing Personnel through Staff Scheduling Algorithms. Proceedings of the Joint Conference on Information Sciences, 5(2), 829-835.

Punnakitikashem P., Rosenberger J. M., 2008. Stochastic programming for nurse assignment . Computational Optimization Applications, 40 (3), 321–349.

Rudd A. G., Jenkinson D., Grant R. L. and Hoffman A., 2009. Staffing levels and patient dependence in English stroke units. Clinical Medicine, 9 (2), 110–115.

Siferd S. P., Benton W. C., 1994. A decision modes for shift scheduling of nurses. European Journal of Operational Research, 74 (3), 519–527.

Villarreal M. C., Keskinocak P., 2014. Staff planning for operating rooms with different surgical services lines, Health Care Manag Science, nov. 2014.

Wittenauer R., Smit L. 2013. Priority Medicines for Europe and the World 2013 Update. Background Paper 6.6 - Ischaemic and Haemorrhagic Stroke.

THE DEVELOPMENT OF A LOW-COST OBSTETRIC SIMULATOR TO TRAIN MIDWIFERY STUDENTS AND TEST OBJECTIVE EXAMINATIONS' SKILLS

S. Ricci[(a)], A. Paci[(b)], S. Marcutti[(c)], P. Marchiolè[(d)], G. Torre[(e)], M. Casadio[(f)], G. Vercelli[(g)], M. Cordone[(h)]

[(a),(b),(c),(f),(g)] University of Genova - Dept. Informatics, Bioengineering, Robotics and Systems Engineering
[(d)] ASL3 Genova (Italy) - Gynecology and Obstetric Villa Scassi Hospital
[(e),(h)] University of Genova - Centre of Advanced Simulation

[(a)]ricci_serena@ymail.com, [(b)]andrea.paci90@gmail.com,[(c)]simone.marcutti@simarlab.it,[(d)]pmarchiole@yahoo.com, [(e)]gctorre@unige.it, [(f)]maura.casadio@unige.it, [(g)]gianni.vercelli@unige.it, [(h)]massimocordone@ospedale-gaslini.ge.it

ABSTRACT

The study presents the design a low cost simulator that allows precise identification of the fetal position, enabling doctors and students to train and improve their skills by inspecting visually and manually what happens inside a simulated birth canal. The system consists on a female pelvis, a custom-made fetal mannequin, and a visual display to show in real time the birth canal and the position of the fetus. Students are often unable not only to identify correctly the fetal head position, but also to discriminate between the two fontanels. This system can help them to train this ability and could be an important instrument for the instructors to objectively assess the clinical skill of each student.

Keywords: obstetric, simulations, fetopelvic relationships, OSCE

1. INTRODUCTION

The knowledge of the correct position and orientation of the fetal head is important for obstetricians and midwives during spontaneous deliveries and especially before operative vaginal deliveries. Nevertheless, these parameters are estimated in a subjective way. This fact leads to discordant evaluations, errors and failures in ventouse extraction and forceps application, worse outcomes for mother and newborn, increased use of urgency cesarean section.

The problem is longstanding. In 1952 E. Parry Jones, in his famous book about Kielland's forceps, stated: *"Kielland did much for obstetrics, but perhaps his most important contribution was his emphasis on the need for determining the exact position of the fetal head.."* (Parry Jones 1952).

Nowadays, students can practice deliveries only in cases where there is no danger for both the mother and the fetus. However, when they start their career, they could come across emergency situations in which they have to act quickly (Macedonia et al. 2003). Thus the birth simulation is very important to improve the skill of midwifery students and residents and to test their progresses during Objective Structured Clinical Examination (OSCE).

In 1988-1989 R. H. Allen, J. Sorab and G. Gonik from the Huston University, measured the forces applied by clinicians during birth, using tactile sensing technology. In particular they used sensors applied on a clinician's hand in order to investigate the relation between applied forces and the risk of birth injury (Allen et al. 1988, Sorab et al. 1988).

In 2002 C. M. Pugh and P. Youngblood, from the Stanford University, implemented the simulator "E-Pelvis" to simulate pelvic examinations; it consists of a partial mannequin instrumented internally with electronic sensors that are interfaced with a data acquisition card and a graphic software to visualize the examinations (Pugh and Youngblood 2002).

In 2003 the "Laboratoire Ampère" of Lyon (France) developed the Birth simulator: it includes a fetal mannequin; the maternal anatomically correct pelvic model; an interface pressure system mimicking the pelvic muscles; a software to visualize in real time the head location (Dupuis et al. 2005, Moreau et al. 2008).

One of the main problems of the commercially available simulators is the high price. Moreover, most of them do not allow detecting the fetal position and its orientation with respect to the female ischial spines (Dupuis et al. 2005). The birth simulator presented in this article is a low cost model that overcomes this problem allowing an identification of the fetal position.

2. THE DELIVERY: FETAL HEAD AND MATERNAL PELVIS

According to the "Williams Obstetrics" textbook (Cunningham et al. 2010) the pelvis is composed of four bones: the sacrum, coccyx, and two innominate bones, formed by the fusion of the ilium, ischium, and pubis. The pelvic cavity can be divided into the false and the true pelvis. The false pelvis is bounded posteriorly by the lumbar vertebra and laterally by the iliac fossa, whereas the true pelvis is bounded above by the sacrum, the linea terminalis, and the upper margins of the pubic bones, and below by the pelvic outlet.

Extending from the middle of the posterior margin of each ischium are the ischial spines. These are of great

obstetrical importance because the distance between them usually represents the shortest diameter of the pelvic cavity. They also serve as valuable landmarks in assessing the level to which the presenting part of the fetus has descended into the true pelvis.

Four diameters of the pelvic inlet are usually described (fig. 1):

- anteroposterior is the shortest distance between the promontory of the sacrum and the symphysis pubis and it normally measures 10 cm or more;
- transverse measures 13 cm and represents the greatest distance between the linea terminalis on either side;
- oblique extends from one of the sacroiliac synchondroses to the iliopectineal eminence on the opposite side. They average less than 13 cm.

The fetal head is composed of two frontal, two parietal, and two temporal bones, connected by a thin layer of fibrous tissue. These bones are separated by membranous spaces that are termed sutures. The most important sutures are:

- the frontal, located between the two frontal bones;
- the sagittal, placed between the two parietal bones;
- the two coronal, situated between the frontal and parietal bones;
- the two lambdoid, located between the posterior margins of the parietal bones and upper margin of the occipital bone.

Where several sutures meet, an irregular space forms, which is enclosed by amembrane and designated as a fontanel. The greater, or anterior, fontanel is a lozenge-shaped space that is situated at the junction of the sagittal and the coronal sutures. The lesser, or posterior, fontanel is represented by a small triangular area at the intersection of the sagittal and lambdoid sutures.

The fetal diameters include (fig. 2):

- The occipitofrontal (11.5 cm), which follows a line extending from a point just above the root of the nose to the most prominent portion of the occipital bone;
- The biparietal (9.5 cm), the greatest transverse diameter of the head, which extends from one parietal boss to the other;
- The bitemporal (8.0 cm), which is the greatest distance between the two temporal sutures.
- The occipitomental (12.5 cm), which extends from the chin to the most prominent portion of the occiput;
- The suboccipitobregmatic (9.5 cm), which follows a line drawn from the middle of the large fontanel to the undersurface of the occipital bone just where it joins the neck.

At the onset of labor, the position of the fetus with respect to the birth canal is critical to the route of delivery. Fetal orientation relative to the maternal pelvis is described in terms of:

- Fetal lie that is the relation of the fetal long axis to that of the mother;
- Presenting part which is the portion of the fetal body that is either foremost within the birth canal or in closest proximity to it;
- Attitude is the characteristic posture assumed by the fetus in the later months of pregnancy;
- Position refers to the relationship of an arbitrarily chosen portion of the fetal presenting part to the right or left side of the birth canal.

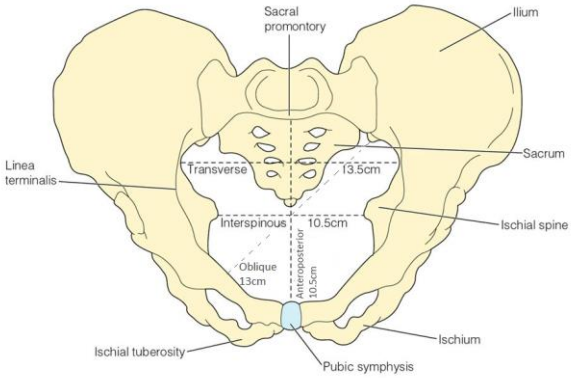

Figure 1 Main pelvic diameters and bones (Floresta 2011)

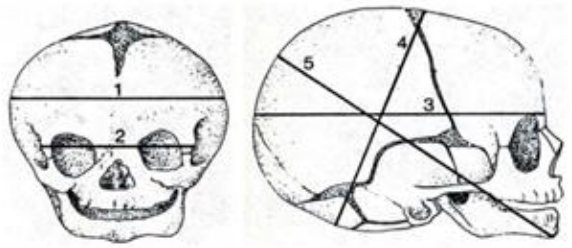

Figure 2 Fetal head diameters 1. Biparietal, 2. Bitemporal, 3. Occipitofrontal, 4. Subooccipitobregmatic, 5. Occipitomental (Barbone et al. 2012).

3. BACKGROUND

The simulator consists of a female pelvis, a custom-made fetal head and a visual display, connected to custom electronics, able to show in real time the birth canal and the position of the fetus. More specifically the system has four parts:

- A physical model of the fetus and the pelvis;
- A correspondent graphic model;
- A client side web application which allows the users' authentication and the registration of the subjects' performance during the OSCE;
- A server-side subsystem to manage communications among the physical model, the graphic model and the web application;

3.1. The birth simulator project: main goals

Our goal is to develop a system

- to train the ability in internal examination during labor;
- to discriminate between the two fetal fontanels;
- to estimate correctly the position and the orientation of the fetal head with respect to the female ischial spines;
- to measure the force applied on the fetal head.

An analysis of commercially available birth simulators revealed that most of them are not able to detect and display the position of the fetus in the birth canal. They focus on the delivery as a situation in which the mother and the newborn need help; moreover, commercially available simulators are very expensive.

We decided to implement a birth simulator able to detect physically and visually the position of the fetus with respect to maternal ischial spines and the forces applied on the fetal fontanels. The system will have also the following features:

- Low-cost
- Wireless
- Plug and play
- Space-saving

3.2. Communication and data visualization

The communication sub-system is based on a Raspberry Pi 2 model B, which acts as a bridge connecting physical and virtual simulator. Raspberry Pi 2 model B is a low cost single-board computer that plugs into a computer monitor. It has various functionalities including the ability to interact with the outside world. All data, coming from the fetal head, are received and transmitted to Raspberry via Bluetooth and from Raspberry to the client via Wi-Fi (fig. 3).

This system doesn't have cables coming out from the pelvis. All sensors, which send data to the Raspberry, are connected to the open-source electronics platform Arduino, powered by a rechargeable battery and positioned inside the fetal head.

The software is implemented with Node.js, that is a platform used to build applications based on JavaScript V8 runtime. It uses sockets (software abstraction) such as Socket.IO or UDP to communicate in real time: the first socket is used to communicate in release mode, whereas the second one is used to send information in development mode. Socket.IO enables real-time bidirectional event-based communication; UDP is used to connect Node.js and the graphic editor Unity.

Unity is a graphical shell for a desktop environment; it is a cross-platform game engine known for its ability to target projects to multiple platforms.

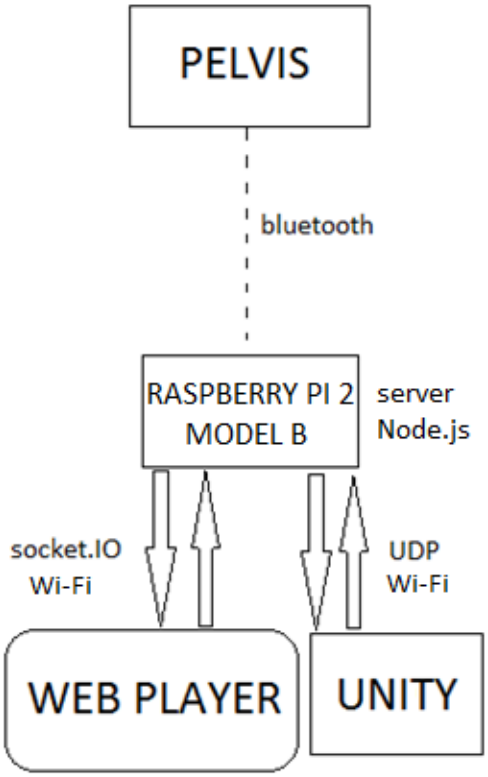

Figure 3 The communication system of the birth simulator

3.3. The physical model

We bought a model of a female pelvis, the female pelvis skeleton A61, distributed by 3b Scientific (Hamburg, Germany) and we printed a 3D fetal head with the main anatomical landmarks.

3.3.1. The fetal head

The free fetus model available online (http://www.3dxtras.com/3dxtras-free-3d-models-details.asp?prodid=38) is used as a base to made the printable fetal head (fig. 4); starting from this model we edited the head using Blender and Geomagic; Blender is an open-source 3D computer graphics software product used for creating animated films, visual effect, 3D applications, video games and 3D printed models, whereas Geomagic Studio is a mechanical Computer-Aided Design software, used for the design of mechanical systems and assemblies.

We changed the head's dimensions so that they were compatible with our pelvis; then we cut the head at the beginning of the neck, so that it can join an existing body and we divided the head in two parts, both to make the printing process easier and to locate sensors correctly (fig. 5).

Before printing the fetal head, we choose the right material which form the final model; that material must have features similar to the skin: it can be elastic but, at the same time, stiff enough so that the measurement are not affected by error caused by surface deformation.

Our first model, was very realistic and too much complex to be printed. As a matter of fact, we decided to simplify it using Geomagic, i.e. we reduced the number of vertices in order to have a lighter model usable to print the head and to visualize the scene. In figure 6 there are shown the phases of our work, while the result of printing is observable in figure 7.

The 3D printed head has the main anatomical landmarks, i.e. the anterior and posterior fontanels connected by the sagittal suture. The diameters of the printed head are:

- bitemporal: 7.5 cm;
- biparietal: 9 cm.
- occipital-frontal: 11.3 cm;
- suboccipitobregmatic: 9.2 cm.
- occipitomental: 13 cm.

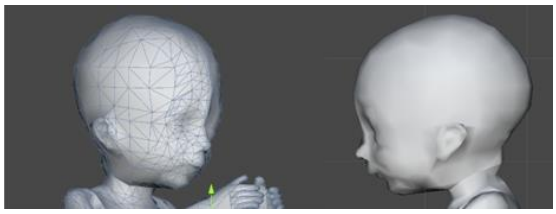

Figure 4 The free fetus model

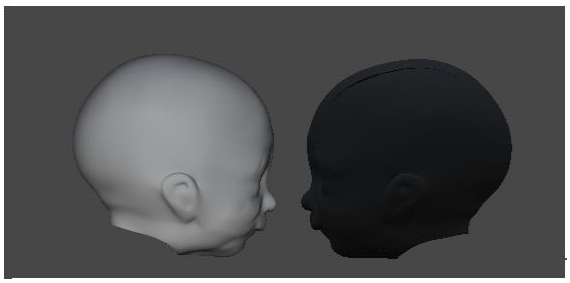

Figure 5 The model's editing

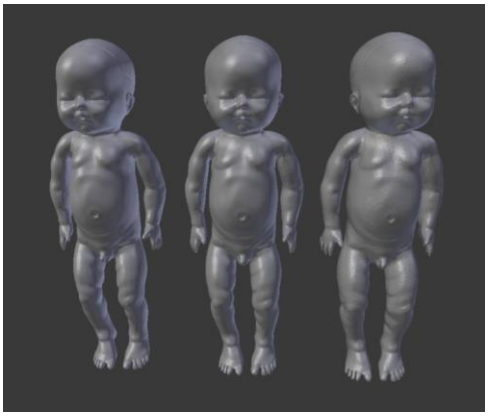

Figure 6 The starting model, the model used, a simpler model not usable for printing because of its defects on the head caused by an excessive reduction of the vertices.

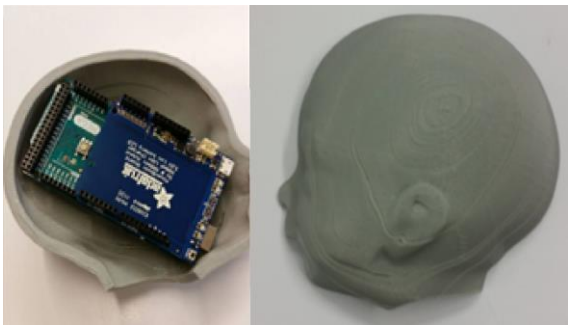

Figure 7 The two parts of the printed head. On the left it is possible to see some electronic component: the Arduino Mega and the Adafruit powerBoost. Furthermore the fetal head contains two IMUs and two pressure sensors.

3.3.2. Sensor used in the model

The head position and the orientation of the fetal head with respect to maternal ischial spinesare detected by two Inertial Measurement Units (IMUs).

The contact force of the user's hand on the mannequin's fontanels is measured by two pressure sensors.

The IMUs are inside the head whereas the pressure sensors are on the surface, in correspondence with the anterior and posterior fontanels. Thus, we chose small sensors so as they could be placed easily in the head, which contains:

- One Arduino Mega;
- Two IMUs;
- Two pressure sensors;
- One Bluetooth component;
- One rechargeable battery.

The two IMUs MPU6050 have an embedded 3-axis MEMS gyroscope, a 3-axis MEMS accelerometer and a Digital Motion Processor hardware accelerator engine with an auxiliary I2C port. The MPU-6050 features three 16-bit analog-to-digital converters (ADCs) for digitizing the gyroscope outputs and three 16-bit ADCs for digitizing the accelerometer outputs. For precision tracking of both fast and slow motions, the parts feature a user-programmable gyroscope full-scale range of ±250, ±500, ±1000, and ±2000°/s(dps) and a user-programmable accelerometer full-scale range of ±2*g*, ±4*g*, ±8*g*, and ±16*g*. The MPU-6050 operates from VDD power supply voltage range of 2.375V-3.46V.

Each force sensing resistors is composed by a polymer thick film device, which exhibits a decrease in resistance with an increase in the force applied to the active surface. Its force sensitivity is optimized for use in human touch control of electronic devices and it is able to measure forces up to 10 kg; the pressure sensitivity range from 0.1 kg/cm^3 to 10 kg/cm^3. It has a 18.3 mm diameter with an active area of 12.7 mm. It is composed by three substrates: a flexible substrate with printed semiconductor; a spacer adhesive; a flexible

substrate with printed interdigitating electrodes, the overall thickness is of 0.47 mm.

Bluetooth nRF8001 Bluefruit Low Energy Breakout allows establishing a wireless link between Arduino and any compatible iOS or Android (4.3+) device. It works by simulating a UART device beneath the surface. It sends and receives data up to 10 meters away, from your Arduino to a device.

Adafruit powerBoost shield goes onto Arduino and provides a slim rechargeable power pack, with a built in battery charger as well as DC/DC booster. The powerBoost shield can run off of any Lithium Ion Battery. We chose a Lion Rechargeable Battery able to power the mannequin for six/eight hours. Its model is 103456A-1S-3M, its nominal voltage is 3.7V and its capacity is 2050 mAh.

3.3.3. The physical model's features

Starting from these sensors' measures, a calibration procedure allows to precisely define in real time the head position with respect to the pelvis.

The head position is defined according to the eleven stations postulated by the American College of Obstetrician and Gynecologists (ACOG), i.e. eleven positions where the head can be placed in the birth canal with respect to the maternal ischial spines (fig. 8). The position '0' corresponds to the vertices at the ischial spines and then there are five stations over and five under it. Each fifth station is located a centimeter above or below the spines. Thus, as the presenting fetal part descends from the inlet toward the ischial spines, the designation is –5, –4, –3, –2, –1, then 0 station. Below the spines, as the presenting fetal part descends, it passes +1, +2, +3, +4 and +5 stations to delivery. (Cunningham et al. 2010, Hagadorn-Freathy et al. 1991, Robertson et al. 1990).

The manual evaluation of these stations is not easy, as Dupuis demonstrated in his prospective study: *"transvaginal assessment of fetal head station is poorly reliable, meaning clinical training should be promoted"* (Dupuis et al. 2005).

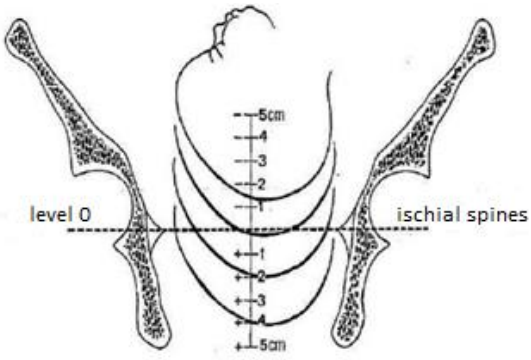

Figure 8 Head levels with respect to maternal ischial spines according to ACOG classification (Moreau 2007).

3.4. Graphic model

The graphic model allows users to visualize what happens inside the birth canal in real time. It consists of a female pelvic 3D model and a fetus 3D model (fig. 9). The first one is a free model available online (http://www.3dxtras.com/3dxtras-free-3d-models-details.asp?prodid=10508), edited so that its dimensions are the same as the physical pelvic model; the second one is the model used to build the fetal head (fig. 4).

The graphic representation can be used both in training and in examination mode. During a training session the student makes a pelvic examination and he checks his skills by a feedback provided on a screen. In particular, he has to detect the correct position and orientation of the fetus with respect to the female ischial spines. Moreover, the graphic model shows in real time the correct identification of the fontanels thanks to pressure sensors: when a user touches a fontanel, i.e. a pressure sensor, the graphic model highlights that fontanels.

In examination mode the student cannot take advantage of the virtual representation, which is visualized only by the doctor so that he can evaluate the student's performance.

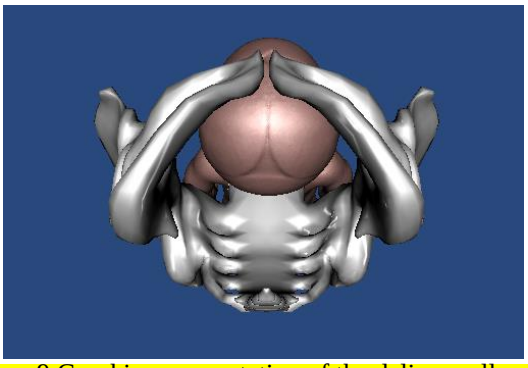

Figure 9 Graphic representation of the delivery allowing users to visualize what happens inside the birth canal

3.4.1. Calibration system

An important point for the correct representation of the graphic model is the calibration process that is necessary to identify the starting fetus position in the birth canal. Calibration allows a unique correlation between the pivot of physical fetus head and the system of reference inside the pelvis. Without calibration the computer is not able to detect properly the physical position and orientation of the mannequin, as a matter of fact the two IMUs cannot return an absolute position of the fetal head in the world coordinates.

At the beginning we decided to implement an internal calibration, i.e. to define a starting position of the fetus inside the birth canal; before each session the user should have placed the fetus in the same position. However, this procedure could generate errors if the user positioned the mannequin in a wrong way. For this reason we opted for an external calibration where the starting position is outside the birth canal and it is a bound positionin which the fetus must be located before starting a session (fig. 10).

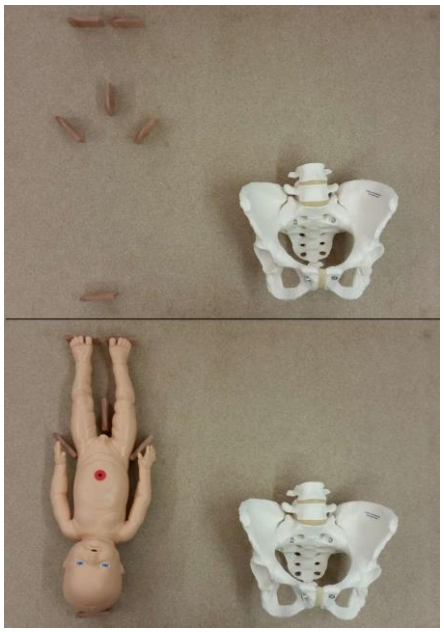

Figure 10 On the top there is the pelvis and the shape which defines the starting position; below it is shown an example of external calibration: the fetus must be positioned according to the shape before each session.

3.5. User interface

The birth simulator is a didactic instrument made to improve students' skills and knowledge concerning the delivery. For this reason, we implemented a web player application, which is a platform with all the data. After authentication each user accesses to his personal page: the student's page gives information about previous sessions and it allows students to start a training session. Users can also check their improvement and difficulties (fig. 11); the doctor's page has information about the whole class; the teacher can visualize the list of students and their past evaluation, moreover he can start an exam session. When an evaluation has started, he must validate the calibration and gives performance scores (fig. 12).

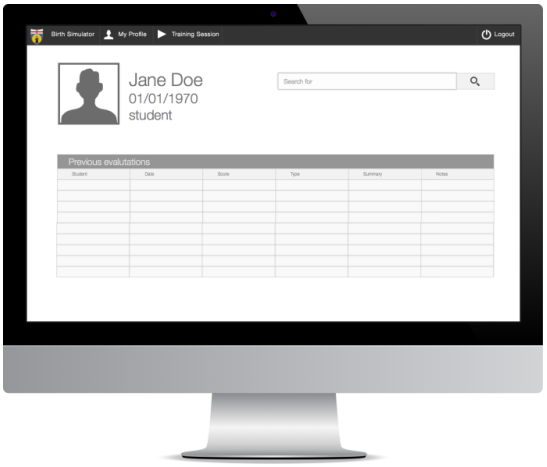

Figure 11 Student's page in which each student can visualize his own profile, examine his past training, write notes and start a new training session.

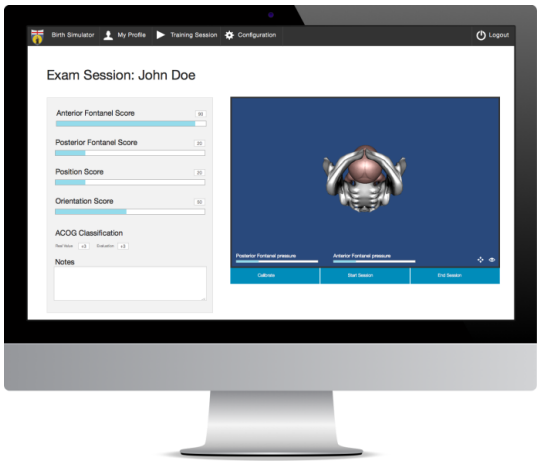

Figure 12 In the exam mode, the teacher has the possibility to give scoresto the students and record his impression.

4. CONCLUSION

The aims of the project are:

- to implement a birth-simulator able to detect properly the position and orientation of a fetus with respect to maternal ischial spines.
- to develop a portable low-cost device.
- to create an instrument that can train and evaluate students' OSCE skills to improve their obstetric abilities.

The communication had to be wireless, in order to have no cables coming out from the pelvis, that's why we chose a Bluetooth low-energy device. However, this device only allows a point-to-point communication and presents difficulties in software management. For these reasons we use a Raspberry Pi 2 model B in order to expand communication possibilities. This system facilitates the development of new functionalities linked to multiple simultaneous connections. Moreover it will allow the development of mobile applications, which will make the simulator even more portable.

Each electronic component of the simulator had to be low-cost and with dimension that were adequate to the head dimension. This made the research hard, but we succeeded in sensorizing the simulator, buying the pelvis and implementing the software using free tools by spending less than 400 euros. To prevent errors caused by the undesirable movement of the IMUs, we modeled the head so that the inner part had grooves in which locate the IMUs. We did not have any problem with the pressure sensors because they are located on the head's surface and they cannot move improperly.

5. FUTURE DEVELOPMENT

It will be useful to know the whole force applied on the fetal head during the delivery and the corresponding strain. These measurements can be obtained covering the fetal with a Roboskin layer. Roboskin is based on conformable mesh of sensors having triangular shape

and interconnected in order to form a networked structure. Each sensor is supported on a flexible substrate allowing the sensor to conform to smooth curved surfaces, implementing 12 taxels based on capacitive transducers (Cannata et al. 2008).

To parallel it is useful to display the head's strain in the graphic visualization so that users can get a visual feedback about the forces they applied; this leads to the modification of the virtual head: currently it behaves as a rigid body, butin the future the head's behavior might be turned into a deformable body. This development can be realized using the *cloth* component in the Unity Editor, which will allow a more realistic graphic representation.

Another important step will be to test and validate the prototype of the simulator in the Centre of Advanced Simulation of Genoa University. In that occasion a selected group of doctors and students will be asked to use and become familiar with the prototype, in order to give us some feedback and suggestions to improve the simulator.

ACKNOWLEDGMENT

Serena Ricci, Andrea Paci and Simone Marcutti contributed equally to this work.

The authors thanks Andrea Canessa, Silvio Sabatini, Filippo Sante and Edoardo Bellanti for their help in the initial stage of the work.

REFERENCES

Allen R., Sorab J., Gonik B., 1988. Measuring clinician-applied forces during birth using tactile sensing technology. IEEE Eng in medicine and biology society 1285-1286.

Barbone S., Castiello M., Alborino P., 2012. Igiene e cultura medico-sanitaria. Milano: Franco Lucisano Editore.

Cannata G., Maggiali M., Metta G., Sandini G., 2008. An Embedded Artificial Skin for Humanoid Robots. IEEE International Conference on Multisensor Fusion and Integration for Intelligent Systems 434-438.

Cunningham G., Leveno K., Bloom S., HauthJ., Rouse D., Spong C., 2010. William Obstetrics: 23rd Edition. New York: McGraw-Hill Medical.

Dupuis O., Silveira R., Zentner A., Dittmar A., Gaucherand P., Cucherat M., Redarche T., Rudigoz R., 2005. Birth simulator: Reliability of transvaginal assessment of fetal head station as defined by the American College of Obstetrician and Gynecologists classification. American Journal of Obstetrics and Gynecology 192:868-874.

Floresta F., 2011. Nursing Care Management 101 Care of mother, child and family. Slideshare. Available from: http://www.slideshare.net/conradincubus?utm_campaign=profiletracking&utm_medium=sssite&utm_source=ssslideview [July 2015]

Hagadorn-Freathy A., Yeomans E., Hankins G., 1991. Validation of the 1988 ACOG forceps classification system. Obstet Gynecol 77:356-60.

Macedonia C., Gherman R., Satin A., 2003. Simulation Laboratories for Training in Obstetric and Gynecology. The American College of Obstetrician and Gynecologists 102(2):388-392.

Moreau R., 2007. Le simulateur d'accouchement BirtSIM: un outil complet pour la formation sans risque en obstétrique. PhD Thesis. National Institute of Applied Sciences of Lyon.

Moreau R., Ochoa V., Pham M.T., Boulanger P., Redarche T., Dupuis O., 2008. A method to evaluate skill transfer and acquisition of obstetric gestures based on the curvatures analysis of the position and the orientation. Journal of Biomedical Informatics 41:991-1000.

Parry Jones E., 1952. Kielland's forceps. London: Butterworth & Co, 2.

Pugh C., Youngblood P., 2002. Development and Validation of assessment measures for a newly developed physical examination simulator. Journal of the American Medical Informatics Association 9(5):448-460.

Robertson P., Laros R., Zhao R., 1990. Neonatal and maternal outcome in low-pelvic and midpelvic operative deliveries. American Journal of Obstetrics and Gynecology 162:1436-44.

Sorab J., Allen R.H., Gonik B., 1988. Tactile sensory evaluation of clinician-applied forces during delivery of newborns. IEEE Trans on biomedical engineering 35(12): 1090-1093.

THE FOUNDATION FOR MULTI-SCALE MODELING OF THE DIGITAL PATIENT

C. Donald Combs, Ph.D.
Vice President and Dean, School of Health Professions
Eastern Virginia Medical School
Norfolk, Virginia USA
combscd@evms.edu

ABSTRACT
The Digital Patient is a technological platform that has the potential to transform personal and public health care, as well as pharmaceutical and device development and testing, research, and patient and professional education. It is the ultimate Big Data project in healthcare; however, its power will derive not from the volume of data, but from the integration of disparate sources of data into valid and reliable information—about biological processes, social context and treatment efficacy. That integration, in turn, is largely dependent on the evolving theoretical approach known as systems biology and the successful meshing of multi-scale models. This paper provides an overview of the digital patient, the domains of systems biology and multi-scale modeling and the implications for personalized medicine.

Keywords: systems biology, multi-scale modeling, digital patient, convergence

1. INTRODUCTION

What is a Digital Patient? It is a digital representation of 'health' and 'disease' and a sophisticated decision support system that can be customized to represent each one of us, individually or collectively. Imagine a "virtual twin" of sorts, living in digital form, inside a computer. *That virtual twin is shaped by your medical history. It keeps inside a digital record of your insulin levels, which are constantly tracked by that micro-sensor the doctors installed when they did your angioplasty and stented one of your carotids. Your virtual twin is a bit sleep-deprived, just like you, since you are not sleeping so well due to that back injury. It is allergic to some antibiotics and has 'let itself go,' after overeating for the past few years.*

This description represents a vision of truly personalized medicine, which was at the heart of the project DISCIPULUS. That project was given the task of engaging the European Union (EU) research community in order to develop a Roadmap towards the *Digital Patient*, a key component and conceptual child of the Virtual Physiological Human (VPH) initiative (www.vph-institute.org). Within the scope of DISCIPULUS, the Digital Patient was defined as "*a technological framework that, once fully developed, will make it possible to create a computer representation of the health status of each citizen that is descriptive and interpretive, integrative and predictive*".

2. CONVERGENCE, SYSTEMS BIOLOGY AND MULTI-SCALE MODELING

In January 2011 the Massachusetts Institute of Technology submitted a report to the health science research community introducing a new research model that is essential to the continued development of the Digital Patient. The research paradigm they developed is called *convergence*, the merging of distinct technologies, processing disciplines, or devices into a unified whole to create a host of new pathways and opportunities. Convergence implies the technical tools, as well as the disciplined analytic approaches, from design, engineering and physics and their adaptation to the life sciences. The strength in this research methodology is that it does not rest on a particular scientific advance, but on an integrated approach for achieving advances.

Focusing more directly on the type of convergence essential to the Digital Patient is systems biology. Systems biology addresses interactions in biological systems at different scales of biological organization, from the molecular to the cellular, organ, organism, societal and ecosystem levels. It is characterized by its integrative nature as compared to the reductionist nature of molecular biology. It is also characterized by quantitative descriptions of biological processes, using a variety of mathematical and computational techniques. Thus, systems biology combines the development and application of predictive mathematical and computational modeling with experimental studies. The modeling techniques that are employed incorporate multiple spatial and

temporal scales that are consistent with the integrative perspective of systems biology. Just as physiology is a branch of biology, systems physiology, systems medicine and personalized medicine are subsets of systems biology. These levels of systems and their supporting informatics are shown in *Figure 1*. The Digital Patient will eventually integrate data and models across scales and time and thereby enable the realization of truly personalized medicine.

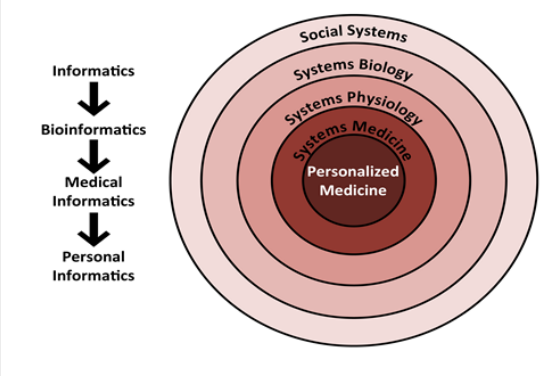

Figure 1: System of Systems and Levels of Informatics

Systems physiology focuses on the function of interacting parts of the system at the cell, tissue, organ and organ system scales, and is tightly coupled with structural anatomical information. Systems medicine is a subset of systems biology that addresses applications to clinical problems. Examples include the application of the systems biology framework to develop quantitative understandings of disease processes, to drug discovery, and to the design of diagnostic tools. A subset of systems medicine that relies on individual patient data or the data from a specific group of similar patients is the emerging domain of personalized medicine.

The interest in systems biology has been growing steadily during the past decade. As Noble noted: "Systems biology … is about putting together rather than taking apart, integration rather than reduction. It requires that we develop ways of thinking about integration that are as rigorous as our reductionist programs, but different. … It means changing our philosophy, in the full sense of the term."

Although the framework is being developed, many currently available systems biology studies are not multilevel; they do not integrate physiological responses from the molecular to the cellular, organ and whole organism levels. The development of an integrated model of human physiology is essential for the understanding of how molecular, cellular, organ and system levels interact for a total physiological response. Then, of course, the higher levels of biological systems and social systems must ultimately be integrated into the analytic framework.

3. MULTI-SCALE MODELING

Biological and physiological systems are highly complex. This complexity results in large measure from the following factors:

Non-linearities: Many responses have upper and lower boundaries with different levels of sensitivity in between.

Redundancy: Many physiological states are the result of multiple mechanisms pushing and pulling on the observable response. Redundancy makes it difficult to identify important causal mechanisms.

Disparate time constants: The importance of an observation often depends on the timing of the protocol. For instance, the control of arterial blood pressure is a mix of fast-acting neural mechanisms, slow-acting hormonal mechanisms, and long-term effects of body fluid volume and composition.

Individual variation: Physiological responses are a qualitative and quantitative function of sex, age, body composition and other individual characteristics.

Emergence: Many high-level, integrative behaviors of the biological system cannot be described solely by aggregating the respective inputs from basic processes.

Biomedical researchers are increasingly using integrative physiological and biological models to better understand fundamental relationships that have been hidden in the complexity.

4. SYSTEMS BIOLOGY, MULTI-SCALE MODELING AND PERSONALIZED MEDICINE

Translational biomedical research has made the integrative analysis of human physiology more relevant to clinical practice. The explosion of data over the past twenty years is providing novel opportunities to develop new clinical treatments. New technologies such as DNA sequencing, imaging, and proteomics provide massive amounts of new information about the human body. The ability to extract useful information from these data is beginning to lead to custom treatments for diseases, such as cancer, infectious diseases, and hematological and metabolic disorders. The existence of these newly available data sources has created a necessity for new methods of analysis. Genetic analysis suggests which genes may be important for clinical outcomes; however, the physiological relevance of changes in genetic makeup is not yet clear. This

ambiguity necessitates a systematic approach to the integrative analysis.

Systems biology has the potential to provide valuable insights into the physiological workings of the human body. The current goal of systems biology research is to utilize scientific advancements from the past two decades, such as genomics and proteomics, in an effort to develop targeted therapeutic strategies. The effective creation of these strategies, however, can only be realized with an in-depth understanding of the multi-faceted etiologies of complex diseases.

The highly complex nature of biomedical systems results from several distinct factors previously mentioned. These factors include non-linearities, redundancy of physiological states as a result of "multiple mechanisms pushing and pulling on the observable response", disparate time constraints, individual variation, as well as the concept that many high-level and integrative behaviors of the biological system cannot be described solely through the sum of inputs from basic processes. Despite the extensive complexities of biomedical systems, researchers are using sophisticated biological and physiological models to better understand fundamental relationships within the biological system.

Some scientists predict that understanding the data resulting from the systems biology approach will ultimately lead to the widespread availability of personalized medicine. In order to accomplish this feat, scientists must analyze data in a manner that recognizes the data as "a highly complex system comprising multiple inputs and feedback mechanisms." Translational medicine, a growing domain within biomedical and population oriented health research that aims to improve the health of individuals by converting research findings into diagnostic tools and procedures, requires complex functional and conceptual linkages. These linkages include the association of genetics to proteins, proteins to cells, cells to organs, organs to complete systems, as well as systems to the organism itself and to the surrounding social environment.

The creation of a comprehensive mathematical model is essential to understand the integration of these systems and to successfully apply a systems biology approach. Such a mathematical model would accurately link the functioning of all organs and systems, providing a useful framework for the development and testing of new hypotheses likely to contribute to improved clinical outcomes.

There are currently several intensive efforts underway to develop a human model.

A number of centers around the world are in the process of developing specific environments to facilitate the creation of integrative models of human physiology, or 'physiomes'. The Physiome Project is an effort to develop databases and models with the intent to understand human physiological responses. The International Union of Physiological Sciences (IUPS) Physiome Project focuses on providing a "computational framework for understanding human and other eukaryotic physiology," and comprises databases, markup languages, software for computational models of cell function, as well as software for interacting with organ models. Currently, the primary limitation with the Physiome Project is the lack of integration of the multiple narrow-focus models that could, if successfully integrated, lead to a comprehensive and integrative model of human physiology.

Many scientists are currently working on various systems biology-driven studies ranging from gene analysis to cellular metabolism and localized blood flow responses. Technological developments during the past few decades have also provided unique opportunities in the development of new clinical treatments. These technologies, such as DNA sequencing, imaging and proteomics, provide a vast array of new and untapped information about the human body. As scientists are able to extract usable information from the massive amounts of raw data, the research will infiltrate clinical practice in the form of customized treatments for disease in specific individuals. One notable example of this research effort to improve healthcare at the individual patient level follows.

Systems biology seeks an understanding of how and why complex systems behave as they do, and thus will have far-reaching implications for agriculture, energy production, environmental protection, and many other human activities. As Dr. Leroy Hood has noted, biology will be the dominant science of the 21st century, just as chemistry was in the 19th century and physics was in the 20th century.

Dr. Hood and his colleagues envision personalized medicine in a construct they call P4 medicine: predictive, preventive, personalized and participatory. Key benefits of P4 medicine to the patient and to the healthcare system will potentially include being able to:

- Detect disease at an earlier stage, when it is easier and less expensive to treat effectively;
- Stratify patients into groups that enable the selection of optimal therapy;
- Reduce adverse drug reactions by more effective early assessment of individual drug responses;
- Improve the selection of new biochemical targets for drug discovery;

- Reduce the time, cost, and failure rate of clinical trials for new therapies; and
- Shift the emphasis in medicine from reaction to prevention and from disease to wellness.

A coordinated and integrated program is envisioned by the Institute for Systems Biology (ISB) to accelerate the solving of technical challenges of P4 medicine. The program includes:

- Developing methods for determining individualized genomes and for integrating the findings with diagnostic measurement data;
- Developing methods for determining the levels of organ-specific proteins, microRNAs and other possible biomarkers, including cells, in the blood to assess the health or disease in all major human organ systems and thus enabling the monitoring of the earliest onset of disease;
- Digitizing medical records and creating effective, secure databases for individual patient records (new, data intense records with gigabytes of data);
- Developing new mathematical and computational methods for extracting maximum information from molecular information on individuals (including their genomes), and from other clinical data and personal history;
- Developing new computational techniques for building dynamic and disease-predictive networks from massive amounts of integrated genomic, proteomic, metabolic and higher level phenotypic data (This is the heart of the emerging field of personalized medicine: new methods for interrogating data and understanding the interaction between the environment and the genome of the individual.);
- Predicting drug perturbations of biological networks and developing therapeutic perturbations of biological networks (that is, re-engineering of networks in higher organisms with drugs, moving from a diseased state back to normal);
- Creating pluripotent cells (stem cells) from normal, differentiated cells, and then differentiating them to specific body cell types. The ability to create stem cells with a given individual's genome will be remarkable, understanding it will be revolutionary;
- Developing new *in vivo* molecular imaging methods and analysis methods to follow disease, drug response, drug effectiveness, and drug dosage determinations;
- Effectively managing the enormous personalized data sets that will result, which requires the development of broadly accepted policies addressing security, quality control, data mining, privacy protection, and reporting;

5. CONCLUDING DISCUSSION

Data is everywhere now, being aggregated, analyzed, and repackaged. We are in an era of Big Data, living with the recognition that almost everything we do is being captured as one or another type of data, with the hope that all that data can be used to help us become smarter, healthier, safer and richer and with the fear that our privacy is being invaded and that our risk for harm is increasing. It is in this broader context that this article addresses one of the more hopeful Big Data undertakings—that is, the construction and deployment of the Digital Patient.

The capacity to measure one's personal physiological and social metrics, compare those metrics with the metrics of millions of other humans, personalize needed therapeutic interventions and measure the resulting changes will ultimately realize the vision of personalized medicine—wherein patients and their providers will be able to detect disease at an earlier age; provide optimal therapy based on the characteristics of each individual and reduce adverse responses to therapy; where pharmaceutical companies can improve the process of drug discovery and clinical trials; and where the healthcare industry's emphasis truly shifts from reaction to disease to prevention of disease and promotion of wellness. Implicit in this vision is the integration of a sustained focus on improving the outcome measures of healthcare—safety, effectiveness, patient-centeredness, timeliness, efficiency, and equity—into clinical practice. Underlying this focus is, of course, the development and integration of multi-scale models based on the understandings emerging from systems biology.

REFERENCES

Combs, C.D. 2016. "The digital patient." In *The digital patient: Advancing medical research, education, and practice*, edited by C.D. Combs, J. A. Sokolowski, an C. M. Banks. Hoboken, NJ: John Wiley and Sons. Forthcoming.

Hester, R.L., Iliescu, R, Summers, R, Coleman, T.G. Systems biology and integrative physiological modelling. *The Journal of Physiology*. 011; 589(5):1053-1060.

doi:10.1113/jphysiol.2010.201558.
Hood, L, Balling, R, and Auffray, C. (2012). Revolutionizing medicine in the 21st century through systems approaches. *Biotechnology Journal*, 7: 992-1001. doi: 10.1002/biot.201100306
Hood, L. Systems biology and P4 (Predictive, Preventive, Participatory and Personalized Health) medicine: Past, present, and future. *RMMJ* 2013;4 (2):e0012. doi:10.5041/RMMJ.10112
Institute for Systems Biology. About systems biology. Accessed November 25, 2014.Available at http://www.systemsbiology.org/about-systems-biology
Massachusetts Institute of Technology. (2011, Jan.). The third revolution: The convergence of the life sciences, physical sciences, and engineering. MIT Washington Office: Washington, DC.
Noble, D. Biophysics and systems biology. *Philosophical Transactions A*. February 1, 2010. Available at: http://rsta.royalsocietypublishing.org/content/368/1914/1125.long
"Roadmap for the Digital Patient" (DISCIPULUS Consortium). Vanessa Díaz-Zuccarini, Marco Viceconti, Veli Stroetmann (editors). 2013.

LEAN MANAGEMENT PRACTICIES TO IMPROVE PERFORMANCES IN OPERATING ROOMS

Antonio Calogero [(a)], Francesco Longo[(b)], Letizia Nicoletti[(c)], Marina Massei[(d)], Adriano Solis[(e)]

[(a) (b)] DIMEG, University of Calabria, Italy
[(c)]CAL-TEK SRL, Italy
[(d)]DIME, University of Genoa, Italy
[(e)]York University, Canada

[(a)]calogero.antonio@alice.it, [(b)]f.longo@unical.it, [(c)]l.nicoletti@cal-tek.eu, [(d)]massei@itim.unige.it, [(e)]asolis@yorku.ca

ABSTRACT

The proposed research work is meant to present a Surgical Department simulation model developed for a public healthcare facility in South Italy. Such work is grounded on a careful analysis of available data and of the entire surgical process whose components, activities and workflow have been mapped through specific charts. In the scope of the proposed research, after the simulation model has been developed and validated, specific analysis on actual and potential capacities have been carried out. In particular, the potential impact of Lean Management principles and methods are explored with a focus on the "Pull method". As a result the paper contribution is twofold: from one side it comes up with a tool devoted to streamline decision-making processes and from the other side it explores the possibility to apply Lean Management practices in domains that are different from Manufacturing. The main results show, indeed, that the pull method can bring substantial benefits in terms of patients waiting times reduction, increased productivity and better resources allocation.

Keywords: Modeling, Simulation, Healthcare Facilities, Lean Management, Pull method.

1. INTRODUCTION

The Lean approach featured by lower costs, higher quality and customer service is an interesting but challenging research area. To date, it has been mainly applied to manufacturing systems and therefore, within the scope of this research, a particular effort has been done to evaluate the potential applicability of lean practices to healthcare facility management processes. On the other hand, Modeling and Simulation has been used as investigation tool providing the playground for almost unbiased evaluations and analytical assessments before implementation in the real system. Particular attention has been paid to the "Pull method" application and related effects in Operating Rooms management. As Operating Rooms are among the most costly units within a hospital, increasing productivity while preserving cares quality is a top priority and the main rationale behind the research discussed herein. Productivity can be assessed in terms of cases average duration, idle times, surgeries scheduling and resources level of use without overlooking the role human factors such as motivation and teamwork (R. Marjamaa et al., 2008). In particular, when dealing with elective surgery departments, both internal and external indicators need to be considered. External indicators include waiting times and waiting lists length, which impact on the perceived quality, while internal performance indicators include "throughput" time (time from arrival to dismissal), bed occupancy rate, dismissal rate and resources utilization rate. Needless to say that these parameters cannot be evaluated under emergency conditions given the impossibility, in such a case, of any scheduling activity. For the purposes of the study presented in this research work, a large public hospital located in South Italy has been considered. Here the Elective Surgery Department includes eight operating rooms and the main research effort has been oriented toward the definition of a reference model for surgeries planning and

scheduling. To this end, the approach being adopted is in two levels. The former, is mainly concerned with upstream planning while the latter is centered on how to best organize those activities that usually take place during the preoperative period. At this level, the Pull method, from Lean Management theory, has been applied and as a result pull systems have been created whenever a patient is moved from one point of care to the next. Here, according to Lean Management Principles, potential obstacles and/or sources of delay have been detected and removed.

As mentioned above, the proposed approach has been tested and validated in a tailor-made simulation environment that, as shown in Longo et al (2014), provides the ideal framework to look into possible achievable benefits and improvements before implementation in the real system.

Thus, from a methodological point of view, this work gives further evidence that Lean management and discrete-event simulation (DES) can be jointly used for process improvement and service delivery enhancement as already highlighted by Robinson et al. (2012). Moreover, it is worth noticing that simulation approaches have been successfully applied to health care facilities To mention a few, relevant contributions on this matter can be found in Holm et al (2013), Weerawat et al. (2013) and Bruzzone et al. (2013). Nevertheless, Lean Management practices are mostly related to the manufacturing sector with very limited applicability to healthcare facilities management.

2. CONTEXT ANALYSIS

After an internal audit, the operating room department considered in this research work, has been required to improve its overall performances especially in terms of resources utilization. The scenario under investigation is really complicated due to the numerous restrictions and interdependencies with other hospital functions and departments. Considering that scheduling activities have a not negligible impact over the main performances indicators such as waiting time, staff utilization, overtime and affect the performances of interrelated departments such as surgical wards, finding out best practices for scheduling and activities planning can substantially contribute to achieve the intended outcomes. However, creating a schedule that states which patients have to undergo a surgery and at which moment in time is a rather cumbersome task.

In general, a Surgical department includes four planning levels: strategic planning, tactical planning, offline and online operational planning. At the strategic level, capacities sizing and allocation is dealt with whereas at the tactical level, slots of operating room time are assigned to medical specialties and the surgical staff is planned. At the offline operational level, elective patients are scheduled in advance, and the staff is assigned to specific operating rooms. Lastly, at the online operational planning level, day-to-day disturbances such as unexpected delays or emergency surgeries are dealt with (Van Houdenhoven et al., 2006). This research focuses on the offline operational planning that entails patients allocation and scheduling seeking to minimize waiting times and wastes.

Indeed, besides the hospital management purpose of improving performances, other stakeholders perceive different problems in and around the operating room, for example:

- the operating room personnel faces high variability in actual surgery duration with variable daily workloads;
- Surgical wards deal with large fluctuations in patient flows, which lead to low average bed utilization and frequent overstaffing as well as understaffing;
- The operating room planners deal with unexpected daily changes due to not received or wrong lists of patients;
- Surgeries scheduling is often tightly constrained by limited availability of additional equipment, sterile surgical instrument sets and/or anesthetist physicians;

In addition, other issues have been directly detected during the context analysis. Many of them are related to unsuitable organizational methods affecting the planning phase. For

instance, among the observed practices, any surgical ward is used to send the list of patients for surgery only the day before the surgery is required creating organizational difficulties related to staff and materials allocation.
Hence, a poor planning leads to downtime of Operating Rooms and prevents surgery from being cost-effective. Patients entering the Operating Block at the wrong time can slow down the whole process just as patients who cannot leave immediately after surgery due to complications upon wakening. Furthermore, keeping in mind that often there are fixed overheads and personnel costs as well as expensive and sophisticated equipment, it follows that the early closing of one or more Operating Rooms or an Operating Block, is an unrecoverable loss. A classic example of waste is the sudden cancellation of surgeries due solely to organizational reasons. Moreover a poor coordination prevents patients' shifts from being speedy and effective and causes operating rooms to be used longer than necessary. As a consequence, aside from an optimal use of equipment, it is also crucial to encourage synergies among the staff.

2.1 Offline Operational planning

From a patient's perspective, the process starts when, based on medical examination, the patient is required to undergo a surgery. At this point in time, the patient gets in touch with a medical specialist that fills in an admission registration form where relevant information for planning are collected. Such information consists of treatment description, expected surgery, expected length of stay in the hospital, urgency and relevant data for preoperative preparation. This form is the processed at the central planning department and, as a consequence, the patient is added to the current waiting list for admission at the surgical ward. Surgery and admission planning depend on the expected length of stay as well as on the bed occupancy level. Figure 1 shows the scheduling process.

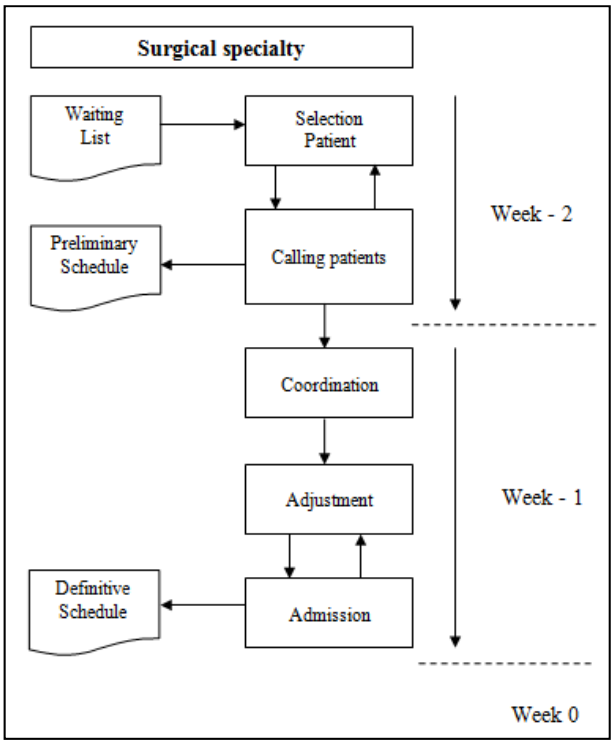

Fig.1: Flowchart process scheduling

- **Patients Selection**

Patients selection occurs two weeks ahead of the surgery week and is based on the information reported on the waiting list. This phase comes up with a preliminary operating room schedule where patients are randomly sequenced within a session. The planned duration is based on the information supplied by the surgeon.

- **Calling patients:**

After patients selection, planners inform the anesthesiology department since each patient requires a preoperative screening by the anesthesiologist before surgery. Screening are carried out in the week before the surgery is expected and if a patient is not fit for surgery, the surgery is cancelled and another patient from the waiting list is selected. Then the preliminary operating room schedule is updated accordingly.

- **Coordination:**

In the week before surgery is scheduled, the preliminary operating room schedule is sent to the operating room managers, the surgeons involved, the surgical wards and the radiology department to check and establish the right surgeries.

- **Adjustment:**

Communication with some actors may bring about the need to adjust the preliminary schedule, because of several reasons. Estimates of operation durations may be adjusted, surgeons may want to add patients to the schedule (e.g. in case of high urgency), surgical wards may foresee problems with accommodating all patients, etc. Such reasons require adjustment of the preliminary schedule, by shifting patients between wards, assigning patients to another day in the same week or removing patients from the week , etc. Adjustments can be done until Thursday (morning) in the week before surgeries. After this deadline, the operating room schedule is definitive.

- **Admission:**

After finalizing the operating room schedule, the operating room planners call the patients involved and inform them about the planned date and time for surgery providing details about preparation and time for check-in at the hospital.

However, changes are likely to occur. Indeed, it can happen that the patients in the definitive schedule cannot come at the planned time and therefore have to be immediately replaced by other patients from the waiting list. There can be also internal reasons (i.e lack of tools and medical products) that do not allow fulfilling the schedule. As a consequence, many last-minute changes can occur.

3. PULL SYSTEM APPROACH

Tools that support strategy and planning as well as those that help solving problems are numerous, but in this context, it is necessary to focus on those that are able to support day-to-day operations and to deal with the specific features outlined in Section 2. Therefore the "pull system method" has been considered. The basic idea this method pursues is to take up the operating room only when the patient is ready that is to say pre-operative activities have been carried out and resources (people and materials) are available. In a pull system of service, the timely transition from one-step in the process to the following is the primary responsibility of the downstream (i.e., subsequent) process that, in such a case, is the surgical department. In 'pull' systems rather than pushing patients into a waiting queue for the next step in their care, available resources are requested to 'pull' patients towards them.

At the offline operational planning level (that is referred to in this research work) , the "pull system" seeks to provide the information necessary to control and to speed up the flow of patients throughout the surgical process. Making the scheduling process a "pull system" may result in significant waiting time reductions and improved customer services. The pull method implementation will require specific scheduling rules as well as the possible redesign of supporting processes but not only. Greater involvement of the staff is also envisaged. Indeed, as mentioned before, synergies and coordination play a crucial role. To this end, substantial improvements can be achieved informing and involving surgeons, nurses and all the staff in:

- Scheduling rules and regulations;
- Consistent monitoring of processing times;
- Establishing quality indicators.

Furthermore, a proper implementation of the pull system may require processes re-engineering and activities streamlining (i.e. Supply processes). Responsibilities should be assigned, and procedures documented to allow performance monitoring.

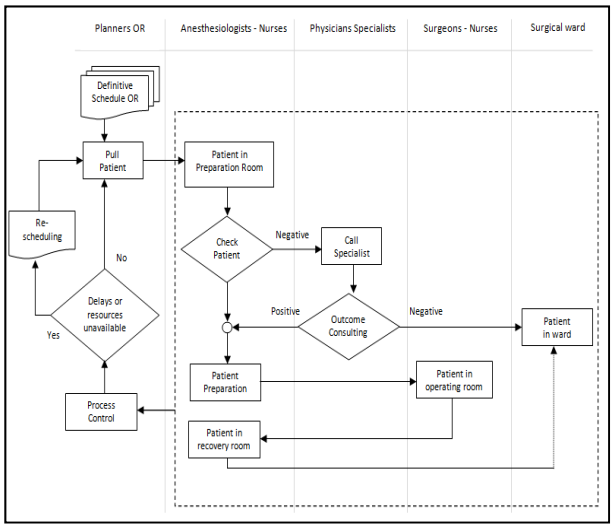

Fig.2: Pull system conceptual model

Surgical speciality	Average Process Time (APT) [min]	Average Surgery Time (AST) [min]	% AST on APT	Average Time pre - surgeries [min]	Average Time post - surgeries [min]	Non-Surgical Time (NST) [min]	% NST on APT
Neurosurgery	270	150	56%	80	40	120	44%
General Surgery	210	110	52%	75	25	100	48%
Vascular Surgery	165	80	48%	50	35	85	52%
Ortho Surgery	150	60	40%	60	30	90	60%
Ear-Nose-Throat Surgery	120	50	42%	40	30	70	58%
Gynaecology Surgery	170	90	53%	55	25	80	47%
Urology Surgery	180	95	53%	60	25	85	47%

TAB.1: Average Times Analysis

4. DATA ANALYSIS AND CURRENT PERFORMENCE

A common indicator for performance measurement in an operating room department is utilization. Although different definitions can be found in literature, commonly utilization measures the percentage of use compared to the resource capacity. As expected, the target value is 100% that means the highest utilization. Values below this threshold may be attributable to three different factors: starting late, finishing early or idle times between operations. For evaluating the actual performances of the Surgical Department, a dataset covering 52 weeks from January 1, 2014 to December 31, 2014, has been taken into account. Table 1 shows the current values of average process time, average surgery time, pre-surgery, post-surgery average time and average waiting time for each surgical specialty. In particular Process time results from three time components that include the pre-op time, the surgery time and the time interval between the surgery end and the transfer to the patient room. At first sight, it is possible to notice that in the current scenario, utilization levels are far below the target. Indeed, Average Non-surgical Time is over the 40% of the Average Process Time so that idle time percentage compared to surgery time is very high.

AUT for each Specialty [hours/Day]												
	Jan	Feb	Mar	Apr	May	Jun	Jul	Aug	Sep	Oct	Nov	Dec
Neurosurgery	4,20	6,50	6,50	5,20	7,00	6,40	7,50	6,30	7,50	7,40	6,40	7,50
n°surgeries	9	15	16	13	8	11	19	14	12	17	18	22
General Surgery 1	8,00	7,50	8,00	5,30	3,30	5,40	5,30	7,30	7,40	6,30	9,30	7,30
n°surgeries	30	37	35	27	8	23	33	29	33	41	48	32
General Surgery 2	7,40	6,00	6,40	4,00	4,30	4,00	4,40	8,00	7,40	6,40	7,40	7,40
n°surgeries	23	12	14	6	1	1	11	15	17	23	23	17
Vascular Surgery	2,30	4,40	4,40	3,30	2,40	3,30	5,40	5,30	5,00	4,40	6,50	4,40
n°surgeries	8	22	12	11	4	19	36	27	22	25	23	21
Ortho Surgery	6,30	6,00	5,40	3,40	4,30	5,40	6,30	7,00	6,20	7,40	6,20	5,40
n°surgeries	48	50	52	37	34	46	57	60	41	61	50	49
Ear-Nose-Throat Surgery	4,00	5,40	4,20	4,00	-	3,50	3,10	2,40	3,50	4,10	4,30	2,20
n°surgeries	22	26	31	24	-	17	20	18	20	25	20	15
Gynaecology Surgery	3,20	3,20	4,20	6,10	5,40	2,10	3,50	4,10	4,20	4,20	5,50	6,00
n°surgeries	5	1	4	2	1	3	6	9	11	4	17	14
Urology Surgery	4,50	4,50	5,20	5,30	3,10	5,30	5,20	7,00	4,50	5,30	6,40	5,50
n°surgeries	31	42	37	39	22	51	41	43	41	45	47	46

TAB. 2 - Average Time Utilization Daily – Operating Room

Table 2 shows the average utilization time in hours on a daily basis for each month. On average each operating room is open for less than a surgery/day. Therefore despite long waiting lists the available time (and resources) is only partially used. Inefficiency becomes even more evident when considering aggregated data over a one year period (see table 3 and 4). In such a case it is possible to notice that on average the utilization level is under the 50% of the total available time.

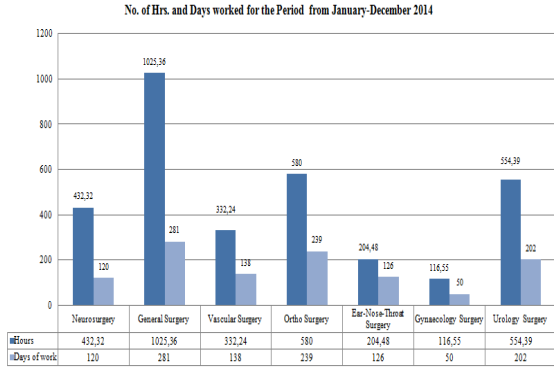

TAB. 3 - No. of Hrs. and Days worked

Operating Room	Total hours of surgery / year	% Utilization
Neurosurgery	432,32	29%
General Surgery 1	712,16	47%
General Surgery 2	313,2	21%
Vascular Surgery	332,24	22%
Ortho Surgery	580	39%
Ear-Nose-Throat Surgery	204,48	14%
Gynaecology Surgery	116,55	8%
Urology Surgery	554,39	37%

TAB. 4 - Utilization – Operating Room

5. SIMULATION MODEL DEVELOPMENT

To come up with an effective and easy to deploy solution for both performance monitoring and what-if analysis, a discrete event simulation tool has been developed. The simulation model is specifically designed to support the Surgical Department in evaluating operating rooms current and potential capacities enabling a preliminary and cost effective evaluation of the potential benefit that can be achieved integrating the "pull method" from Lean Management into offline operational programming processes.

5.1 Simulation Model Flow Chart

The simulation model flow chart is centered on flows of patients scheduled ahead of time for elective surgery. The available types of surgeries include Neurosurgery, General Surgery (two operating rooms), Vascular Surgery, Orthopedic Surgery, Ear-Nose-Throat Surgery, Gynecological and Urological Surgery (one operating room for each). The Operating Block that has been modeled as part of the simulation model consists of eight pre and post-operating rooms and eight operating rooms. While preparation rooms can be used by patients of any type, operating rooms are distinct for each specialty and come equipped with special instruments enabling particular types of surgery. The simulation model takes as input the final schedule that is used to evaluate which resources (humans and machines) are required to comply with all the activities in it. To this end, human resources in the operating block have been modeled. In greater detail, the simulation model includes two teams dealing with four operating rooms each. As depicted in figure 3, each team, includes:

- Anesthesiologists
- Nurses anesthetists
- Operating Block Nurses (or Circulating Nurses)
- Operating Room Nurses (or Scrub Nurses)
- Surgeons (for each specialty surgical)

By default assignments are as follows: an anesthesiologist for two operating rooms, a sterilized nurse (or scrubs) for each operating room, a scrub nurse for each operating room, a anesthetist nurse for two operating rooms. In addition, the number of health workers can be chosen in the initial settings of the simulation while surgeons are in a fixed number that is a first surgeon and an assistant surgeon for each operating room.

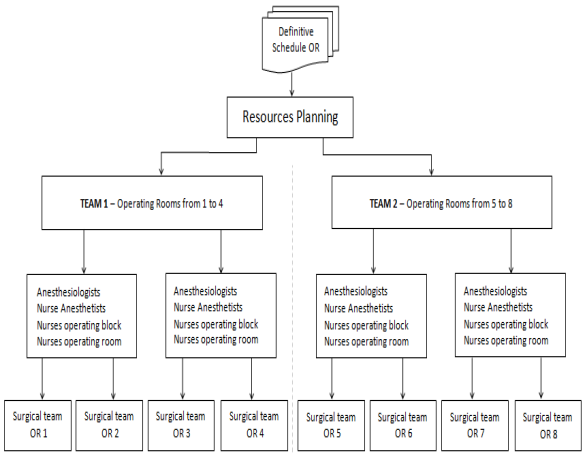

Figure 3 : Simulation Model Resources Organization

The first process implemented is the operating rooms preparation and checklist control process that starts every day at 7:00 AM and lasts one hour. In this process, which is shown in figure 4, are involved nurses in the operating room (sterilized, assistant surgeon) and nurses of operating block (non-sterilized).

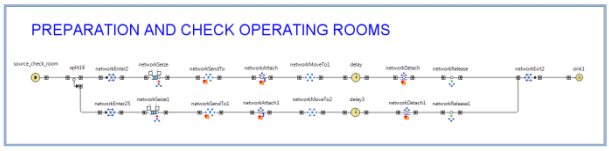

Figure 4: Simulation model Flow Chart: Preparation and Check Operating Rooms

In figure 5 is shown the simulation model flow chart of the Neurosurgery preoperative process. Nevertheless similar models have been built for the other specialties.
The pull method has been implemented within the simulation model. Hence, when the patient entity is generated some build-in controls are carried out. Such controls, have been implemented from scratch in Java and include:

- Checking for the operating room availability from the definitive schedule;
- Reading the start time and end time of regular working shifts for each operating room;
- Checking if there is an anesthesiologist ready to start the pre-operative stage;

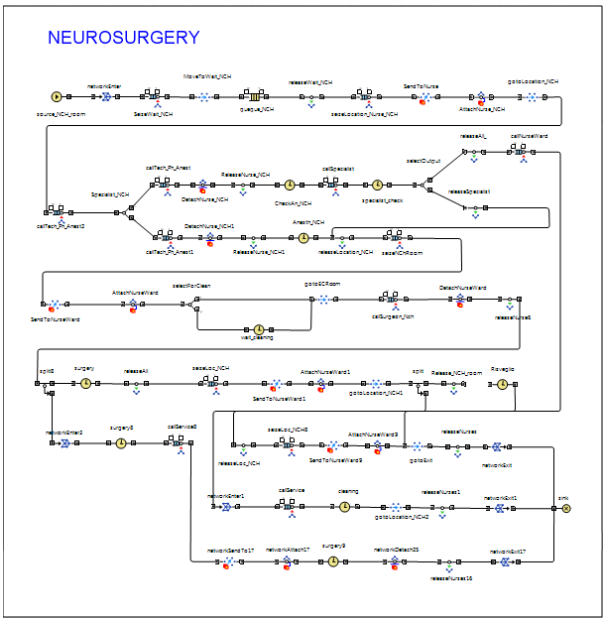

Figure 5: Simulation model Flow Chart: Pull System for Patient and preoperative process (NCH – OR)

- Comparing the remaining time before the operating room closes to the surgery estimated time. This comparison is necessary to prevent overtime. Indeed, if overtime occurs the system pulls another patient with lower estimated surgery time and postpones the patient that may cause overtime to the day after.

After such controls, the patient is treated (pulled) only when resources are available (as it happens in manufacturing systems where the pull method is applied). The advantages are the reduction the waiting time in the operating block, reduction of overtime work (and related costs), optimization of elective surgeries. Furthermore, as the simulation model is meant for what if analysis, several scenarios can be investigated changing the parameters in the input dialog window shown in fig. 6. Some of the basic parameters include:

- number of operating room nurses (for each team);
- number of operating block nurses (for each team);
- number of anesthetists nurses (for each team);
- number of anesthesiologists doctors (for each team);

- choice of weekly opening days for each operating room;
- time opening daily for each operating room;
- define the estimated time for each type of surgery (for each operating room);

Figure 6 : Parameters input window

In addition, times for anesthesia induction vary according to the surgery type based on real data provided by the Department of Anesthesiology and Intensive Care of the Hospital.

It is worth mentioning that along the development process the simulation model has been extensively tested with real data about the estimated time of surgery, time of preparation of patients, the arrival times of the patients in the surgical unit, the time required for patients awakening after anesthesia, time for operating rooms preparation and cleaning. In addition, the model has been also validated with the Sanitary Direction.

6. SIMULATION ANALYSES AND RESULTS COMPARISON

The simulation model can be considered an accurate representation of the operating block, especially for the purpose of testing ideas and concepts. This model explores the dynamics of patients flows and of all healthcare operators involved in operating rooms processes. In order to facilitate the use of the simulation model, a graphic user interface has been added to provide the user with the possibility to monitor performance evolution during the simulation (see figure 7).

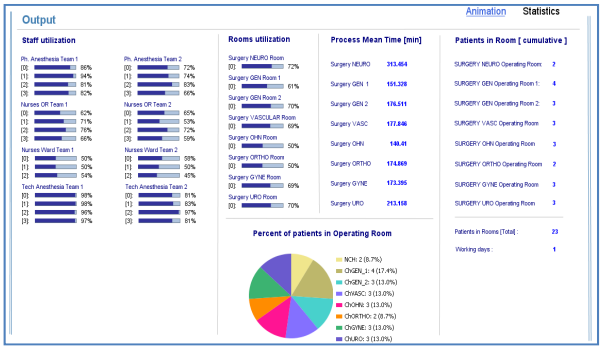

Figure 7 Output of the simulation model

In particular, the output section includes the measure of the following output parameters:

- operating rooms daily, monthly and yearly level of use (for each room and average value);
- waiting time before surgery (for each room and average value);
- waiting time after surgery (for each room and average value);
- circulating nurses level of use (for each nurse and average value);
- scrub nurses level of use (for each nurse and average value);
- auxiliary workers level of use (for each worker and average value);
- anesthetist nurses level of use (for each nurse and average value);
- anesthesiologist doctor level of use (for each doctor and average value);
- average process time (for each operating room and surgery type)
- patients rate for each operating room;
- daily , monthly and yearly number of patients for each operating room;

For the analysis that have been carried out as part of this research workand that will be discussed in the sequel, some basic settings include:

1. operating rooms standard opening times include: six hours in the morning assigned to four rooms and six hours in the afternoon assigned to the remaining four rooms;

2. Health care professionals assigned as shown in table 5.

Healthcare Professionals	Assigned [8:00 am to 2 pm]	Assigned [2:00 pm to 8 pm]
Anesthesiologist	2	2
Nurses anesthetist	2	2
Nurses circulating	4	4
Nurses scrub	4	4
Cleaning staff	1	1

Tab.5: Staff assigned to perioperative process

Simulation results allow ascertaining that compared to the actual performances, significant improvements can be achieved thanks to the "pull method implementation". Indeed, as shown in figure 8, comparing 2014 performance levels calculated in section 4 with those obtained in the simulated scenario, it results that the productivity is greatly increased. Some surgical specialties double the number of surgical procedures, such as Ear-Nose-Throat Surgery and General Surgery, while other specialties benefit from significant increases in productivity ranging from 20% to 40%

Operating Room	Hours Utilization actual	OR Utilization actual	OR Utilization simulated
Neurosurgery	6,00	41%	82%
General Surgery 1	6,30	55%	83%
General Surgery 2	6,30	55%	83%
Vascular Surgery	4,46	45%	68%
Ortho Surgery	6,00	58%	77%
Ear-Nose-Throat Surgery	3,52	33%	76%
Gynaecology Surgery	4,40	47%	70%
Urology Surgery	5,12	52%	78%

Tab.6 : Rate utilization Operating rooms

The simulation results reported in table 6, in particular, those reported in the third column of the table, provide an overall picture of operating rooms efficiency in the simulated scenario compared to the efficiency levels of the real facility.

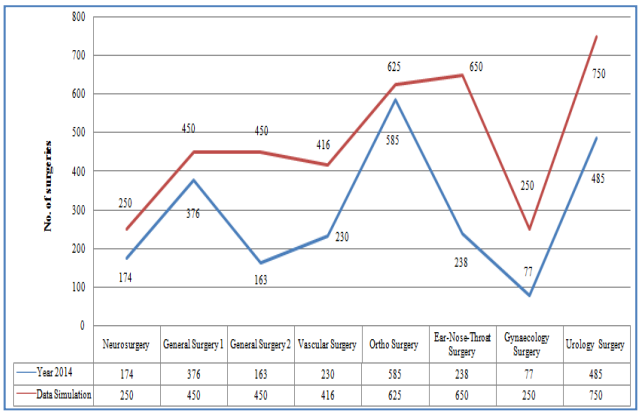

Figure 8: Comparison number of surgeries (Year 2014 – Simulated Data)

Furthermore another important outcome of the simulated scenario is the substantial reduction (60%) of patients waiting times before surgery. This result, that is analytically shown in table 7, is in line with the essence of the pull method. It is worth noticing that waiting times in the simulated scenario cannot be further reduced due to the activities that are required before the pre-anesthesia phase for preparing the surgery.

Operating Room	Average waiting time [min]	Average Waiting Time Simulated [min]	% of improvement
Neurosurgery	70	15	78,6%
G. Surgery 1	70	10	85,7%
G.Surgery 2	70	10	85,7%
Vascular S.	45	15	66,7%
Ortho S.	50	15	70,0%
ENT Surgery	40	10	75,0%
Gynae S.	50	10	80,0%
Urology S.	55	10	81,8%

Tab.7 : Waiting time improvement

CONCLUSIONS

This paper presents the results of a simulation study that has involved the Surgical Department of a public healthcare facility located in South Italy. After a preliminary work devoted to map the surgical process and after data collection and analysis, a simulation model of the operating rooms has been developed. The model, that has been validated by stakeholders and through comparison with

real data, can be used for evaluating actual and maximum capacities but also for testing alternative scenarios before the implementation in the real system. Moreover, thanks to the model parametrization, the proposed tool can be easily adopted in other similar facilities or for evaluating different configurations in terms of resources allocation and availability. In addition, the simulation model has been equipped with build-in functions implementing the "pull method" from Lean Management practices showing that substantial performance improvements can be achieved . As a matter of facts, most healthcare organizations push patients from one area to another, from wards to operating blocks, without knowing when the patient will be treated. Instead, according the pull method, thanks to a definitive scheduling and some basic preconditions such as continuous checking and resources availability, patients are pulled when they are actually needed and as a result wastes are reduced and productivity is enhanced. The effects of the pull method implementation are accurately investigated in the simulated environment that has served as playground to assess the potential impact of the proposed approach.

REFERENCES

Bennis, F., Amghar M., Sbiti N., Elouadi A., Modeling and Performance Evaluation of the Operating Room in a Hospital, I*nternational Journal of Emerging Science and Engineering (IJESE) ISSN: 2319–6378, Volume-1, Issue-4, February 2013*

Brailsford, S.C., Harper, P.R., Patel, B., Pitt, M., 2009. An analysis of the academic literature on simulation and modelling in health care. *Journal of Simulation*, 3, 130–140.

Brandeau, M.L., Sainfort, F., Pierskalla, W.P., 2004. *Operations Research and Health Care: A Handbook of Methods and Applications*. Springer.

Brecht Cardoen, Erik Demeulemeester, Jeroen Belien, 2010. Operating Room Planning and Scheduling Problems: A Classification Scheme. *International Journal of Health Management and Information (IJHMI) Volume 1, Number 1, 2010, pp. 71 – 83*

Bruzzone, A., Longo, F., Nicoletti, L., Spadafora, F., Diaz, R., Behr, J. (2013). Health care facility improvement through simulation. *Proceedings of the 2nd International Workshop on Innovative Simulation for Health Innovative Simulation for Health, IWISH 2013*, Held at the Int. Multidisciplinary Modeling and Simulation Multiconference, I3M 2012, pp. 115-123.

Bruzzone, A.G., Massei, M., Madeo, F., Tarone, F., Petuhova, J., 2011-a. Intelligent Agents for pandemic Modeling. *Emerging M and S Applications in Industry and Academia Symposium, EAIA, Spring Simulation Multiconference*, pp. 23-30

Bruzzone, A.G., Novak, V., Madeo, F., Cerada C., 2011-b. modeling of obesity epidemics by intelligent agents. *Proceedings oof the 23rd European Modeling & Simulation Symposium, EMSS 2011*, pp. 768-774.

Bruzzone, A.G., Frascio, M., Longo, F., Massei, M., Siri, A., Tremori, A. 2012. MARIA: An Agent Driven Simulation for a Web Based Serious Game devoted to Renew Education Processes in Health Care. *Proceedings of the International Workshop on Innovative Simulation for Health Care*, pp. 188-195, September 19-21, Vienna, Austria,

Diaz, R., Behr, J., Jeng, A., Lu, H., Longo, F., 2012-a. Analyzing the Effects of Policy Options to Mitigate the Effect of Sea Level Rise on the Public Health: A System Dynamics Approach. *Proceedings of the Emerging M&S Applications in Industry and Academia Symposium*, pp. 47-54, Orlando, FL, USA.

Diaz, R., Behr, J.G., Longo, F., Liu, H., 2013. A Systems Framework for Modeling Health Disparities in the Prevalence in Chronic Conditions following a Natural Disaster Event. *International Journal of Privacy and Health Information Management*, 1(1), Vol 1(1), 12-28.

Diaz, R., Khattak, A., Behr, J., Jeng, A., Longo, F., Duanmu, J., 2012-b. The effects

of transit corridor developments on the healthcare access of medically fragile vulnerable populations. *Proceedings of the 24th European Modeling and Simulation Symposium*, pp. 565-572, September 19-21, Vienna, Austria.

England, W., Roberts, S.D., 1978. Applications of computer simulation in health care. *Proceedings of the 10th Winter simulation Conference*, pp 665-677, December 4-6, FL, USA.

Flagle, C.D., 2002. Some origins of operations research in the health services. *Opns Res*, 50(1), 52–60.

Fone, D., Hollinghurst, S., Temple, M., Round, A., Lester, N., Weightman, A., Roberts, K., Coyle, E., Bevan, G., Palmer, S., 2003. Systematic review of the use and value of computer simulation modelling in population health and health care delivery. *J Public Hlth Med*, 25(4), 325–335.

Gehmlich, V. (2008). _Opportunities of supply chain management in healthcare‘, In Hübner, U. and Elmhorst, M. (eds.), eBusiness in healthcare; from eprocurement to supply chain management, Springer-Verlag London Limited.

Günal M.M., Pidd M., 2010. Discrete event simulation for performance modelling in health care: a review of the literature. *Journal of Simulation*, 4, 42–51.

Holm, L.B., Luras, H., Dahl, F.A., 2013. Improving hospital bed utilisation through simulation and optimisation: With application to a 40% increase in patient volume in a Norwegian general hospital. *International Journal of Medical Informatics*, 82(2), 80–89.

Martin L.D., Rampersad S.E., Low D.K.W., Reed M.A. 2014. Process improvement in the operating room using Toyota (Lean) methods. *Rev Colomb Anestesiol* 42(3):220-228.

Longo F, Calogero A, Nicoletti L, Massei M, De Felice F, Petrillo A (2014). Lean management approaches applied to healthcare systems. In: *Proceedings of the International Workshop on Innovative Simulation for Healthcare*. p. 60-69, ISBN: 978-88-97999-37-9, Bordeaux, France, September 10-12, 2014

Marjamaa R., Vakkuri A., Kirvela O., 2008, Operating Room Management: why, how and by whom? *Acta Anaesthesiologica Scandinavica 52: 596-600.*

Jacobson, S.H., Hall, S.N., Swisher, J.R., 2006. Discrete-Event Simulation of Health Care Systems. In: Hall R.W. ed. *Patient Flow: Reducing Delay in Healthcare Delivery*. Springer, 211-252.

Jimmerson, C. (2007). *A3 Problem Solving for Healthcare: A Practical Method for Eliminating Waste.* New York: Productivity Press

Jun, J.B, Jacobson, S.H., Swisher, J.R., 1999. Applications of discrete event simulation in health care clinics: A survey. *J Opl Res Soc*, 50, 109–123.

Jun, J.B., Jacobson S.H., Swisher J.R., 1999. Application of discrete-event simulation in health care clinics: a survey *journal of the operational research society*, 50(2), 109-123.

Lehaney, B., Hlupic, V., 1995. Simulation modelling for resource allocation and planning in the health sector. *J Royal Soc Hlth*, 115(6), 382–385.

Porter M.E., 2008. Competitive Advantage: Creating and Sustaining Superior Performance. Eds. Simon and Schuster, 2008.

Robinson S., Z. J. Radnor, N. Burgess, C. Worthington (2012), Utilising Simulation in the implementation of Lean in Healthcare. *European Journal of Operational Research, vol.219, Issue 1,16 may 2012, pp. 188-197.*

Smith-Daniels, V.L., Schweikhart S.B., Smith-Daniels D.E, 1988. Capacity management in health care services: Review and future research directions. *Dec Sci* 19, 889–918.

Swisher, J.R., Jacobson , S.H., Jun, J.B., Balci, O., 2001. Modeling and analyzing a physician clinic environment using discrete-event (visual) simulation. *Computers & Operations Research*, 28(2), 105-125.

Wang, J., Li, J., Tussey, K., Ross, K., 2012. Reducing Length of Stay in Emergency Department: A Simulation Study at a Community Hospital. *Systems, Man and Cybernetics, Part A: Systems and Humans, IEEE Transactions on*, 42(6), 1314-1322.

Winkler S.M., Affenzeller, M., Kronberger, K., Kommenda, M:, Wagner, S., Jacak, W., Stekel, H., 2011. On the use of estimated tuomor marker classification in tumor diagnosis prediction. A case study for breast cancer. Proceedings of the 23rd Europeran Modeling & Simulation Symposium, EMSS 2011, Rome, Italy

Weerawat, W., Pichitlamken, J., Subsombat, P., 2013. A Generic Discrete-Event Simulation Model for Outpatient Clinics in a Large Public Hospital. *Journal of Healthcare Engineering*, 4(2), 285-306.

Author's Index